Universidade Federal do Espírito Santo

Programa de Pós-Graduação em Astrofísica, Cosmologia e Gravitação

Black hole ringdown, and theoretical considerations concerning k-essence, Rastall and entangled gravity

Edison Cesar de Oliveira Santos

Thesis submitted as part of the requirements for the degree of
Doctor of Philosophy in Astronomy & Physics

Supervisor: Prof. Júlio César Fabris
Universidade Federal do Espírito Santo, Vitória, Brasil

2021

Universidade Federal do Espírito Santo
Centro de Ciências Exatas
Programa de Pós-Graduação em Astrofísica, Cosmologia e Gravitação

Black hole ringdown, and theoretical considerations concerning k-essence, Rastall and entangled gravity

Edison Cesar de Oliveira Santos

A presente tese "*Black hole ringdown, and theoretical considerations concerning k-essence, Rastall and entangled gravity*" foi submetida no ano de 2021 ao PPGCosmo por *Edison Cesar de Oliveira Santos* como parte dos requisitos para a obtenção do título de Doutor em Astronomia e Física.

Caso esta tese venha a ser aprovada, esta folha deverá ser substituída pela correspondente de aprovação.

"You can try the best you can,
you can try the best you can,
the best you can is good enough."
Radiohead - Optimistic

Abstract

While the detection of gravitational waves was an outstanding achievement in theoretical and observational physics, data science, computer science and engineering on their own merit, it also allowed us to observe black holes for the first time. Black hole physics had a tumultuous research history, from a nearly non-existent field to work, in the first years of general relativity, culminating in the *golden age of general relativity* in the sixties and mid-seventies, where black holes entered the mainstream theoretical physics. We could be arguably living in the second *golden age of general relativity*, but this time around black holes entered the mainstream observational physics. In light of this, this thesis tackle some problems in black hole physics, or in a broader sense, the current understanding of gravity. The first part of this thesis is devoted to developing the machinery of first-order perturbation theory in order to obtain the quasi-normal modes from both singular and non-singular black holes, that is, the frequencies related to the oscillation of a black hole after its merging. In the next section we contrast how a particular analytical model, that works from the merger up to the ringdown phase, constrains both the final mass and spin parameter when compared to the published results. In the second part, we investigate a series of works related to spherically-symmetric solutions of both k-essence and Rastall theories, where a possible solution to what seems a coincidence in both theories, might be related to a formulation of a lagrangian formalism for the latter theory. We end this thesis finding black hole solutions to a novel theory of gravity, entangled gravity. This model is not defined in the absence of any matter field, but we argue that black hole solutions satisfying the *near vacuum* condition resembles solutions obtained in standard general relativity.

Keywords: black hole, perturbation theory, quasi-normal modes, stability, modified gravity.

Resumo

A detecção de ondas gravitacionais foi uma incrível conquista da física teórica e observacional, ciência de dados, ciência da computação e engenharia, cada qual com seus próprios méritos, que nos permitiu observar buracos negros pela primeira vez. A física de buracos negros teve uma tumultuada história em sua pesquisa, desde um campo de trabalho quase inexistente, culminando na *era de ouro da relatividade geral* nos anos sessenta e meados nos anos setenta, onde buracos negros entraram na física teórica tradicional. Nós podemos, discutivelmente, estar vivendo na segunda *era de ouro da relatividade geral*, mas desta vez buracos negros entraram na física observacional convencional. Por meio disso, esta tese aborda alguns problemas da física de buracos negros, ou em um sentido mais amplo, no atual entendimento da gravitação. A primeira parte desta tese é direcionada no desenvolvimento da teoria perturbativa de primeira-ordem para obter of modos quasi-normais de buracos negros singulares e não-singulares, ou seja, as frequências relacionadas com a oscilação do buraco negro após sua fusão. Na próxima seção comparamos como um modelo analítico particular, que funciona desde a fusão até a fase de ringdown, restringe a massa e o parâmetro de rotação quando comparado com os resultados publicados. Na segunda parte investigamos uma série de trabalhos relacionados à soluções esfericamente-simétricas das teorias de k-essência e Rastall, onde uma possível resolução para o que parece ser uma coincidência em ambas teorias, pode estar relacionada com a formulação de um formalismo lagrangiano para este modelo. Terminamos essa tese encontrando soluções de buraco negro em uma nova teoria de gravitação, chamada gravidade "entangled". Este modelo não é definido na ausência de campos de matéria, mas argumentamos que soluções de buraco negro satisfazendo a condição de *quase vácuo* se assemelham às soluções obtidas na relatividade geral padrão.
Palavras-chaves: buraco negro, teoria de perturbação, modos quasi-normais, estabilidade, teoria modificada da gravitação.

Acknowledgments / Agradecimentos

Muito obrigado aos meus pais que me deram condições para conseguir chegar até aqui. Obrigado por nunca terem desistido dos meus estudos e terem me dado as oportunidades que eu precisava.

Thank you for supporting, advising, helping and loving me Tassia Ferreira. I have no idea how I would have finished this work without you. Having you by my side has been the greatest gift I ever had. Wherever we are headed next, let us go together!

I thank Júlio Fabris for making this work possible and for sharing some of your vast knowledge with me.

I am particularly thankful for Nelson Christensen, Marie-Anne Bizouard and Olivier Minazzoli for the hospitality and the fruitful discussions about physics (some of them over wine). You have provided me great personal and scientific experiences that I will carry on with me for my whole life.

Contents

List of Figures

List of Tables

Introduction

It is an exciting time to be a young researcher in the gravitation-related field. We have a well established mathematical toolbox: general relativity (GR), which has survived the test of time for more than a hundred years. Lots of open questions yet to be solved: Can we find a renormalization procedure that works for gravity? Can we get rid of the singularities? Is there any way to merge this theory with quantum-field theory? What is the deal with both dark matter and dark energy? And now we are finally having some answers: Yes, gravitational waves exist [3]. It propagates at the speed of light [4]. The universe is expanding at an accelerating pace [5]. Black holes (BH) do exist [6].

With more questions than answers, we have many possibilities to circumvent some questions: What if the universe is not four-dimensional [7]? Dark matter may be just BHs [8]. Graviton's mass may be hiding under some screening mechanism [9]. Gravity may emerge from thermodynamics [10]. Bearing that in mind, in this thesis we investigate some of these problems, and potential explanations to these questions.

After two BHs merge together in the coalescence process, the single remnant BH emits gravitational waves in the form of quasi-normal modes. Contrary to the usual normal modes, where the oscillation process keeps perpetually ringing, in this case the oscillations are damped since the waves are either entering the BH's event horizon, or propagating to the radial infinity. This is what we go over on chapter 2. In a more mathematical approach, we uncover the spatial angular rotation symmetry, investigate the spherical harmonics decomposition of the two orthogonal parities, discuss about the test-fields and its perturbation types, while developing two different methods to analyze the quasi-normal frequencies.

As we established, one of the main issues in gravitation is the existence of singularities within BHs. Some authors may agree[1] that this may be an indication of something ill-defined in our current understanding of gravity. One possible way to remedy this situation is to add some kind of matter inside the BH, which turns the solution non-singular, or regular. We explore these solutions, and compare the quasi-normal frequencies with the singular ones.

While modeling the merging process of a binary system throughout its entirety is a great endeavor accomplished, it was done matching several different methods for each stage. In chapter 2.7 we investigate one model that tries to encapsulate the merger-ringdown stage of the coalescence process, through the merger to the ringdown into a single framework. This model takes the remnant final BH and trace it back to the before-merger state, when the two bodies were still afar from each other. We use this model to check how we can estimate both the mass and the dimensionless spin parameter for two different gravitational waves signals, and how they compare to the results already obtained.

[1] Me included.

Taking into account that GR may not be our final theory of gravity, we check some peculiarities in two different extensions to GR. Using two different models of gravity, k-essence and Rastall with a scalar field, it was possible to obtain the same BH-like solution for the metric field. This result, at first really surprising due to the different nature of the two theories, must be checked and thoroughly investigated. Therefore, in chapter 3, much more as an exploratory investigation, we try to answer some questions concerning this coincidence: under which conditions are these two theories alike each other? Are the solutions stable in each case?

We could argue that between these two theories, Rastall bears more exotic traits since it is a fundamentally non-conservative theory that may encapsulate some yet to be found effect in curved space time. With this, in chapter 4 we tackle its main issue: Rastall theory does not posses any lagrangian, that is, its field equations are induced to give the field equations that satisfy some desired conditions. We will show that all the proposals in the literature does not recover the expected results, while we convey one possible way out of this conundrum.

We finish this thesis in chapter 5 where we check a theory cast as a particular case of a $f(R, \mathcal{L}_m)$ model, called entangled gravity. This model "entangles" the gravity lagrangian and the matter component into a single term, that is, it is impossible to exist gravity without matter, and vice-versa. One of the main properties of this theory is the lack of a vacuum solution, the total lagrangian density vanishes when setting the matter lagrangian to zero. Despite this, we will argue that the BH solutions that we found resembles the BHs solutions obtained in GR satisfying the *near vacuum* condition.

Black holes quasi-normal modes

2.1. Introduction

One of the main solutions obtained in general relativity (GR) are black holes (BH) spacetimes. In agreement with the *no-hair theorem* [11], the BH solutions are fully described by its mass M, charge Q and the angular momentum parameter a, aside from the cosmological constant, Λ, that may be directly introduced into the field equations. These solutions can be classified as a sub-class of the *Kerr-Newman (anti) de-Sitter* space-time.

When the spin of the BH is not considered, that is, assuming that the solution is not only stationary but also static, the general spherically-symmetric metric[1] $g_{\mu\nu}$ can be arranged in the form

$$ds^2 = f(r)dt^2 - f(r)^{-1}dr^2 - r^2 d\Omega^2, \tag{2.1}$$

where the lapse function $f(r)$ contains the BHs properties.

In this given form, Schwarzschild obtained the first analytic solution for GR [12]. Assuming no matter content, the inner region of this solution describes a BH, presenting a point of no-return described by its *event horizon*. Adding some matter to its core, this metric now describes the outer region of spherically-symmetric objects like stars or planets, making the classical examples of GR's prediction possible, like the perihelion precession of Mercury and the deflection of light by the Sun [13].

Another proposed prediction from GR is the emission of gravitational waves. Although these waves were first proposed by Einstein in 1916 [14], they were only discovered a hundred years later by the LIGO-Virgo collaboration [15] due to the coalescence of two BHs.

This coalescence process is roughly divided into three different stages, each with their own unique features: the first stage is the *inspiral phase*, where both bodies are spiraling inward due to the emission of gravitational waves, albeit far enough from each other to be distinguished as two objects. The horizons then coincide and the *merger phase* begins; this is where the strongest gravitational waves are emitted. The modeling of this phase requires the computation of the full-solution of Einstein's non-linear equations, which is only possible through numerical analysis. The remnant of this collision is a single vibrating BH, with its frequency decaying exponentially. The last stage of the coalescence is known as the *ringdown phase* and is well described by perturbation theory.

Perturbation theory was first applied to BH physics by Regge and Wheeler [16] and was picked up more than a decade later by Zerilli [17]. The main result obtained in these papers was the reduction of the cumbersome set of perturbed equations into a single Schrödinger-like equation for the radial perturbations. Subsequently, the first paper to effectively calculate quasi-normal

[1] In standard GR.

modes, that is, the damped oscillation signal of a BH, was done by Vishveshwara [18]. Thereafter, the calculation of quasi-normal modes for singular BHs in a wide variety of contexts and methods was initiated ([19, 20, 21] and references therein).

Although the singularities are unavoidable due to the singularities theorems, they may be overlooked in some considerations related to BHs. But in the last stages of BH evaporation, due to Hawking radiation in the semiclassical regime of GR [22], these singular regions cannot be discarded either due to the *information loss paradox* (see [23] for a review in the subject) or to establish how BHs evolve in the last stages of evaporation. One of the proposed solutions for both of these issues, is to assume that as a result of some quantum effect, yet to be fully described by a quantum gravity theory, the singular regions in BHs would be regularized. Thus the BH's centre would not present any divergences, neither in the sense of its curvature scalars nor due to geodesic incompleteness of the spacetime. These solution are called regular, or non-singular, BHs.

In light of this, in section 2.2 we review the basics of BH perturbation theory. In section 2.3 we uncover the main properties of the singular and regular BHs which will be examined later on. In the next two sections, 2.4 and 2.5, we examine two different methods to obtain the oscillation frequencies: first we review the method of Pöschl-Teller potential, where a closed form for the frequencies are obtained using an approximate effective potential; then we describe the semi-analytical WKB method, where we generalize it to the third-order. We present and discuss the plots of the frequencies against the BHs parameters obtained for each solution in section 2.6. Section 2.7 ends this chapter focusing in the ringdown gravitational waveform, where we compare how a novel analytical waveform model contrasts with the results already obtained for two different gravitational waves signals.

2.2. Black hole perturbation theory

BH perturbation theory began with the pioneering work of Regge and Wheeler [16], where they investigated whether Schwarzschild's metric was stable under the general perturbation

$$g'_{\mu\nu}(x^\lambda) = g_{\mu\nu}(x^\lambda) + h_{\mu\nu}(x^\lambda), \tag{2.2}$$

where $g_{\mu\nu}(x^\lambda)$ is the background metric and $h_{\mu\nu}(x^\lambda)$ is the perturbed metric. To guarantee the validity of the linearized field equations, the following condition must be satisfied

$$\left|\frac{h_{\mu\nu}(x^\lambda)}{g_{\mu\nu}(x^\lambda)}\right| \ll 1, \tag{2.3}$$

that is, the perturbation term is never dominant over the background metric.

2.2.1. Perturbation of the Einstein equations

The standard theory of gravitation, using the geometrized unit system $8\pi G = c = 1$, is given by the Einstein field equations (EFE) as

$$G_{\mu\nu} = T_{\mu\nu}, \tag{2.4}$$

where $G_{\mu\nu}$ is the usual definition of the Einstein tensor given by $G_{\mu\nu} = R_{\mu\nu} - \frac{1}{2}g_{\mu\nu}R$, in terms of the Ricci tensor, $R_{\mu\nu}$, and its correspondent scalar, R, and $T_{\mu\nu}$ is the stress-energy tensor (SET).

With the well-established background solutions for BHs (like Schwarzschild, Reissner-Nordström and Kerr, for example), we can check what happens to these solutions under a perturbation of

the type (2.2). Therefore, the main objective of this section is to outline the procedure to obtain the general perturbed EFE. To achieve this, we first revise the main elements of the EFE. The components of the Christoffel symbols may be evaluated via

$$\Gamma^{\lambda}_{\mu\nu} = \frac{1}{2} g^{\lambda\alpha}(\partial_\mu g_{\alpha\nu} + \partial_\nu g_{\mu\alpha} - \partial_\alpha g_{\mu\nu}), \tag{2.5}$$

and the Riemann tensor as

$$R^{\alpha}{}_{\mu\beta\nu} = \partial_\beta \Gamma^{\alpha}_{\mu\nu} - \partial_\nu \Gamma^{\alpha}_{\mu\beta} + \Gamma^{\alpha}_{\rho\beta}\Gamma^{\rho}_{\mu\nu} - \Gamma^{\alpha}_{\rho\nu}\Gamma^{\rho}_{\mu\beta}. \tag{2.6}$$

The Ricci tensor, and its correspondent scalar, are obtained by contracting the Riemann tensor via

$$R_{\mu\nu} = R^{\alpha}{}_{\mu\alpha\nu}, \tag{2.7}$$

and

$$R = R^{\alpha}{}_{\alpha}. \tag{2.8}$$

To obtain the perturbed EFE, we have to calculate how each of these quantities behave under first-oder perturbation separately. In the linear regime, where we denote each perturbed component with a δ, the perturbed affine connection may be obtained via

$$\delta\Gamma^{\lambda}_{\mu\nu} = \frac{1}{2} g^{\lambda\alpha}(\nabla_\mu h_{\alpha\nu} + \nabla_\nu h_{\mu\alpha} - \nabla_\alpha h_{\mu\nu}). \tag{2.9}$$

Using the same method, the perturbed Riemann tensor may be obtained through the use of

$$\delta R^{\alpha}{}_{\mu\beta\nu} = \nabla_\beta \delta\Gamma^{\alpha}_{\mu\nu} - \nabla_\nu \delta\Gamma^{\alpha}_{\mu\beta}, \tag{2.10}$$

which may be recast in terms of the perturbed metric $h_{\mu\nu}$ as

$$\delta R^{\alpha}{}_{\mu\beta\nu} = \frac{1}{2}(\nabla_\beta \nabla_\mu h_\nu{}^\alpha + \nabla_\beta \nabla_\nu h_\mu{}^\alpha - \nabla_\beta \nabla^\alpha h_{\mu\nu} - \nabla_\nu \nabla_\mu h_\beta{}^\alpha - \nabla_\nu \nabla_\beta h_\mu{}^\alpha + \nabla_\nu \nabla^\alpha h_{\mu\beta}). \tag{2.11}$$

Through the contraction of the perturbed Riemann tensor we get the following perturbed Ricci tensor

$$\delta R_{\mu\nu} = \frac{1}{2}(\nabla_\rho \nabla_\mu h_\nu{}^\rho + \nabla_\rho \nabla_\nu h_\mu{}^\rho - \Box h_{\mu\nu} - \nabla_\nu \nabla_\mu h), \tag{2.12}$$

where we defined the trace of the perturbed metric as $h = h^\rho{}_\rho$. With a final contraction of the remaining indices of the perturbed Ricci tensor, we determine the perturbed Ricci scalar as

$$\delta R = -h^{\mu\nu} R_{\mu\nu} + \nabla_\mu \nabla_\nu h^{\mu\nu} - \Box h. \tag{2.13}$$

By the definition of the Einstein tensor, its perturbation is

$$\delta G_{\mu\nu} = \delta R_{\mu\nu} - \frac{1}{2} R h_{\mu\nu} - \frac{1}{2} g_{\mu\nu} \delta R, \tag{2.14}$$

and we may use the quantities that we calculated to cast it in terms of h

$$\delta G_{\mu\nu} = \frac{1}{2}[(\nabla_\alpha \nabla_\mu h_\nu{}^\alpha + \nabla_\alpha \nabla_\nu h_\mu{}^\alpha - \nabla_\nu \nabla_\mu h) + g_{\mu\nu}(h^{\alpha\beta} R_{\alpha\beta} - \nabla_\alpha \nabla_\beta h^{\alpha\beta} + \Box h) - h_{\mu\nu} R]. \tag{2.15}$$

With all the main components evaluated the perturbed EFE may be written as

$$\delta G_{\mu\nu} = \delta T_{\mu\nu}, \tag{2.16}$$

in which we defined a general SET perturbation as $\delta T_{\mu\nu}$.

Up to this point this whole structure of equations is general for any linear perturbation given by equation (2.2). However, despite the linear nature of the perturbed EFE, it is clear that dealing with them is still a difficult task. Since in this work we are dealing solely with spherically-symmetric BHs solutions, we must exploit this symmetry to further simplify the equations. In the next section we set the mathematical ground, using the spherical harmonics as basis of the two-dimensional sub-space of the sphere, to obtain a simpler set of equations.

2.2.2. Axial and polar decomposition

A second-rank tensor possess the following general transformation law

$$g_{\mu'\nu'}(x^{\lambda'}) = \frac{\partial x^{\mu'}}{\partial x^{\mu}} \frac{\partial x^{\nu'}}{\partial x^{\nu}} g_{\mu\nu}(x^{\lambda}). \tag{2.17}$$

The BHs solutions that we are analyzing possess spherical symmetry, with this we can check how each component of this metric behave under a general two-dimensional rotation, given by the following transformation

$$\frac{\partial x^{\mu'}}{\partial x^{\mu}} = \begin{pmatrix} 1 & 0 & 0 & 0 \\ 0 & 1 & 0 & 0 \\ 0 & 0 & & \\ 0 & 0 & & \mathcal{R}_i^{\ j} \end{pmatrix}. \tag{2.18}$$

Each component of the metric transforms as [24]

$$\begin{aligned} g'_{00} &= g_{00}, & g'_{11} &= g_{11}, & g'_{01} &= g_{01}, \\ g'_{0i} &= \mathcal{R}_i^{\ k} g_{0k}, & g'_{1i} &= \mathcal{R}_i^{\ k} g_{1k}, & & \\ g'_{ij} &= \mathcal{R}_i^{\ k} \mathcal{R}_j^{\ l} g_{kl}, & & & & \end{aligned} \tag{2.19}$$

that is, under a two-dimensional rotation, a general four-dimensional metric transforms as: three scalars (g_{00}, g_{01} and g_{11}), two vectors (g_{0i} and g_{1i}) and one tensor (g_{ij}). This may be summarized via the matrix representation of the metric

$$g_{\mu\nu} = \begin{pmatrix} S_1 & S_2 & V_1 & V_1 \\ sym & S_3 & V_2 & V_2 \\ sym & sym & T & T \\ sym & sym & sym & T \end{pmatrix}, \tag{2.20}$$

with the *sym* indicating the symmetric terms of the metric. This procedure is known as Scalar, Vector and Tensor (SVT) decomposition. The ease of using this scheme is that each perturbation type decouple and they can be treated separately.

Usually in BH physics, the scalar perturbations are called of the *polar type*, which causes deformation on the BH horizon, and the vector ones as the *axial type*, responsible for small increments on the BH's rotation. As we will see in the following sections, the tensor perturbation may be gauged-off with a suitable choice, hence they are not dynamical [19].

Due to the spherical symmetry, we use the spherical-harmonics to decompose the *axial* and *polar* perturbations, which form an orthogonal set. Any scalar function may be directly decomposed using the spherical-harmonic function, with the usual notation $Y_\ell^m(\theta, \phi)$[2]. It is clear that

[2] A quick review of its main properties may be found in appendix A

since it is a scalar, it must be invariant under rotation, thus it is of the *polar* type. However we are decomposing the functions over the two-dimensional sphere, hence the vector and tensor parts must also be decomposed using what is known as *vectorial* and *tensorial harmonics.* Since the *axial* and *polar* functions form an orthogonal group, we can assemble the vector-harmonics into its *axial* and *polar* components, and the same can be done to the tensor-harmonics.

The vector-harmonics decomposed in its *polar* part are defined as

$$Y^m_{\ell \boldsymbol{i}} = \partial_i Y^m_\ell \tag{2.21}$$

while the *axial*-part is

$$X^m_{\ell \boldsymbol{i}} = \epsilon_i^{\ j} \partial_j Y^m_\ell, \tag{2.22}$$

where we defined the pseudo-tensor

$$\epsilon_i^{\ j} = \begin{pmatrix} 0 & -1/\sin\theta \\ \sin\theta & 0 \end{pmatrix}. \tag{2.23}$$

Similarly, the tensor-harmonic of the *polar* type is

$$Y^m_{\ell \boldsymbol{ij}} = \nabla_i \partial_j Y^m_\ell \tag{2.24}$$

and the correspondent *axial* type is

$$X^m_{\ell \boldsymbol{ij}} = \frac{1}{2}(\epsilon_i^{\ k} \nabla_j + \epsilon_j^{\ k} \nabla_i) \partial_k Y^m_\ell. \tag{2.25}$$

Through direct inspection, it can be seen that equations (2.21) and (2.24), under parity transformation transforms as $(-1)^\ell$, exactly as the (scalar) spherical-harmonic transforms via $Y^m_\ell(\theta, \phi) = (-1)^\ell Y^m_\ell(\theta, \phi)$. In comparison, the axial parts, equations (2.22) and (2.25) transforms as $(-1)^{\ell+1}$. Due to this reason, the *axial* part is also known as the *odd*-parity class, and the *polar* part as the *even*-parity class.

These *vectorial* and *tensorial* harmonics (as it is used in reference [25]) are a generalization of the usual spherical-harmonics. This whole set of harmonics are unified in what is called *spin-weighted spherical harmonics*, ${}_sY^m_\ell$. For $s = 0$ we would have ${}_0Y^m_\ell$, which are the usual (scalar) spherical-harmonics used to decompose scalar functions; the vector-harmonics would be of spin equal to 1, ${}_1Y^m_\ell$; and the tensor-harmonics would be represented as ${}_2Y^m_\ell$, with $s = 2$. This formalism was rediscovered, and first applied to gravitational radiation, by Newman and Penrose in reference [26]. For an approach more inclined to the mathematical aspects of this decomposition, we refer the reader to reference [27].

2.2.2.1. Axial-parity

Since the scalar part, expanded in spherical harmonic transforms as $(-1)^\ell$, its *axial* contribution is equal to zero.

Using equation (2.22), the *vectorial* harmonics are

$$\begin{aligned} X^m_{\ell \boldsymbol{\theta}} &= -\frac{1}{\sin\theta} \partial_\phi Y^m_\ell, \\ X^m_{\ell \boldsymbol{\phi}} &= \sin\theta \partial_\theta Y^m_\ell. \end{aligned} \tag{2.26}$$

Its *tensorial* part, through the use of equation (2.25), may be written as

$$\begin{aligned} X^m_{\ell\boldsymbol{\theta\theta}} &= -\frac{1}{\sin\theta}(\partial_\theta\partial_\phi - \cot\theta\partial_\phi)Y^m_\ell, \\ X^m_{\ell\boldsymbol{\phi\phi}} &= (\sin\theta\partial_\theta\partial_\phi - \cos\theta\partial_\phi)Y^m_\ell, \\ X^m_{\ell\boldsymbol{\theta\phi}} &= 1/2\left(\sin\theta\partial^2_\theta - \csc\theta\partial^2_\phi - \cos\theta\partial_\theta\right)Y^m_\ell. \end{aligned} \tag{2.27}$$

With each component of the matrix (2.20) decomposed in its *axial*-parity part, we can rewrite it in the most general way as

$$h^a_{\mu\nu} = \begin{pmatrix} 0 & 0 & -h_0(t,r)\frac{1}{\sin\theta}\partial_\phi Y^m_\ell & h_0(t,r)\sin\theta\partial_\theta Y^m_\ell \\ sym & 0 & -h_1(t,r)\frac{1}{\sin\theta}\partial_\phi Y^m_\ell & h_1(t,r)\sin\theta\partial_\theta Y^m_\ell \\ sym & sym & -K(t,r)\frac{1}{\sin\theta}(\partial_\theta\partial_\phi - \cot\theta\partial_\phi)Y^m_\ell & K(t,r)\frac{1}{2}\left(\sin\theta\partial^2_\theta - \frac{1}{\sin\theta}\partial^2_\phi - \cos\theta\partial_\theta\right)Y^m_\ell \\ sym & sym & sym & K(t,r)(\sin\theta\partial_\theta\partial_\phi - \cos\theta\partial_\phi)Y^m_\ell \end{pmatrix} \tag{2.28}$$

whereas we defined the general functions $h_0(t,r)$, $h_1(t,r)$ and $K(t,r)$, depending on both the radial coordinate r and the time coordinate t. What we have obtained with equation (2.28) is the most general metric of the *axial* type. That is, from here we could plug these components back into equation (2.16), to obtain the perturbed *axial* EFE. But we have another trick up our sleeve: a suitable gauge choice to further simplify this set of equations.

The gauge freedom in general relativity is expressed by the following expression

$$\begin{aligned} h^{new}_{\mu\nu} &= h^{old}_{\mu\nu} + \nabla_\mu\xi_\nu + \nabla_\nu\xi_\mu, \\ &= h^{old}_{\mu\nu} + \partial_\mu\xi_\nu + \partial_\nu\xi_\mu - 2\Gamma^\alpha_{\mu\nu}\xi_\alpha. \end{aligned} \tag{2.29}$$

In other words, this equation relates how the perturbed metric $h^{old}_{\mu\nu}$ changes along the vector ξ_μ. This transformation leaves the linearized Riemann tensor, equation (2.11), unchanged, hence the new perturbed metric $h^{new}_{\mu\nu}$ is physically the same as the previous one, allowing the freedom on choosing a convenient ξ_μ. The ξ_μ vector components can also be decomposed in its *axial*-part through the use of (2.22). That is

$$\begin{aligned} \xi_t = 0, \quad \xi_\theta &= -\Lambda(t,r)\frac{1}{\sin\theta}\partial_\phi Y^m_\ell, \\ \xi_r = 0, \quad \xi_\phi &= \Lambda(t,r)\sin\theta\partial_\theta Y^m_\ell. \end{aligned} \tag{2.30}$$

With the gauge-freedom explicit in $\Lambda(t,r)$, we can suitably choose this function to annul $K(t,r)$ in the metric (2.28). This choice is known as *Regge-Wheeler gauge*.

Since we are looking after wave solutions with frequency ω, to further simplify the equations we choose the temporal coordinate to behave as $e^{-i\omega t}$. Applying these simplifications, and relabelling some functions, we are left with the following *axial*-parity metric

$$h^a_{\mu\nu} = \begin{pmatrix} 0 & 0 & -h_0(r)\frac{1}{\sin\theta}\partial_\phi & h_0(r)\sin\theta\partial_\theta \\ sym & 0 & -h_1(r)\frac{1}{\sin\theta}\partial_\phi & h_1(r)\sin\theta\partial_\theta \\ sym & sym & 0 & 0 \\ sym & sym & sym & 0 \end{pmatrix} e^{-i\omega t}Y^m_\ell. \tag{2.31}$$

A last simplification may be performed realizing that it is not necessary to work for a general value of m. GR is a covariant theory, therefore we can choose any value of m and the radial

equations must still be the same. With this we set $m = 0$, which makes any dependence of the ϕ coordinate to vanish without any loss of generality. Employing this choice we obtain

$$h^a_{\mu\nu} = \begin{pmatrix} 0 & 0 & 0 & h_0(r) \\ sym & 0 & 0 & h_1(r) \\ sym & sym & 0 & 0 \\ sym & sym & sym & 0 \end{pmatrix} e^{-i\omega t} \sin\theta \partial_\theta P_\ell. \tag{2.32}$$

This is what Regge-Wheeler called as the "canonical form of *axial* waves".

With all these simplifications we were able to eliminate one variable from our set of equations and the spherical harmonics Y^m_ℓ lost their ϕ dependence reducing to the Legendre polynomial.

2.2.2.2. Polar-parity

We closely follow the procedure performed for the *axial* parity section to obtain the *polar* decomposition. Since the scalar part transforms as $(-1)^{(\ell+1)}$, it will have a contribution of the type $Y^m_\ell(\theta, \phi)$.

Through the use of equation (2.21) we can decompose the vector part into

$$\begin{aligned} Y^m_{\ell\boldsymbol{\theta}} &= \partial_\theta Y^m_\ell, \\ Y^m_{\ell\boldsymbol{\phi}} &= \partial_\phi Y^m_\ell. \end{aligned} \tag{2.33}$$

Similarly, using the tensor *polar*-parity decomposition in equation (2.24) we get

$$\begin{aligned} Y^m_{\ell\boldsymbol{\theta\theta}} &= \partial^2_\theta Y^m_\ell, \\ Y^m_{\ell\boldsymbol{\phi\phi}} &= (\partial^2_\phi + \sin\theta\cos\theta\partial_\theta) Y^m_\ell, \\ Y^m_{\ell\boldsymbol{\theta\phi}} &= (\partial_\theta\partial_\phi - \cot\theta\partial_\phi) Y^m_\ell. \end{aligned} \tag{2.34}$$

As we just did for the metric with the other parity, we define the arbitrary functions with the radial and time coordinate dependence as $h_0(t,r)$, $h_1(t,r)$, $H_0(t,r)$, $H_1(t,r)$, $G(t,r)$ and $K(t,r)$. We may use this back into (2.20) to obtain the most general metric for the *polar*-parity decomposition

$$h^p_{\mu\nu} = \begin{pmatrix} H_0(t,r)Y^m_\ell & H_1(t,r)Y^m_\ell & h_0(t,r)\partial_\theta Y^m_\ell & h_0(t,r)\partial_\phi Y^m_\ell \\ sym & H_2(t,r)Y^m_\ell & h_1(t,r)\partial_\theta Y^m_\ell & h_1(t,r)\partial_\phi Y^m_\ell \\ sym & sym & [K(t,r) + G(t,r)\partial^2_\theta]Y^m_\ell & G(t,r)(\partial_\theta\partial_\phi - \cot\theta\partial_\phi)Y^m_\ell \\ sym & sym & sym & [K(t,r)\sin^2(\theta) + G(t,r)(\partial^2_\phi + \sin\theta\cos\theta\partial_\theta)]Y^m_\ell \end{pmatrix}. \tag{2.35}$$

To better simplify these rather cumbersome quantities, we use the gauge-freedom in GR, equation (2.29), with the *polar* decomposition to obtain

$$\begin{aligned} \xi_t &= M_0(t,r)Y^m_\ell, \quad \xi_\theta = M(t,r)\partial_\theta Y^m_\ell, \\ \xi_r &= M_1(t,r)Y^m_\ell, \quad \xi_\phi = M(t,r)\partial_\phi Y^m_\ell. \end{aligned} \tag{2.36}$$

Since now we have three different variables originating from the gauge-freedom equation, we can choose a suitable $M_0(t,r)$, $M_1(t,r)$ and $M(t,r)$ to cancel out $G(t,r)$, $h_0(t,r)$ and $h_1(t,r)$. Once again we choose a wave solution with frequency ω, setting the time dependence as $e^{-i\omega t}$ and we

may choose $m = 0$, without any loss of generality. With all these simplifications we are left with the *polar*-parity metric

$$h^p_{\mu\nu} = \begin{pmatrix} H_0(r) & H_1(r) & 0 & 0 \\ sym & H_2(r) & 0 & 0 \\ sym & sym & K(r) & 0 \\ sym & sym & sym & K(r)\sin^2(\theta) \end{pmatrix} e^{-i\omega t} P_\ell. \tag{2.37}$$

In Regge-Wheeler's paper, this is known as the "cannonical form of the *polar* waves" in the *Regge-Wheeler gauge*. With all these steps we were able to reduce the set of variables from seven to only four.

After obtaining both parities metrics, (2.32) and (2.37), we can use them back in the perturbed EFE, equation (2.16), after setting an appropriate perturbed SET. Each of these set of equations may be assembled to obtain a a Schroödinger-lie equation that rules the radial perturbation

$$\frac{d^2\psi(r)}{dr_*^2} + (\omega^2 - V(r))\psi(r) = 0, \tag{2.38}$$

where r_* is defined as the tortoise coordinate $\frac{dr}{dr_*} = f(r)$. This equation is known as the *master equation* and its effective potential, $V(r)$, depends on the characteristics of the given BH solution and on the type of the perturbation.

2.2.3. Perturbation types

Taking Schwarzschild BH as example, if we set the perturbed SET to be equal to zero we obtain the *gravitational perturbation*. Since the metric is a tensor, we could borrow the quantum-field theory terminology and interpret it as a perturbation of a spin-2 test-field.

It is also possible to check how the metric would behave due to different test-fields. To find the perturbation caused by an electromagnetic field, we must perform the perturbation of the electromagnetic quadri-potential as

$$A'_\mu(x^\lambda) = A_\mu(x^\lambda) + \delta A_\mu(x^\lambda), \tag{2.39}$$

which must also obey the sourceless Maxwell's equations

$$\nabla_\mu F^{\mu\nu} = 0, \quad \nabla_{[\alpha} F_{\mu\nu]} = 0, \tag{2.40}$$

where $F_{\mu\nu} = \partial_\mu A_\nu - \partial_\nu A_\mu$ is the Faraday tensor. Closely following the procedure of the previous section, we can expand the A_μ quadri-vector using the *axial* parity

$$\begin{aligned} \delta A_t = 0, \quad \delta A_\theta = -a_0(t,r)\frac{1}{\sin\theta}\partial_\phi Y^m_\ell, \\ \delta A_r = 0, \qquad \delta A_\phi = a_0(t,r)\sin\theta\partial_\theta Y^m_\ell. \end{aligned} \tag{2.41}$$

and the *polar* decomposition

$$\begin{aligned} \delta A_t = a_1(t,r)Y^m_\ell, \quad \delta A_\theta = a_2(t,r)\partial_\theta Y^m_\ell, \\ \delta A_r = a_3(t,r)Y^m_\ell, \quad \delta A_\phi = a_3(t,r)\partial_\phi Y^m_\ell. \end{aligned} \tag{2.42}$$

This perturbation will be of the *electromagnetic type* and this may also be recognized as the perturbation of a spin-1 test-field.

Similarly, we can inspect the perturbation of a spin-0 test-field, that is, a scalar field. This field must obey the Klein-Gordon equation given as[3]

$$\Box\phi(r) = 0, \tag{2.43}$$

in the given background curved space-time. This case is particularly interesting because for any (electro-) vacuum space-time described by equation (2.1), its effective potential is given by the following general formula

$$V^s(r) = f(r)\left[\frac{\ell(\ell+1)}{r^2} + \frac{f'(r)}{r}\right], \tag{2.44}$$

where the prime denotes a derivative in respect to the radial coordinate r.

One of the main results in BH perturbation theory, is that any spherically-symmetric metric[4], in the context of GR, for any perturbed test-field, is ruled by the same *master equation* (2.38). The intrinsic characteristics of the BH are embedded within the effective potential $V(r)$. Due to this, the study of perturbed BHs turns out to be a problem of analysing their respective effective potential.

2.3. Singular and Regular Black Holes

In this section we first analyse the singular BHs solutions, Schwarzschild, Reissner-Nordström and Schwarzschild de-Sitter, and then we move on to the regular ones, Bardeen and Hayward. For both cases we discuss the general traits of the solutions and show the effective potentials for various cases.

2.3.1. Singular Solutions

2.3.1.1. Schwarzschild

The simplest BH solution is described by the Schwarzschild space-time. The *lapse function* $f(r)$ is

$$f_{Sch}(r) = 1 - \frac{2M}{r}. \tag{2.45}$$

Schwarzschild's BH is a simple example of what usually is encountered in BHs solutions: there is a region where after an observer crosses it, any possible future-light cone will be pointed towards its centre and, therefore, nothing can return from it. This region is called *event horizon*, and for this case it is located at $r = 2M$. Within it, there is a point that is geodesic incomplete, at $r = 0$, meaning that no geodesic can cross through it. Due to this behavior, these points are called *singularities*, and they are an unavoidable structure of GR under some certain reasonable conditions of the manifold (it must be globally hyperbolic) and the correspondent SET (it must satisfy the weak-energy condition). These results are well enclosed on the singularity theorems developed by Hawking and Penrose [29].

Mathematically, there is no issue in setting a negative value for the mass, but physically it will not recover the Newtonian limit at spatial infinity, therefore it is more appropriate to refer to it as the *mass parameter*. Doing so, the radius of the event horizon becomes negative, nonexistent. With this we are stripping-off the event horizon, making the *singularity* in its centre apparent

[3] In this thesis we assume massless spin-zero particles.

[4] For Kerr(-Newman) solution, the method must be changed. The radial equation obtained is in the form of a Teukolsky equation, first introduced in [28].

for any observer. As a result, space-times like this are called *naked singularities* and due to their eccentric nature, Penrose postulated in the *cosmic censorship conjecture* that they should not physically exist [30].

For this solution, the effective potential ruling the radial perturbations may be enclosed in a single equation

$$V_{Sch}(r) = f_{Sch}\left[\frac{\ell(\ell+1)}{r^2} + 2\frac{\beta M}{r^3}\right]. \tag{2.46}$$

The parameter β is related to the spin of the field through $\beta = 1 - S^2$, also called the *field's spin weight* [20]. Thus, when we set $S = 0$ ($\beta = 1$), $S = 1$ ($\beta = 0$) and $S = 2$ ($\beta = -3$), we acquire the *scalar*, *electromagnetic* and the *axial gravitational* perturbation, respectively. The latter was the potential first obtained by Regge-Wheeler in reference [16] and is widely recognized as the *Regge-Wheeler potential*.

Lastly, the effective potential for the *polar gravitational* perturbations, known as *Zerilli potential* [17], is given as

$$V^{p}_{Sch}(r) = \frac{f_{Sch}}{r^3(\eta r + 3M)^2}[2\eta^2(\eta+1)r^3 + 6\eta^2 M r^2 + 18\eta M^2 r + 18M^3], \tag{2.47}$$

with $2\eta = (\ell-1)(\ell+2)$.

Chandrasekhar [31] has shown that the two potentials for the *gravitational* perturbations, described by equations (2.46) (setting $S = 2$), and (2.47), are related by

$$V^{a}_{Sch}(r) = \pm\alpha\frac{dW}{dr_*} + \alpha^2 W^2 + \kappa W, \tag{2.48}$$

with

$$W = f_{Sch}\frac{1}{2r^3(\ell r + 3M)}, \quad \alpha = 6M, \quad \kappa = 4\eta(\eta+1). \tag{2.49}$$

This relationship between the potentials is called the *super-partner potentials*, which is a typical term in the context of supersymmetric theories [32]. Such feature arises from the fact that these potentials possess the same amplitudes for both the transmitted and reflected waves [33]. This property is known as the *isospectral relation*, since they have the same quasi-normal spectrum and this structure imply a relation between the wave-functions ψ^a and ψ^p of the type

$$\psi^{a}_{p} = \frac{1}{\alpha - \omega^2}\left(\mp W + \frac{d}{dr_*}\right)\psi^{p}_{a}, \tag{2.50}$$

hence, after obtaining the wave-function for one potential, the other can be easily derived [20].

2.3.1.2. Reissner-Nordström

The line element describing a charged BH with charge Q is known as the Reissner-Nordström space-time. The event horizons are situated at $r_\pm = M \pm \sqrt{M^2 - Q^2}$, and thus three different cases are possible: i) $M > Q$ gives a BH where the outer horizon is an event horizon and the inner one a Cauchy horizon; ii) $M = Q$ has both horizons coinciding and is called the *extremal solution*; iii) $Q > M$ admits no horizons and a charged *naked singularity* space-time is described. The line element for this space-time is described by

$$f_{RN}(r) = 1 - \frac{2M}{r} + \frac{Q^2}{r^2}. \tag{2.51}$$

The *polar gravitational* effective potential is given by

$$V^{p}_{j(RN)} = \frac{f_{RN}}{r^3}\left[\ell(\ell+1)r - q_i + \frac{4Q^2}{r}\right], \qquad i,j = 1,2 \text{ for } i \neq j, \tag{2.52}$$

with the following definitions

$$\begin{aligned} q_1 &= 3M + \sqrt{9M^2 + 4(\ell-1)(\ell+1)Q^2}, \\ q_2 &= 3M - \sqrt{9M^2 + 4(\ell-1)(\ell+1)Q^2}. \end{aligned} \tag{2.53}$$

The correspondent *axial* perturbation effective potential is

$$V^{a}_{j(RN)} = \frac{f_{RN}}{r^3}\left[U \pm \frac{1}{2}(q_1 - q_2)J\right], \tag{2.54}$$

with

$$\begin{aligned} \bar{\omega} &= \eta r + 3M - 2\frac{Q^2}{r}, \\ J &= f_{RN}\frac{r}{\bar{\omega}}^2(2\eta r + 3M) + \frac{\eta r + M}{\bar{\omega}}, \\ U &= (2\eta r + 3M)J + (\bar{\omega} - \eta r - M) - \frac{2\eta r^2}{\bar{\omega}} f_{RN}. \end{aligned} \tag{2.55}$$

As for the Schwarzschild solution, both *gravitational* effective potentials are correlated via

$$V^{p}_{j} = V^{a}_{j} + 2q_i\frac{d}{dr_*}\left[\frac{f_{RN}}{r[(\ell-1)(\ell+2)r + q_i]}\right]. \tag{2.56}$$

Using relation (2.44), the effective potential for a *scalar perturbation* is given by

$$V^{s}_{RN}(r) = f_{RN}\left[\frac{\ell(\ell+1)}{r^2} + 2\frac{M}{r^2} - 2\frac{Q^2}{r^3}\right]. \tag{2.57}$$

We see that if we choose $Q = 0$, we re-obtain the *scalar perturbation* for the Schwarzschild effective potential, defined in (2.46) for $S = 0$ (i.e. $\beta = 1$).

From equations (2.52) and (2.54), it is clear that differently from the uncharged solution, each perturbation type has two different potentials instead of a single one. This stems from the fact that the perturbation of Einstein's and Maxwell's equations cannot be fully disentangled. Due to this there is no purely electromagnetic, nor gravitational, modes of oscillation; there will be an emission of both electromagnetic and gravitational radiation for all kinds of perturbation [34].

Realistic BHs must either contain no charge at all, or a small value when compared to its mass, satisfying the condition $Q \ll M$. In this case we may ignore the coupling of the electromagnetic field and the metric to obtain a distinct potential for the *gravitational* and the *electromagnetic* effective potentials. This procedure is known as *freezing Reissner-Nordström* and more details may be found in reference [35].

2.3.1.3. Schwarzschild de-Sitter

BHs may also be investigated when immersed within a contracting/expanding universe with a cosmological constant Λ. This solution may have either a positive or negative value for Λ

[36]. Despite it being Kotler's discovery, the solution is more commonly known as *Schwarzschild de-Sitter* (positive Λ) or *anti de-Sitter* (negative Λ). This space-time is described by

$$f_{SdS}(r) = 1 - \frac{2M}{r} - \frac{\Lambda}{3}r^2. \tag{2.58}$$

The presence of a mass parameter is associated with the existence of *event horizons*. Therefore, we expect to have at least one horizon for positive mass, while its absence implies a case of naked singularity. On the other hand, the parameter Λ is associated with the cosmological expansion, or contraction, of the universe, which is intrinsically associated with a *cosmological horizon*.

For the Schwarzschild anti-de Sitter case (negative Λ), if the mass parameter is positive, only one horizon solution is possible, which is an event horizon. This space-time describes an observer outside of a BH in an contracting universe, a crucial element for the AdS/CFT[5] correspondence [37]. However, if the mass parameter is negative we are left with a horizonless case, describing a *naked singularity* space-time.

A much richer set of solutions is possible for the Schwarzschild de Sitter (positive Λ) case. The horizons may be localized via the following relations [38]

$$\begin{aligned} r_1 &= \frac{2}{\sqrt{\Lambda}}\sin(\psi), \\ r_2 &= \sqrt{\frac{3}{\Lambda}}\cos(\psi) - \frac{1}{\sqrt{\Lambda}}\sin(\psi), \\ r_3 &= -\sqrt{\frac{3}{\Lambda}}\cos(\psi) - \frac{1}{\sqrt{\Lambda}}\sin(\psi), \end{aligned} \tag{2.59}$$

with

$$\sin(3\psi) = 3\sqrt{\Lambda}M. \tag{2.60}$$

For a negative mass parameter only a cosmological horizon is present, then the observer would be found between the naked singularity and the expanding cosmological horizon. However, if the mass parameter is positive, three different possibilities are available: i) in the range $0 < 9\Lambda M^2 < 1$ an observer is bounded between the cosmological and event horizons, that is, they are in the region between a BH and an expanding universe; ii) when $9\Lambda M^2 = 1$, both horizons coincide and an *extremal* BH is created, this equality is also known as the *Nairiai limit* [39]; iii) lastly, if $9\Lambda M^2 > 1$, no horizons are formed, and this can be interpreted as if the event horizon has grown larger than the cosmological one, making it effectively disappear and its singularity is not screened [38]. We summarize the horizons structure in table 2.1.

	0 horizon	**1 horizon**	**2 horizons**
$M > 0$ **and** $\Lambda > 0$	$9\Lambda M^2 > 1$	$1 = 9\Lambda M^2$	$0 < 9\Lambda M^2 < 1$
$M > 0$ **and** $\Lambda < 0$	Never	Always	Never
$M < 0$ **and** $\Lambda > 0$	Never	Always	Never
$M < 0$ **and** $\Lambda < 0$	Always	Never	Never

Table 2.1.: The different number of horizons are displayed for different values of the cosmological constant, Λ, and mass, M, for the Schwarzschild (anti) de-Sitter solution.

Perturbation theory was first applied to the Schwarzschild de-Sitter solution by Guven and Núñez [40], but we refer the reader to [41], where the whole set of effective potentials is summa-

[5] Anti de Sitter/Conformal Field Theory.

rized. For this case, the effective potential of the *axial gravitational* perturbation is

$$V^{a}_{SdS}(r) = f_{SdS}\left[\frac{\ell(\ell+1)}{r^2} + 2\frac{\beta M}{r^3}\right], \qquad S = 1, 2 \tag{2.61}$$

where, once again, $\beta = 1 - S^2$, but opposed to Schwarzschild case, this potential is only valid for spins-1 and 2. The *gravitational* perturbation of the *polar* type is then

$$V^{p}_{SdS}(r) = \frac{f_{SdS}}{r^3(\eta r + 3M)^2}[2\eta^2(\eta+1)r^3 + 6\eta^2 M r^2 + 3M^2(3\eta r - \Lambda r^3) + 18M^3], \tag{2.62}$$

followed by the definition $\eta = \frac{\ell(\ell+1)}{2} - 1$. The same structure encountered in Schwarzschild relating both potentials, i.e. equations (2.48) and (2.50), also holds true for Schwarzschild de-Sitter. The adjusted definitions of the function W and the constant β can be found in reference [41].

The perturbation for a test scalar-field, $S = 0$, may be obtained using formula (2.44) and is given by

$$V^{s}_{SdS}(r) = f_{SdS}\left[\frac{\ell(\ell+1)}{r^2} + 2\frac{M}{r^3} - \frac{2}{3}\Lambda\right]. \tag{2.63}$$

It is clear from the previous equations that when setting $\Lambda = 0$ the results for Schwarzschild are re-obtained.

2.3.2. Regular Black Holes

Different from the solutions presented in section 2.3.1, singular BHs curvature scalar does not diverge at its center. To avoid these singularities, these BHs are sourced by exotic matter, usually in the form of a particular case of non-linear electrodynamics. In this section we discuss two regular solutions, with their main properties and effective potentials.

2.3.2.1. Bardeen

The first non-singular BH solution was proposed by Bardeen [42]. Its metric is given by

$$f_B(r) = 1 - \frac{2Mr^2}{(r^2+q^2)^{3/2}}. \tag{2.64}$$

It is clear by direct inspection of the line element that as $r \to 0$ the metric becomes regular at the centre. The same occurs to its curvature scalars

$$\begin{aligned} \lim_{r\to 0} R &= -\frac{24M}{q^3}, \\ \lim_{r\to 0} R_{\mu\nu}R^{\mu\nu} &= \frac{144M^2}{q^6}, \\ \lim_{r\to 0} R_{\alpha\mu\beta\nu}R^{\alpha\mu\beta\nu} &= \frac{96M^2}{q^6}. \end{aligned} \tag{2.65}$$

An observer at infinity would not be able to distinguish Bardeen's solution from a Schwarzschild BH since

$$f_B \approx 1 - \frac{2M}{r} + \mathcal{O}\left(\frac{1}{r}\right)^3, \quad r \to \infty. \tag{2.66}$$

However, it is already clear that the charge q does not have the same interpretation as in Reissner-Nordström BH because

$$f_B(r) \approx 1 - \frac{2Mr^2}{q^3} + \mathcal{O}(r)^4, \quad r \to 0, \tag{2.67}$$

that is, it does not decrease with $1/r^2$ as Reissner-Nordström BH, it shows a de-Sitter behavior instead.

The parameter q was first interpreted as the charge of a monopole magnetic field. This is described by a nonlinear electrodynamics generated by the following lagrangian-density [43]

$$\mathcal{L}_B(F) = \frac{3M}{q^3}\left(\frac{\sqrt{2q^2F}}{1+\sqrt{2q^2F}}\right)^{5/2}. \tag{2.68}$$

Sometime later, Bronnikov [44] discovered that a spherically-symmetric spacetime, sourced by a magnetic monopole, may be recast in a purely electric counterpart. This relationship between the two fields is known as the *FP duality*, and Bardeen's BH may be re-interpreted as a solution in the presence of a purely electric source. Even so, despite the fact that the lagrangian-density cannot be written in a closed and analytic form, it was shown that at infinity the field decays with $1/r^3$, that is, it behaves as a non-coulombian electric field [45].

A different way to formulate this regular BH with no need to add magnetic monopoles, is to interpret the parameter q as a scale defining the mass distribution. Setting the density of the BH as

$$\rho(r) = \frac{3Mq^2}{4\pi(r^2+q^2)^5/2}, \tag{2.69}$$

this solution is obtained with neither the necessity of exotic matter, nor through any modification of Einstein equations [46].

As usual in BHs solutions, Bardeen space-time structure depends on the parameters of the metric, in this case both the charge q and the mass M. The zeroes of the function $f_B(r)$ determines the amount and/or the existence of horizons of this solution. If the condition $M > \frac{3\sqrt{3}}{4}q$ is satisfied, this is a BH hole solution with two horizons: an outer event horizon and an inner Cauchy horizon. When $M = \frac{3\sqrt{3}}{4}q$ we have an extremal solution, where the two horizons coincide. When none of these conditions are satisfied, no horizons appear and we are left with a spacetime with no singularity.

Although this regular solution was proposed back in 1968, it was not until recently that the first effective potential, in this case for a massless scalar-field, was evaluated [47]. Using equation (2.44), the correspondent effective potential for a scalar perturbation is

$$V^s(r) = f_B\left[\frac{\ell(\ell+1)}{r^2} + 2M\frac{(r^2-2q^2)}{(r^2+q^2)^{5/2}}\right]. \tag{2.70}$$

The correspondent axial-gravitational perturbation effective potential is given by [48]

$$V^a(r) = f\left[\frac{\ell(\ell+1)+2(f-1)}{r^2} + \frac{f'}{r} + f'' + 2k\mathcal{L}\right], \tag{2.71}$$

where this closed form works out for both regular solutions, Bardeen and Hayward. Using equations, (2.64) and (2.68), back into equation (2.71) we obtain

$$V_B^a(r) = f_B\left[\frac{\ell(\ell+1)}{r^2} - 6M\frac{(q^4-3q^2r^2+r^4)}{(r^2+q^2)^{7/2}}\right]. \tag{2.72}$$

Gravitational and electromagnetic perturbations were also obtained for a Bardeen BH embedded in an universe with a cosmological constant Λ. Much similar to the Schwarzschild (anti) de-Sitter solution, such solution was coined as Bardeen de-Sitter BH and its structure can be found in reference [49], but are out of scope for this work.

2.3.2.2. Hayward

Despite not being the first regular solution proposed, Hayward obtained the simplest regular BH, which is a variation of Bardeen's [50], but with a different motivation behind it. BH evaporation happen when ingoing radiation with negative energy flux draws energy from the BH itself. For static black holes this energy is absorbed in form of mass, and since its event horizon radius is directly proportional to its mass, the BH shrinks until, eventually, it disappears completely. To take this into account, the dynamic region of Hayward's spacetime behaves as a Vaidya-like solution with either ingoing or outgoing radiation [51]. With this, the Hayward lapse-function that satisfies the previous conditions is

$$f_H(r) = 1 - \frac{2Mr^2}{r^3 + 2Ml^2}, \tag{2.73}$$

where l^2 is a convenient encoding of the central energy density, assumed to be positive. This space-time is particularly attractive because an observer at infinity would not be able to distinguish it from a Schwarzschild BH since

$$f_H(r) \approx 1 - \frac{2M}{r} + \mathcal{O}\left(\frac{1}{r}\right)^4, \quad r \to \infty, \tag{2.74}$$

while near the center it becomes de-Sitter space-time as given by

$$f_H(r) \approx 1 - \frac{r^2}{l^2} + \mathcal{O}(r)^4, \quad r \to 0. \tag{2.75}$$

Analyzing its curvatures scalars as $r \to 0$, it becomes apparent that this spacetime is both regular at its centre and that it manifests constant curvature, as the de Sitter spacetime requires

$$\begin{aligned} \lim_{r\to 0} R &= -\frac{12}{l^2}, \\ \lim_{r\to 0} R_{\mu\nu}R^{\mu\nu} &= \frac{36}{l^4}, \\ \lim_{r\to 0} R_{\alpha\mu\beta\nu}R^{\alpha\mu\beta\nu} &= \frac{24}{l^4}. \end{aligned} \tag{2.76}$$

The lagrangian density that sources this BH may be written in terms of the magnetic charge g as

$$\mathcal{L}_H(F) = \frac{12M}{g^3}\frac{(2g^2F)^{3/2}}{(1 + (2g^2F)^{3/4})^2}. \tag{2.77}$$

The constant g relates to l via $g^3 = 2Ml^2$ [52]. Similar to Bardeen BH, the Hayward metric may be reinterpreted through the energy distribution

$$\rho(r) = \frac{3M^2g^2}{2\pi(r^3 + 2Mg^2)^2}, \tag{2.78}$$

where g is interpreted as a scale parameter [46].

Likewise for the other solutions, Hayward solution represents different spacetimes according to the specific range of parameters. For $\frac{3\sqrt{3}}{4}l < M$, we have a BH solution with two horizons; for $\frac{3\sqrt{3}}{4}l = M$ it represents a single horizon, extremal, BH; and a horizonless case if otherwise, characterizing a regular de Sitter spacetime, represented by the constant curvature in (2.76).

The effective potential for a scalar perturbation, through equation (2.44) is

$$V_H^s(r) = f_H\left[\frac{\ell(\ell+1)}{r^2} + 2M\frac{(r^3-4Ml^2)}{(r^3+2Ml^2)^2}\right], \tag{2.79}$$

and the respective axial gravitational perturbation is given by equation (2.71), yielding

$$V_H^a(r) = f_H\Big[\frac{\ell(\ell+1)}{r^2} + \frac{6M}{r^2(r^3+2M\ell^2)^3}(32\ell^6M^3 + 24\ell^4M^2r^3 + 14\ell^2Mr^6 - r^9)\Big]. \tag{2.80}$$

2.4. Pöschl–Teller Potential

As we have discussed in the previous section, the quasi-normal frequencies usually cannot be retrieved analytically due to the rather complicated potentials involved. But with a simplification of the effective potential, the frequencies can be obtained analytically.

In 1933, Pöschl and Teller jointly proposed a potential to obtain the energy eigenvalues of a quantum-mechanical problem [53]. The general potential is given by

$$V_{PT}(x) = -\frac{\mu(\mu+1)}{2}\operatorname{sech}^2(x) - \frac{\mu(\mu+1)}{2}\operatorname{csch}^2(x). \tag{2.81}$$

Besides the analytical eigenvalues property, it allows to compute the scattering data exactly as well, which may be shown to be reflectionless [54]. The reader may check reference [55] for a introductory view about this particular potential.

The precursors to apply this potential in the context of BHs were Ferrari and Mashoon in the early 80s [56]. Instead of using the whole relation stated in equation (2.81), they have used the effective potential as

$$V(r_*) = \frac{V_0}{\cosh^2[\alpha(r_* - r_{*0})]}, \tag{2.82}$$

where r_* is the usual tortoise coordinate, r_{*0} corresponds to the maximum of the potential and the constants V_0 and α are defined as

$$V_0 = V(r_{*0}), \text{ and } \alpha^2 = -\frac{1}{2V_0}\frac{d^2V}{dr_*^2}\bigg|_{r_{*0}}. \tag{2.83}$$

In figure 2.1, we show how the Schwarzschild potential, equation (2.46) for $S = 2$, and the approximate potential, equation (2.82), relates to each other.

With this, the exact frequencies are given by

$$\omega = i\alpha(n+1/2) \pm \alpha\sqrt{\frac{1}{4} - \frac{V_0}{\alpha^2}}, \quad n \in \mathbb{N}. \tag{2.84}$$

Since this is an approximation, it is not expected to fully replicate the results. Nonetheless, the frequencies obtained by this method are a good approximation within the eikonal limit, that is, in the regime of high multipole number ℓ. In addition, the analytical quasi-normal frequencies has

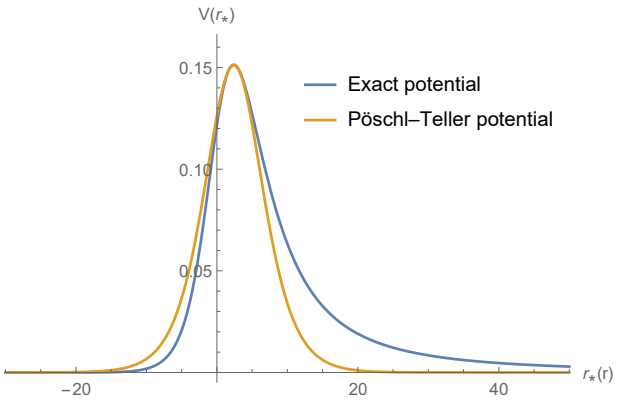

Figure 2.1.: The *axial* gravitational Schwarschild potential, curve in blue, and the Pöschl-Teller potential, curve in orange. We set $M = 1$ and $\ell = 2$.

been obtained using the generalized potential (2.81). As expected, the result is a generalization of the equation (2.84) [57].

Mashhoon's method is a good approximation for Schwarzschild, Reissner-Nordström and Kerr (after some modification) BHs. Surprisingly, it is an exact solution for the first two cases when embedded in a cosmological constant Λ, namely Schwarzschild de-Sitter and Reissner-Nordström de Sitter BHs in the near extremal cases [58]. The same method was further generalized by Molina [59] to d dimensional solutions of these cases.

2.5. The WKB method

The WKB method (named after the physicists Gregor Wentzel, Hendrik Kramers and Léon Brillouin) is an approximate method to solve linear differential equations. The most important and recognizable usage of this method is to solve the time-independent Schrödinger equation [60]

$$\frac{\hbar^2}{2M}\frac{d^2\Psi(x)}{dx^2} + (E - V(x))\Psi(x) = 0. \tag{2.85}$$

Due to the resemblance of equation (2.85) with the master equation (2.38), the idea to employ the same method for BH perturbation theory is evident.

Formally, the WKB method consists of an approximation in a single exponential power series of the type

$$\psi(r) \approx \exp\left[\frac{1}{\epsilon}\sum_{n=0}^{\infty}\epsilon^n S_n(r)\right], \qquad \epsilon \to 0, \tag{2.86}$$

in this case, the differential equation to be analysed has the following general form

$$\frac{d^2\psi(r)}{dr^2} = Q(r)\psi(r), \qquad Q(r) \neq 0. \tag{2.87}$$

The main difference between a quantum mechanical problem, in which you may have different numbers of returning points for the effective potential[6], is that in the BH perturbation theory the function $Q(r)$ contains two turning points, necessarily. For this reason, the matching procedure must be altered, as was developed in reference [61].

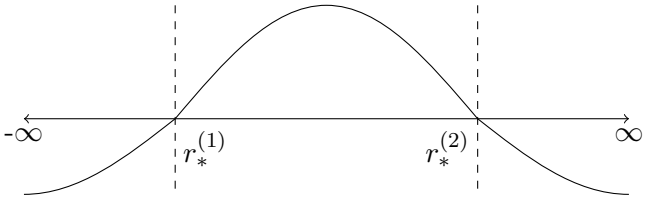

Figure 2.2.: A sketch of a general potential $V(r)$ with two turning points, $r_*^{(1)}$ and $r_*^{(2)}$.

The main peculiarity in a quasi-normal mode problem is that specific boundary conditions must be set. Since waves cannot emerge from the Minkowskian spatial infinity, a purely outgoing waves boundary condition must be chosen

$$\psi(r) = Z_{out}\psi(r)_{out}, \qquad r_* \to \infty, \tag{2.88}$$

while at the event horizon, since waves cannot arise from within the BH, only incoming waves are permitted, then

$$\psi(r) = Z_{in}\psi(r)_{in}, \qquad r_* \to -\infty. \tag{2.89}$$

With these boundary conditions it is clear that the BH itself is losing energy in the form of gravitational waves. This happens either by waves going into the event horizon or by dissipating themselves into the spatial infinity. Using these appropriate boundary conditions, the WKB matching condition throughout the three regions leads to

$$\frac{Q_0}{\sqrt{2Q_0''}} = i(n+1/2), \qquad n \in \mathbb{N}, \tag{2.90}$$

where the subscript 0 represents the function $Q(r)$ evaluated at its maximum and will be omitted from now on in order to simplify the notation.

The factor n is known as the *overtone number*, which is a discrete quantity. To have a better intuition of this quantity, in acoustic physics we can denote the fundamental vibration frequency of any standing wave as f. Integer multiples of this fundamental frequency, $2f$, $3f$, $4f$, are called the first, second and third *overtone*, respectively. Therefore, for $n = 0$ we have the fundamental frequency (first harmonic), then for $n = 1$ the first *overtone* (second harmonic) and so on[7].

Until this point, the method is fully general for any differential equation that obeys equation (2.87), for any given two turning point function $Q(r)$, with $Q''(r) \neq 0$, where the latter implies that a maximum must exist.

For BHs physics, the method was first used by Mashhoon [63], where he indentified $Q(r) = V(r) - \omega^2$, and found the real and imaginary frequencies of the oscillations to be described as

$$\omega^2 = V - i(n+1/2)\sqrt{-2V^{(2)}}, \tag{2.91}$$

with the derivatives of the potentials given by

$$V^{(m)} = \frac{d^m V}{dr_*^m} = f(r)\frac{d}{dr}V^{m-1}, \tag{2.92}$$

which must be evaluated at the potential's maximum.

[6] Usually a single one

[7] In general, the *overtone* is any frequency above the fundamental one, then it may not match exactly the correspondent harmonic. This relationship is dependable on the shape of the instrument. The simplest example of this is a string with one free end and the other one fixed where only the odd harmonics exists [62].

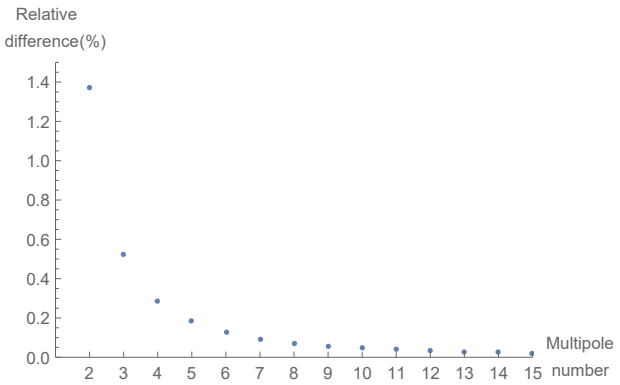

Figure 2.3.: In this plot we evaluate the real part of $(\omega_{PT} - \omega_{WKB})/\omega_{WKB}$ in percentage. That is, the percentile difference between both methods as the multipole number increases. For $\ell = 2$ the difference is of 1.37% and it quickly decreases as the multipole number increases. For $\ell = 4$ the difference is already less than 0.3%, showing that both methods agree for the eikonal limit.

The easiness of the WKB method is well stated in equation (2.91): instead of solving a rather difficult differential equation numerically, the frequencies are obtained by solving a much simpler algebraic one. Furthermore, it can easily be expanded to further orders of approximation by directly adding more terms to the condition above. This method has been first expanded to the third-order by Iyer and Will in reference [64]. Subsequently, a succession of papers arose studying every classical BH solution: Schwarzschild [65], Reissner-Nordström [34] and Kerr [66]. Thereafter, it has been even further developed to the sixth-order for an $N-$dimensional Schwarzschild BH [67].

In the third-order approximation, the condition given in equation (2.91) changes in the following manner

$$\omega^2 = [V + \sqrt{(-2V^{(2)})}\Gamma] - i\sqrt{\alpha(-2V^{(2)})}(1+\Omega), \tag{2.93}$$

whereas the cumbersome quantities Γ and Ω are

$$\Gamma = \frac{1}{\sqrt{-2V^{(2)}}}\left[\frac{1}{8}\left(\frac{V^{(4)}}{V^{(2)}}\right)\left(\frac{1}{4}+\alpha\right) - \frac{1}{288}\left(\frac{V^{(3)}}{V^{(2)}}\right)^2(7+60\alpha)\right], \tag{2.94}$$

$$\begin{aligned}\Omega = -\frac{1}{2V^{(2)}}\Bigg[\frac{5}{6912}\left(\frac{V^{(3)}}{V^{(2)}}\right)^4(77+188\alpha) - \frac{1}{384}\frac{(V^{(3)})^2V^{(4)}}{(V^{(2)})^3}(51+100\alpha) + \\ \frac{1}{2304}\left(\frac{V^{(4)}}{V^{(2)}}\right)^2(67+68\alpha) + \frac{1}{288}\left(\frac{V^{(3)}V^{(5)}}{(V^{(2)})^2}\right)(19+28\alpha) - \frac{1}{288}\left(\frac{V^{(6)}}{V^{(2)}}\right)(5+4\alpha)\Bigg],\end{aligned} \tag{2.95}$$

with $\alpha = (n+1/2)^2$.

In section 2.6, we chose to carry out our analysis using the third-order expansion instead of the sixth-order. The reasoning behind this is that apart from the computational constraints induced by the sixth-order method, this may also obscure the semi-analytical discussion that we implement. Thus, we limit ourselves to the third-order expansion, which is enough for our porpuse.

2.5.1. Stability condition

Throughout the whole mathematical development, we assumed the wave function $\Psi(t, r, \theta, \phi)$, to have a time functional form of the type

$$\Psi(t, r, \theta, \phi) \approx e^{i\omega t}, \tag{2.96}$$

which describes an oscillation in time. However, when analysing equation (2.93), we see that the general frequency also has an imaginary component

$$\Psi(t, r, \theta, \phi) \approx e^{(i\omega_r + \omega_i)t}. \tag{2.97}$$

We stress that the real and imaginary part of ω has been decomposed using a different sign convention $\omega = \omega_r - i\omega_i$.

The real part of the frequency represents the real oscillation of the BH, which is positive definite. Conversely, the imaginary part of the frequency may be either positive or negative. If $\omega_i > 0$, the exponential term diverges as time evolves, and it follows that the oscillation of the BH will always grow, thus describing an *unstable solution*. On the other hand, for $\omega_i < 0$, we have a damped oscillation, since the whole exponential term decreases to zero as the time coordinate infinitely increases and, therefore, the BH ceases its oscillation; this describes a *stable solution*. Finally, $\omega_i = 0$ describes a normal mode, with a BH infinitely vibrating. We must stress that this method does not conceal any formal proof of any stability or instability. Due to the approximative nature of the WKB method, it is, at most, an indication of the general behavior of the solution.

Hence, we can define a quasi-normal mode as a general oscillation which possess an exponential damping factor. Note that this is only true when $\omega_i < 0$.

2.6. Discussion

In this section, we discuss the results we obtained using the WKB method up to the third-order of the first few *overtone* numbers, n, and multipole values, ℓ. We find that most of the plots follow the same general behaviour and, as such, we only present a fraction of them. We believe that the plots displayed summarize well the main results that we obtained.

We use the following convention in all plots to follow: the graphs on the left side are plotted for $n = 0$ and $\ell = [2, 3, 4]$, while the ones on the right side are for $n = [0, 1, 2]$ and $\ell = 2$. The continuous lines represent the real frequencies and the dashed ones are the respective **negative** imaginary frequencies. When not explicitly stated in the figures, we adopted the following values for the constants: $M = 1$, $Q = 0.5$, $\Lambda = 10^{-1}$, $q = 0.5$ and $l = 0.5$.

2.6.1. Schwarzschild

The plots in figure 2.4 are the results that we obtained for the perturbation of the Schwarzschild solution, using the formalism explained in subsection 2.3.1.1. We can see that for a fixed *overtone* number, the imaginary frequencies remain almost unchanged. On the other hand, as it increases and ℓ remains fixed, both real and imaginary frequencies are altered. As the value of n grows the frequency decreases, as does the damping factor. It is also clear that, as the mass of the BH increases, its vibration is reduced and the damping effect becomes less pronounced.

We conclude that the stability condition as defined in 2.5.1 is satisfied and, therefore, the BH is stable.

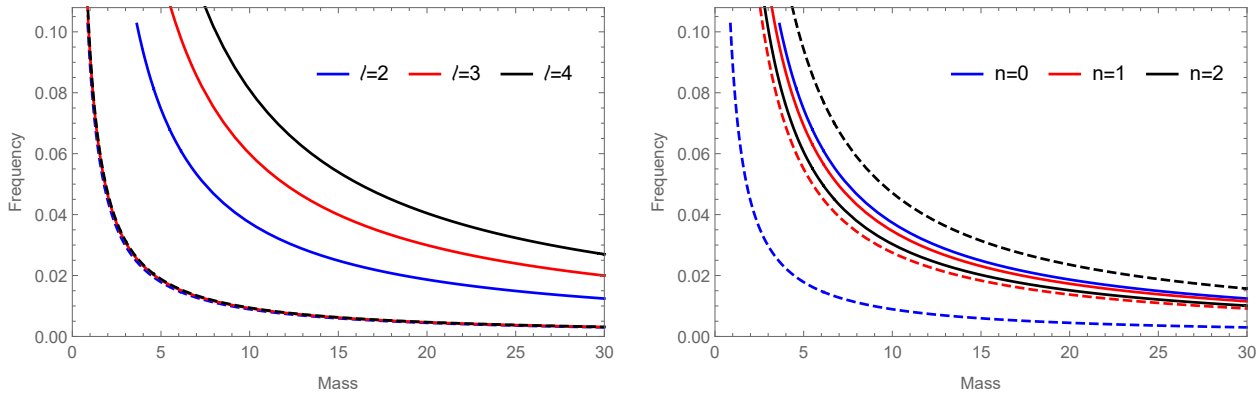

Figure 2.4.: We show the *axial* gravitational perturbation in Schwarzschild space-time for a varying mass. The continuous lines represent the real frequencies and the dashed ones are the respective imaginary frequencies. The plot on the left maintains $n = 0$ constant while ℓ varies through 2 to 4. We see that as ℓ increases the real frequencies also grow, however the imaginary frequencies seem insensible to such changes. The plot on the right maintains $\ell = 2$ constant while n varies through 0 to 2. We can identify that the real frequencies decrease as n increases, while the opposite occurs to the imaginary frequencies. As the mass increases, it damps the oscillation frequency while this effect becomes less evident.

2.6.2. Reissner-Nordström

In what follows, we discuss how the frequencies behaves for the Reissner-Nordström BH, as displayed in figures 2.5 and 2.6.

In figure 2.5, we display an *axial gravitational/electromagnetic* perturbation for the V_1 potential, as defined in equation (2.52), for a fixed charge $Q = 1$ and for a variable mass parameter. Note that the plot starts at $M = 1$, where the condition for existence of a BH is satisfied. Although the value of the frequencies are strictly different from Schwarzschild's, the mass damps the frequencies as well and the same analysis described in the previous subsection applies. We can also see that in the plot on the right side, where the parameter ℓ is kept constant, the real frequencies slightly decreases with the increase of the overtone number.

In figure 2.6, we have an *axial gravitational/electromagnetic* perturbation of the potential V_1, as defined in equation (2.52). We allow the charge to vary until its extremal value, $Q = 1$, for a fixed mass. We were able to check that the imaginary frequencies are weakly dependent on the BH charge, as was first identified in reference [68]. Lastly, we see that the real frequencies of the BH increase as the charges grows, that is, its charge does not act as a damping factor, as the mass does, but as a driving parameter.

As we have established for the Schwarzschild solution, the imaginary frequencies seem to be sensible only to the variation of n. This characteristic may be observed while keeping either the mass or the charge fixed, as displayed in both graphs set.

Briefly, the Reissner-Nordström solution is a stable BH in which the mass damps its vibration. On the other hand, its charge slowly increases its vibration, while keeping the imaginary frequencies unaffected.

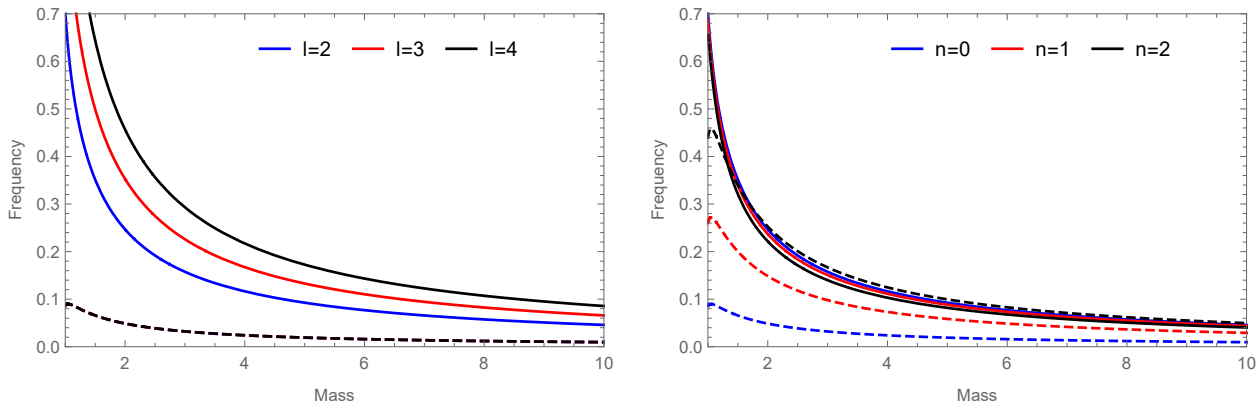

Figure 2.5.: *Axial gravitational/electromagnetic* perturbation of potential V_1 in Reissner-Norström BH for a fixed mass $M = 1$. The continuous lines represent the real frequencies and the dashed ones are the respective imaginary frequencies. The plot on the left maintains $n = 0$ constant while ℓ varies through 2 to 4. We see that as ℓ increases the real frequencies also grow, however the imaginary frequencies seems insensible to such change, exactly as in the Schwarzschild case. The plot on the right maintains $\ell = 2$ constant while n varies through 0 to 2. We can identify that the real frequencies lower their value as n increases, while the opposite occurs to the imaginary frequencies. We see that the mass behave similar to the Schwarzschild BH.

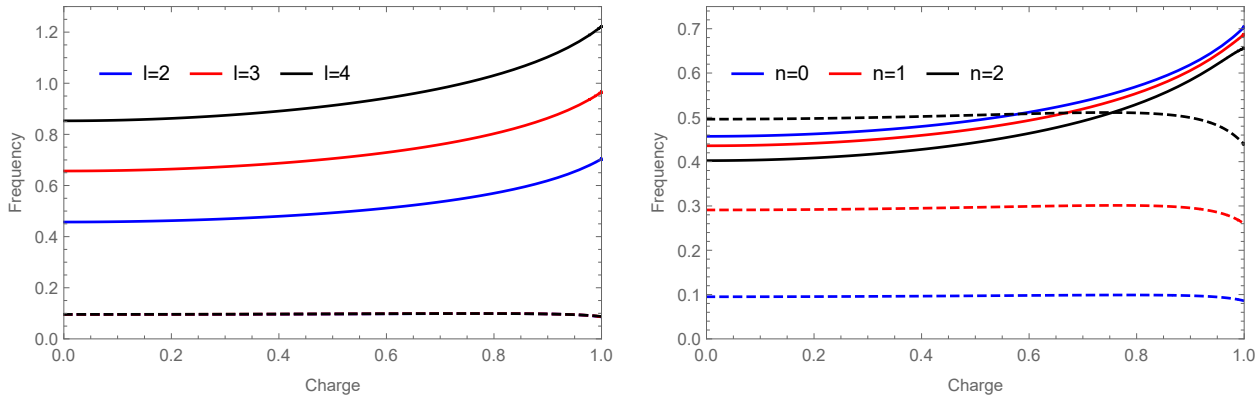

Figure 2.6.: *Axial gravitational/electromagnetic* perturbation of potential V_1 in Reissner-Norström BH for a fixed mass $M = 1$. The continuous lines represent the real frequencies and the dashed ones are the respective imaginary frequencies. The plot on the left maintains $n = 0$ constant while ℓ varies through 2 to 4. We see that as ℓ increases the real frequencies also grow, however the imaginary frequencies seems insensible to such change, exactly as in the Schwarzschild case. The plot on the right maintains $\ell = 2$ constant while n varies through 0 to 2. We can identify that the real frequencies lower their value as n increases, while the opposite occurs to the imaginary frequencies. In both plots it is clear that the frequencies are barely sensitive to the charge variation, while the charge increases the real vibration of the BH.

2.6.3. Schwarzschild de-Sitter

Now we discuss the frequencies of the Schwarzschild de-Sitter BH in figures 2.7, for fixed mass, and 2.8, for fixed Λ.

In figure 2.7 we show the perturbation keeping the cosmological constant Λ constant while varying the mass from $M = 0$ to $M = \frac{\sqrt{10}}{3} \approx 1.05$, within the BH parameter range. We see that the general behavior of the frequencies closely follow Schwarzschild's. However, as we approach the Nairiai limit, both the real and imaginary frequencies rapidly reaches zero. This is compatible with a well-known result that extremal BHs do not emit quasi-normal modes waves.

A different behavior occurs when the mass of the BH is fixed, while Λ varies from $\Lambda = 0$ to $\Lambda = 1/9$, as figure 2.8 shows. For $\Lambda = 0$ the frequencies match the value of Schwarzschild BH, as expected. However, the frequencies possess a general decreasing linear behavior, until reaching next to its extremal value where the frequencies abruptly goes to zero, as it is expected for an extremal BH. Similar to the Reissner-Nordström BH, the plot on the left side shows that the imaginary frequencies are insensible to the variation of the value of the cosmological constant for a fixed multipole-parameter, however the plot on the right side shows that this is not true through the variation of n.

Both the ℓ and n behaves similarly, in both cases. We can also conclude that both parameters of the BH, Λ and M act as a damping parameter, forcing the real frequencies to decrease as it reaches the extremal limit.

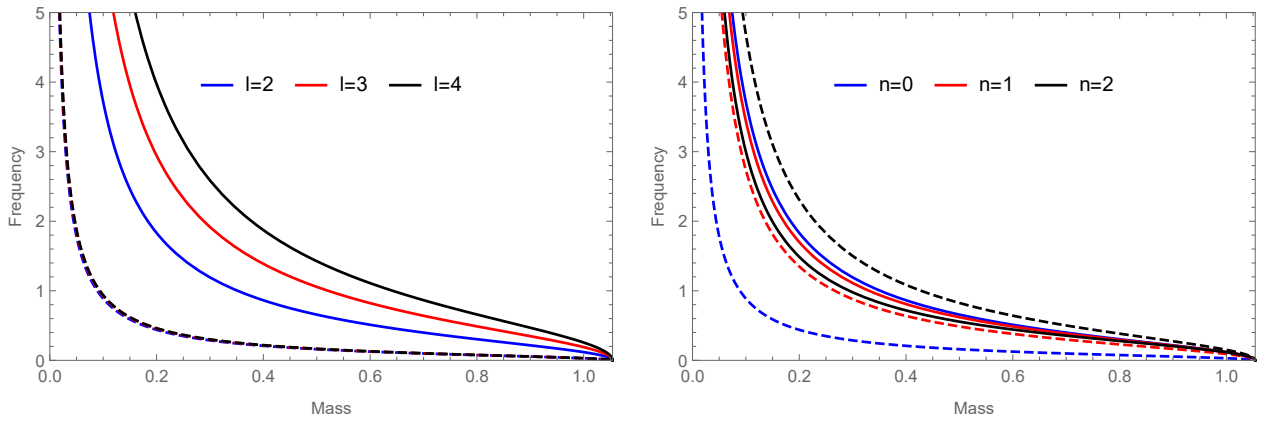

Figure 2.7.: *Axial gravitational/electromagnetic* perturbation Schwarzschild de-Sitter BH for a fixed cosmological constant $\Lambda = 10^{-1}$. The continuous lines represent the real frequencies and the dashed ones are the respective imaginary frequencies. The plot on the left maintains $n = 0$ constant while ℓ varies through 2 to 4. We see that as ℓ increases the real frequencies also grow, however the imaginary frequencies seems insensible to such change, exactly as in the Schwarzschild case. The plot on the right maintains $\ell = 2$ constant while n varies through 0 to 2. As usual, the mass damps the real oscillation frequencies, while making the imaginary ones less pronounced, however they both quickly go to zero as it reaches closer to the extremal condition.

2.6.4. Bardeen

In figures 2.9 and 2.10 we check how the frequencies behave for the *axial* perturbation through the variation of its mass and charge.

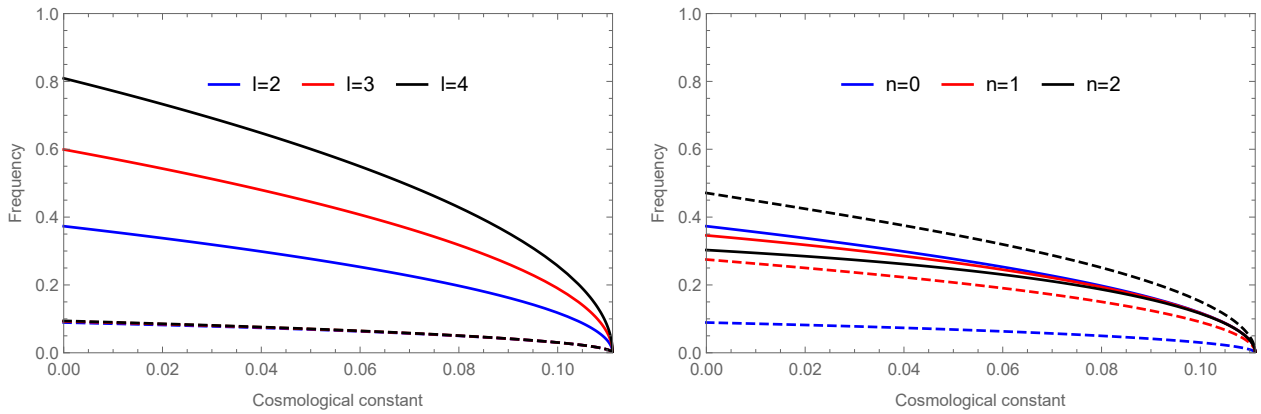

Figure 2.8.: *Axial gravitational/electromagnetic* perturbation Schwarzschild de-Sitter BH for a fixed mass $M = 1$. The continuous lines represent the real frequencies and the dashed ones are the respective imaginary frequencies. The plot on the left maintains $n = 0$ constant while ℓ varies through 2 to 4. We see that as ℓ increases the real frequencies also grow, however the imaginary frequencies seems insensible to such change, exactly as in the Schwarzschild case. The plot on the right maintains $\ell = 2$ constant while n varies through 0 to 2. Particular to this case, the general behavior of the frequencies is almost linear, until reaching close to its extremal limit where the frequencies quickly reach zero. Besides this, it is possible to see that the imaginary frequency is almost not sensible to the variation of Λ through the variation of the parameter ℓ.

First, in figure 2.9, we maintain the mass fixed at $M = 1$ and we vary the charge, obeying the BH condition, from $q = 0$ to $q = \frac{4}{3\sqrt{3}} \approx 0.7698$. This set of graphs are similar to figure 2.6, with the value of the frequencies being a bit lower than the Reissner-Nordström's counterpart, but the increase in the real oscillation frequency occurs a bit more smoothly. It may also been seen in the figure in the right side that as n increases the imaginary frequencies drops sooner as the charge reaches the extremal limit.

For a fixed value of the magnetic charge, $q = 1/2$ in figure 2.10, the usual behavior can be seen: the mass damps the real frequencies and increase the imaginary ones; for a fixed n both frequencies are unchanged through the variation of the multipole number; as ℓ increases, the real frequencies does as well; and as n increases both the real and imaginary frequencies decreases.

In both cases, we check a similar behavior to Reissner-Nordström 's BH, and it shows that it is stable for both parameter variation.

2.6.5. Hayward

We show how the *axial* frequencies change with the BHs parameters mass and l in figures 2.11 and 2.12 for Hayward BH.

From both plots sets, 2.11 and 2.12, we see that the same analysis employed for Bardeen solution holds true. The most noticeable difference is that for ℓ constant, the real frequencies are higher while the imaginary ones lower, when compared to Bardeen BH.

We see that the BH is consistent with being stable for the whole range of the allowed parameters in both cases.

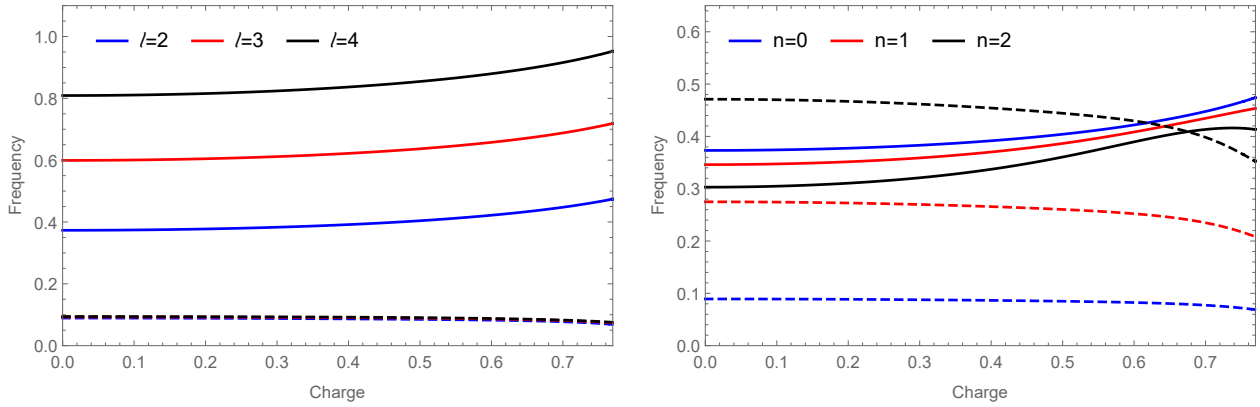

Figure 2.9.: *Axial gravitational/electromagnetic* perturbation of the Bardeen BH for a fixed mass $M = 1$. The continuous lines represent the real frequencies and the dashed ones are the respective imaginary frequencies. The plot on the left maintains $n = 0$ constant while ℓ varies through 2 to 4. We see that the very same analysis performed for Reissner-Nordström BH, when the mass is fixed, holds true. The main difference is that the real oscillation increases more smoothly and the imaginary frequencies start to go to zero quicker as n increases.

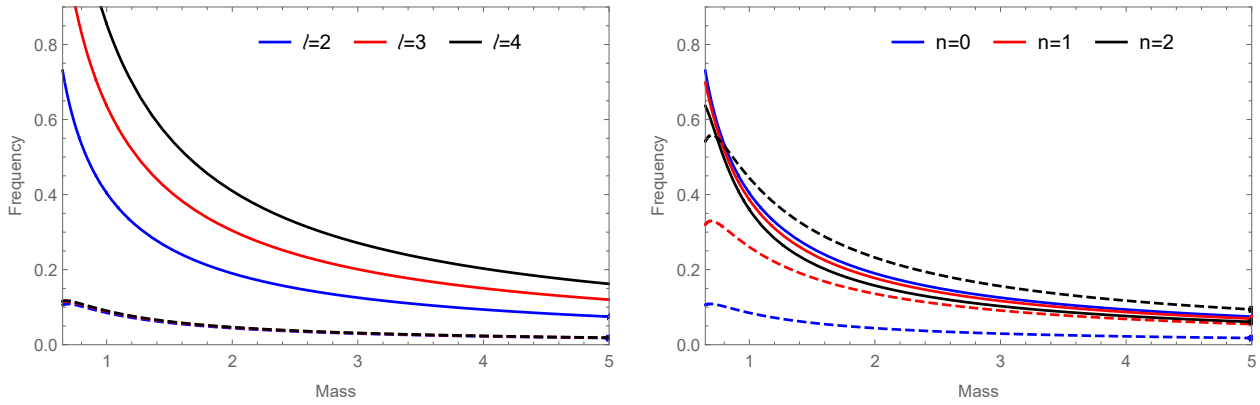

Figure 2.10.: *Axial gravitational/electromagnetic* perturbation of the Bardeen BH for a fixed magnetic charge $q = 1/2$. The continuous lines represent the real frequencies and the dashed ones are the respective imaginary frequencies. The plot on the left maintains $n = 0$ constant while ℓ varies through 2 to 4. The usual damping effect due to the increase of the mass may be seen in both plots.

2.7. The ringdown gravitational wave

The first idea of the gravitational force being propagated through a wave was by Henri Poincaré [69], ten years prior to Einstein's conception of GR. Due to the intrinsic complexities of the GR theory, such as it being inherently non-linear and its ambiguous definition of energy [70], to cite some major concerns, it was deeply debated whether the gravitational waves would carry energy themselves. This discussion came up to a conclusion with a thought experiment given by Feynman in the late 1950s, with what is now known as the "bead argument" [71].

It was settled. Gravitational waves do carry energy. The follow up question seems rather

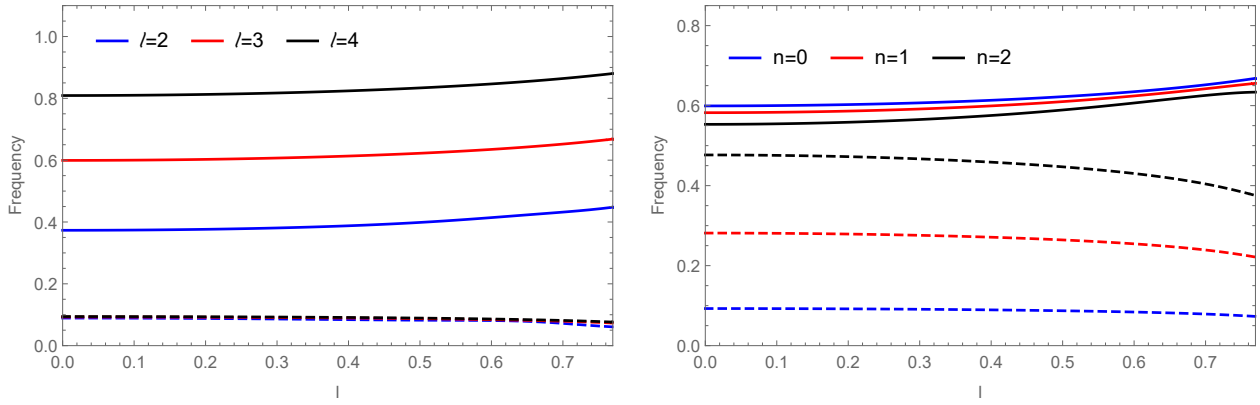

Figure 2.11.: *Axial gravitational/electromagnetic* perturbation of the Hayward BH for a fixed mass $M = 1$. The continuous lines represent the real frequencies and the dashed ones are the respective imaginary frequencies. The plot on the left maintains $n = 0$ constant while ℓ varies through 2 to 4. To this particular case we set $\ell = 3$ on the plot on the right side to better visualize it. Once again we recover similar results obtained for Reissner-Nordström solution.

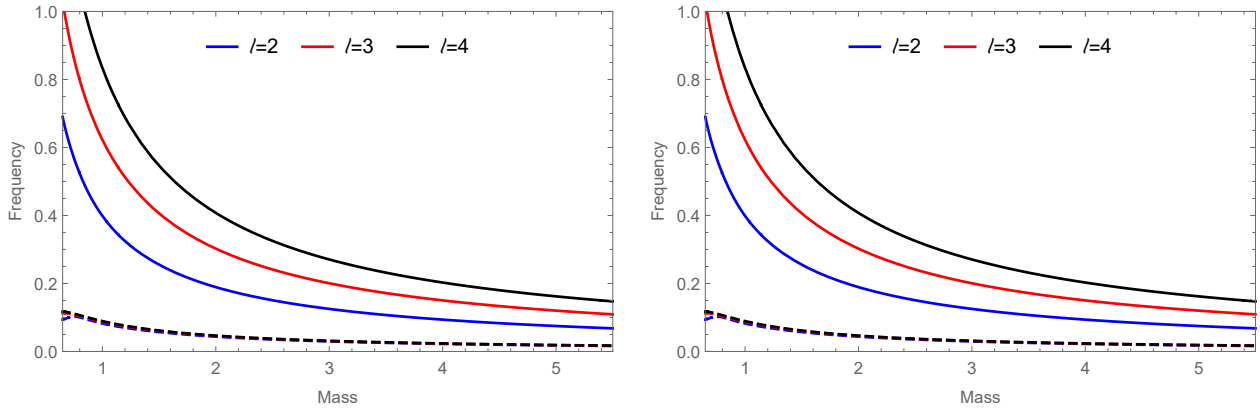

Figure 2.12.: *Axial gravitational/electromagnetic* perturbation of the Hayward BH with $l = 1/2$. The continuous lines represent the real frequencies and the dashed ones are the respective imaginary frequencies. The plot on the left side maintains $n = 0$ constant while ℓ varies through 2 to 4. We see the same general behavior as Bardeen BH, but with slightly difference in the frequencies value for the plot on the right.

obvious then: how do we measure it?

The first generation of experiments that attempted to detect them were based on a huge metal cylinder, working as a kind of "antenna", which would vibrate due to the gravitational wave passing through. Several years were spent trying to improve the apparatus, which culminated in a claimed detection in 1970 [72].

Despite the dubious claim, the search for gravitational waves kept moving forward. Based on the interferometric setup of the Michelson-Morley experiment, the two observatories of the Laser Interferometer Gravitational-Wave Observatory (LIGO) were successfully built in 1997, in the USA, while the Virgo observatory was completed in 2003, in Italy. It was not until 2007 that both observatories agreed to join in a collaborative search for gravitational waves, thus creating

the LIGO-Virgo Science Collaboration (LVSC)[8]

Later, in 2016, the LVSC announced the detection of gravitational waves due to the merger of two BHs [3]. This marked the first direct measurement of gravitational waves and the first BH observation. The LVSC just concluded Observation run 3 (O3). O1 and O2 together detected eleven mergers (seven BHs and one neutron star merger) [73], and with the first part of O3, we have fifty mergers in total [74][9].

One way to test fundamental physics hidden in the gravitational waves, is to look at the remnant, single, BH. The first two phases of the coalescence modeling, the inspiral and the merger, may depend on the environment, accretion disk and the spin direction. While the ringdown phase, the quasi-normal modes are affected solely by the mass (M) and the BH spin parameter (a), fully described by GR[10].

Up to now, the merger phase has only been described using numerical relativity. Thus, the whole coalescence waveform culminated with the Simulating eXtreme Spacetimes (SXS) Collaboration catalog of numerical simulations for merging black holes [75, 76] with thousands of waveforms, for a whole range of parameters, readily available. Despite the numerical success, finding an analytical solution to the whole waveform would enlighten us on the intrinsic details of gravitational wave theory, while opening the possibility to unravel some new details of GR as well.

In light of this, in this section we start by developing an exponential decaying toy model for the ringdown phase, and we show that this recovers the BH's intrinsic parameters. Next, we present a novel analytical model that relies on the remnant BH. It does so by tracing back the light rays to the merger stage.

2.7.1. A toy model

In the ringdown regime, the late-time behavior of the time dependent waves are well described by an exponential tail [77, 78, 79]. That is, the gravitational wave strain $h(t)$ may be approximated to an exponential decaying term with a sine/cosine oscillating function of the type

$$h(t) = Ae^{-\omega_i t}\cos(\omega_r t + \phi), \tag{2.98}$$

where we defined a decaying wave with damping factor ω_i (for $\omega_i > 0$), oscillation frequency ω_r, amplitude A and phase-shift ϕ. In figure 2.7.1 we plot the general behavior of this function.

To understand how we can recover the BH parameters through the analysis of a signal, we simulate a ringdown signal by drawing random samples from a gaussian distribution following model (2.98). Then, we run a Markov Chain Monte Carlo (MCMC) code in Python, using the Metropolis–Hastings algorithm [80, 81], in order to estimate the four free parameters of the model. We show the Probability Density Function (PDF) obtained in figure 2.7.1.

For instance, assuming a Schwarzschild BH, we can match the real and imaginary frequencies to a given mass. Despite the waveform being a superposition of the oscillation modes, the ringdown is mostly dominated by the fundamental one, which corresponds to the least damped [82].

Before moving on to a more accurate model, we must stress the importance of setting where the ringdown regime starts. In other words, at what point in time the transition from the non-linear regime becomes a linear superposition of the damped waves [83].

We have already discussed that the merger is the most energetic phase of the whole process, it is therefore associated with the highest peak of h. On the other hand, several different peaks

[8] With the japanese observatory Kagra joining the collaboration in 2019.

[9] O3 was divided into two different parts, with the second half of the catalog yet to be released.

[10] From now on we are going to assume astrophysical BHs only, that is, they are well described by Kerr solution.

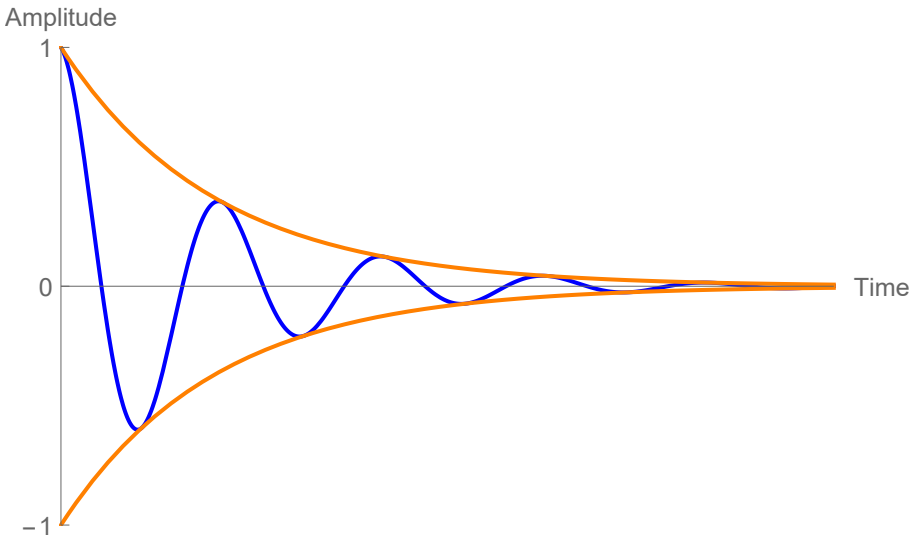

Figure 2.13.: This plot represents a sketch of the general behavior of a damped wave. The blue line is given by equation (2.98), within the orange exponential envelope.

may be used to define the start of the ringdown regime: the strain amplitude and the luminosity peak, both of which are related to the quadrupole moment tensor [84]; and two different peaks related to ψ_4 [11], which are its own peak and the luminosity peak.

Since the Signal-to-Noise Ratio (SNR) in the ringdown is low, compared to all the previous stages of the coalescence, this choice leads to vastly different results for the real and imaginary frequencies of the coalescence. This will directly influence the estimation of the mass and the spin parameter of the remnant BH. For example, in GW150914 of figure 2.7.1, the x-axis represents the real frequency and the y-axis the imaginary one. Four different choices for the start of the ringdown are chosen, $t_0 = t_M + 1, 3, 5, 6.5$ ms, and we can see that the constrain on both frequencies change according to that choice, which potentially leads to different estimations of the mass and spin of this BH.

2.7.2. A merger-ringdown analytical model

In order to obtain the full waveform of all coalescence stages of a binary system we simply glue smaller waves together. The usual approach, to obtain the late dynamical evolution of a two-body problem, in GR is done by mapping their relative motion onto the dynamics of one particle with a reduced mass moving in an effective metric. This method is known as the Effective One-Body (EOB) formalism [87, 88], and is used in the data analysis of the gravitational waves detected by the LVSC.

Instead of trying to evolve the two-body spacetime into the remnant's single body by the end of the merger, we use a novel method that starts from the final perturbative spacetime and retroactively recreate the post-Innermost Stable Circular Orbit (ISCO). This approach is referred to as the Backwards One-Body (BOB) method [89]. This model relies on the fact that the null geodesics on unstable circular orbits, at the BH's light ring, describe the gravitational wave emission of a single perturbed BH. That is, there is a direct correspondence between the quasi normal modes' frequencies, after the merger, and the null rays at the light ring, before the

[11] One of the Newman-Penrose scalars [85], which is associated to the outgoing transverse radiation term [86]

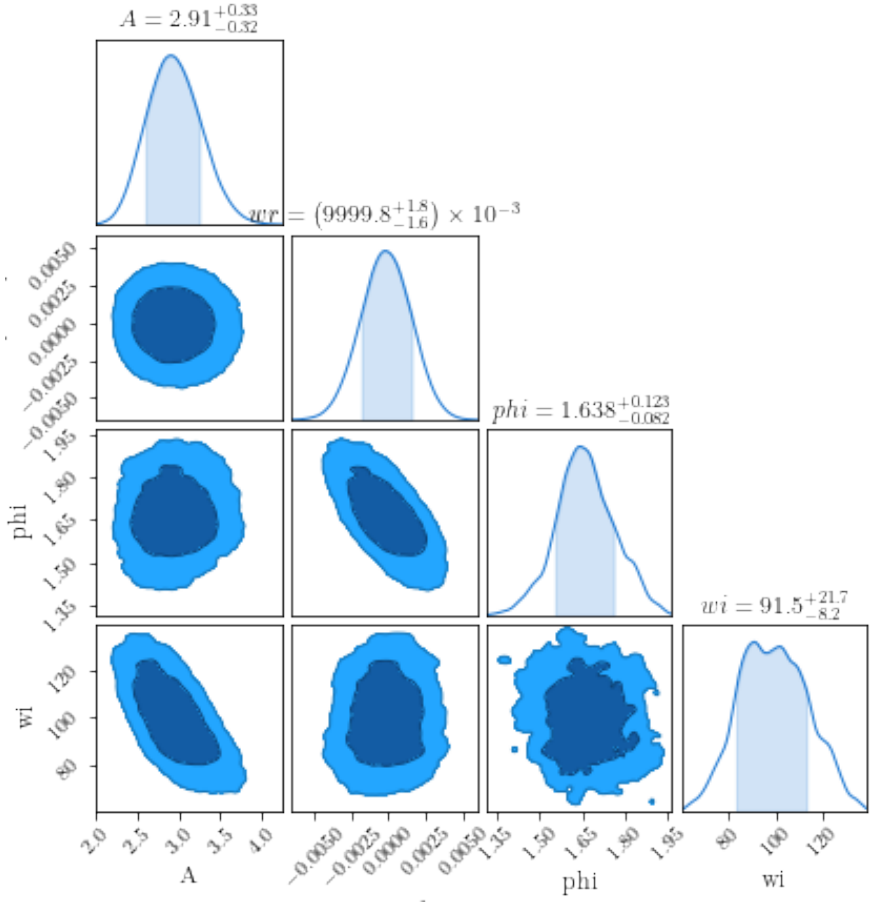

Figure 2.14.: Corner plot showing the parameter constraint on the amplitude, real and imaginary frequencies, and the phase-shift for model in equation (2.7.1) given a gaussian random distribution.

merger.

The exponentially decaying waveform can be found by evaluating how the bundle of null geodesics (null congruence) has diverged from the light ring [90]. It is then possible to trace back the null congruence to the point where the bundle converges, which is expected to be associated with the peak of the strain's amplitude, thus allowing us to predict how the amplitude behaved at earlier times. With the evolution of the amplitude in hand, BOB uses a general relationship between the strain amplitude to compute the frequency, as described in reference [91]. Finally, the phase evolution is acquired through the direct integration of the frequency.

In a nutshell, BOB is a first-principle model that describes the evolution of the amplitude, frequency and phase-shift, of a system in the "merger-ringdown" phase, which englobes the part of the waveform occurring at and after the time of peak amplitude for the waveform strain h. To show that this model is compatible, with the available observed data, would imply in the first analytical model that does not rely on a fit using numerical relativity [89].

In a more straightforward manner, BOB takes the final dimensionless spin a_f, and the final mass M_f, of the merged remnant as its main input, and computes the complex strain $h(t) = h_+(t) + ih_\times(t)$ to be used in equation (2.98).

We test this model using two different gravitational waves, for the data available at the Grav-

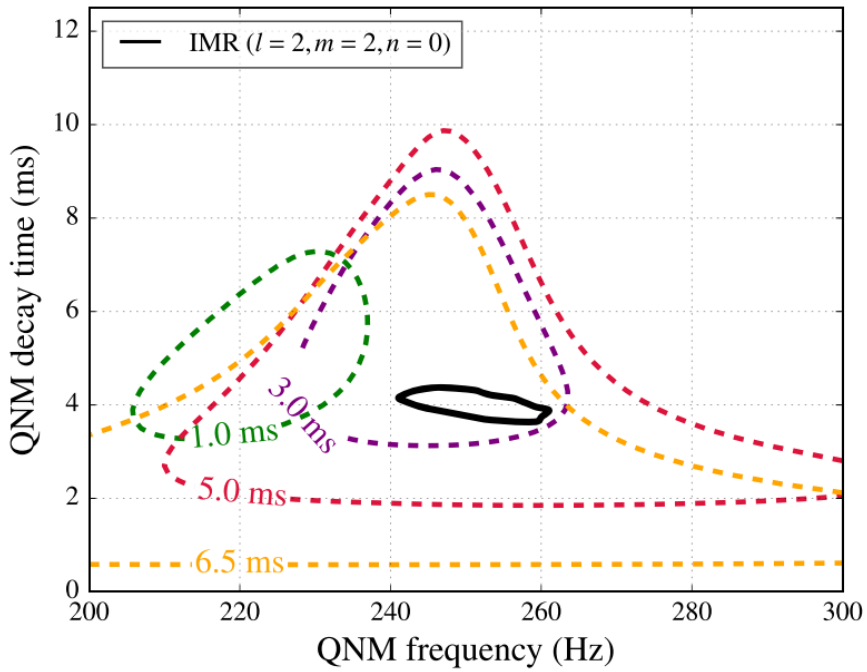

Figure 2.15.: Plot relating the real and imaginary frequencies for different starting points for the ringdown regime: $t = t_M + 1, 3, 5, 6.5$ ms. Figure taken from reference [1].

itational Wave Open Science Center (GWOSC) [92].

2.7.2.1. Some preliminary results

The GW150914 signal was originated by a binary BH system with masses $35.8^{+5.3\pm0.9}_{-3.9\pm0.1} M_\odot$ and $29.1^{+3.8\pm0.1}_{-4.3\pm0.7} M_\odot$. The published results for the mass and spin of the remnant BH are $62.0^{+4.1\pm0.7}_{-3.7\pm0.6} M_\odot$ and $0.67^{+0.05\pm0.01}_{-0.07\pm0.02}$, respectively [93]. In figure 2.7.2.1 we show the PDF for these two parameters using BOB. While the final mass found is substantially higher than the accepted result, $71.92^{+2.31}_{-2.91} M_\odot$, their final spin, $0.74^{+0.04}_{-0.06}$, is compatible within the 68% Contour Levels.

The coalescence signal GW170104 was caused by a primary BH with mass $31.1^{+8.4}_{-6.0} M_\odot$ and a secondary one with $19.4^{+5.3}_{-5.9} M_\odot$. We present the PDF for the mass and spin of the final BH using BOB in figure 2.7.2.1. We estimate the mass to be $64.13^{+5.96}_{-6.37} M_\odot$, respective spin $0.71^{+0.12}_{-0.17}$. Similar to the previous case, the final mass value is fairly higher than the one published, $50.7^{+5.9}_{-5.0} M_\odot$, while the spin parameter is within the expected value of $0.64^{+0.09}_{-0.20}$ [94].

BOB is a fairly new model trying to evolve GR's equation through the merger phase of a binary coalescence. It still needs to be further investigated, both theoretically[12], and against some more data. Being conservative about these preliminary results, we can say that the method is compatible when obtaining the mass of the final BH, but the higher results obtained for the mass must be further investigated.

[12] Still waiting for a more detailed paper Sean!

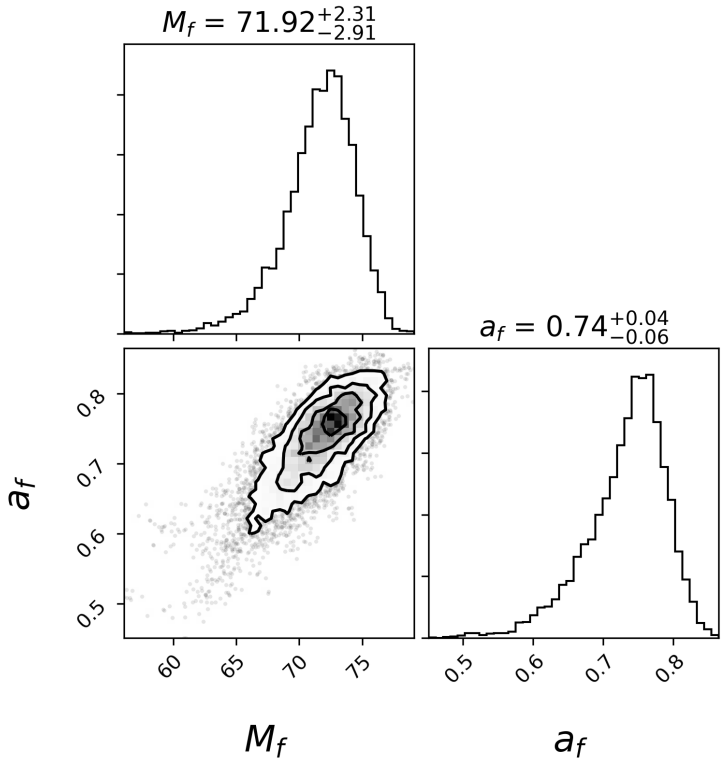

Figure 2.16.: Posterior distribution of the spin parameter a_f and mass M_f for GW150914 using BOB model.

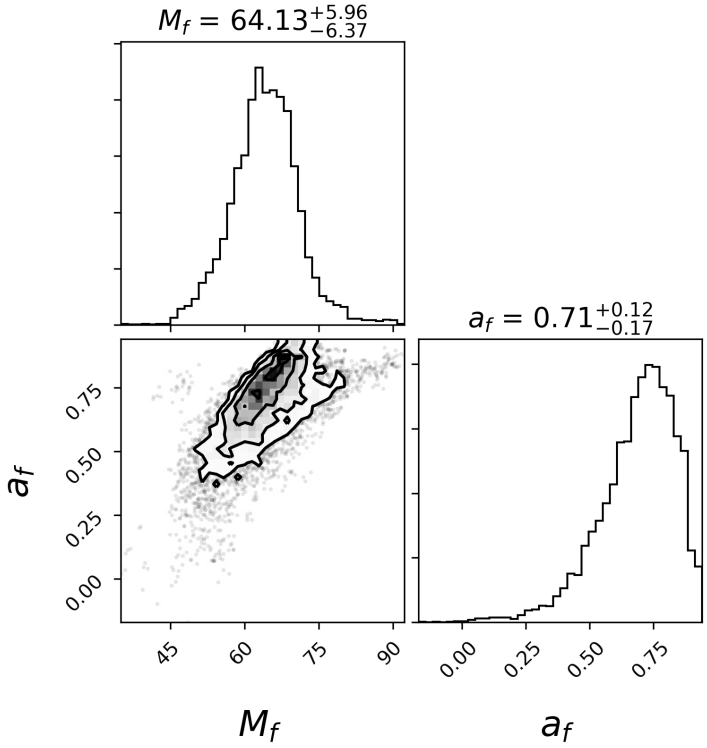

Figure 2.17.: Posterior distribution of the spin parameter a_f and mass M_f for the for GW170104 using BOB model.

The connection between k-essence and Rastall and their stability

3.1. Introduction

Finding similar structures in different contexts, is a recurrent work in both mathematics and physics. One example is the Kaluza-Klein [95, 96] work on a five-dimensional theory of gravity. Their theory naturally[1] gives raise to the standard four-dimensional Einstein gravity and an equation for the scalar field. But the surprising result is that it also gives rise to the classical Maxwell's electromagnetism. The investigation of this "coincidence" played an important role in the evolution of string theory.

In this chapter we step out of BH quasi-normal modes study and investigate a "coincidence" found in two different alternative theories of gravity. In one side we have a scalar-tensor theory, where the source of gravity is not described only by a geometrical tensor, but also by a function of a scalar field: k-essence. In the other side we have a rather exotic theory stating that the conservation of energy and momentum depends on the curvature of spacetime: Rastall theory (see reference [97] for a review in several different gravity theories proposals). If we add a scalar field as a source for gravity for Rastall theory, some static spherically-symmetric solutions mimic k-essence model in its geometric solution.

It is hard to argue that these occurrences happen by only chance, and one should be inclined to further investigate what delves at the bottom of these incidences. This investigation should lead to a deeper connection between these two theories, which may uncover some new intricate relations for some, at first, disconnected models available.

This deepens when we check how the stability of these solutions work in both contexts. A naïve thought would suggest that if one solution is stable/unstable in one context, the same should apply for the other model. However, as we will show, while the k-essence solutions are proven to be unstable, the Rastall counterpart are shown to be inconclusive.

Due to the peculiar nature of Rastall theory, we are prone to assume that this theory holds an intrinsic oddidity that must be further investigated. But we hold this question for the next chapter.

With this, we begin this chapter in, section 3.2, with a quick review of k-essence and Rastall models, making note on the BH-like solutions that we are going to further examine. In the follow-up section, 3.3, we explore under what conditions the two theories relate to each other and how this duality works. We finalize this chapter tackling directly the stability of the BH solutions in both theories, in section 3.4.

[1] Assuming that "naturally" stands for a particular choice of compactification, the cylinder condition hypothesis.

3.2. Reviewing the two theories

3.2.1. K-essence theory

K-essence models [98] consider a general function of a scalar field ϕ. Its lagrangian density is given by

$$\mathcal{L} = \sqrt{-g}[R + F(X, \phi) + \mathcal{L}_m], \tag{3.1}$$

with X being the kinetic term, written as

$$X = \eta \partial_\mu \phi \partial^\mu \phi, \tag{3.2}$$

where $\eta = \pm 1$ is chosen to make X positive, $F(X, \phi)$ is a general function of the kinetic term and the scalar field itself, and $\mathcal{L}_m$ is the lagrangian density for matter fields.

The general field equations for this theory are

$$\begin{aligned} G_{\mu\nu} &= T^{\phi}_{\mu\nu} + T^{m}_{\mu\nu}, \\ T^{\phi}_{\mu\nu} &= \eta F_X \partial_\mu \phi \partial_\nu \phi - \frac{1}{2} g_{\mu\nu} F, \\ \eta \nabla_\lambda (F_X \partial^\lambda \phi) &= \frac{1}{2} F_\phi, \end{aligned} \tag{3.3}$$

where $T^{\phi}_{\mu\nu}$ and $T^{m}_{\mu\nu}$ are the SET due to the scalar field and $\mathcal{L}_m$ respectively. We denote the derivatives in respect to X and ϕ as $F_X = \partial_X F$ and $F_\phi = \partial_\phi F$. We restrict ourselves for a particular choice of the kinetic term as

$$F(X, \phi) = \epsilon X^n + 2V(\phi), \tag{3.4}$$

that is, a general nth power of the kinetic term X and an interacting potential V. With this assumption, the metric and scalar field equations become

$$\begin{aligned} G_{\mu\nu} &= \epsilon \left(\eta \partial_\mu \phi \partial_\nu \phi - \frac{1}{2} g_{\mu\nu} \partial_\lambda \phi \partial^\lambda \phi \right) X^{n-1} + V g_{\mu\nu}, \\ \Box \phi + 2(n-1) &\frac{\nabla_\alpha \phi \nabla_\beta \phi \nabla^\alpha \nabla^\beta \phi}{\partial_\lambda \phi \partial^\lambda \phi} = -\frac{1}{n} V_\phi. \end{aligned} \tag{3.5}$$

Using this set of equations, some static spherically-symmetric solutions were found in reference [2]. We summarize their main structure and properties:

- **Solution 1:** V = 0 and n = 1/3

The solution for the metric field is given by

$$ds^2 = \left(\frac{B_0}{k^2 u} - \frac{k^2 u^3}{2} \right) dt^2 - \left(\frac{B_0}{k^2 u} - \frac{k^2 u^3}{2} \right)^{-1} du^2 - \frac{1}{k^2 u} d\Omega^2. \tag{3.6}$$

This solution has real singularities at $u = \pm\infty$ and $u = 0$, and a coordinate singularity at $u = \frac{(2B_0)^{1/4}}{k}$. Further analysis of this solution is connected to the sign of the constant B_0. For $B_0 < 0$ this solution represents a particular case of a homogeneous, but anisotropic, cosmological solution known as Kantowski–Sachs universe [99]. For $B_0 > 0$, this spacetime represents a BH asymptotically singular and its Penrose diagram, figure 3.2.1, closely resembles the de Sitter space time.

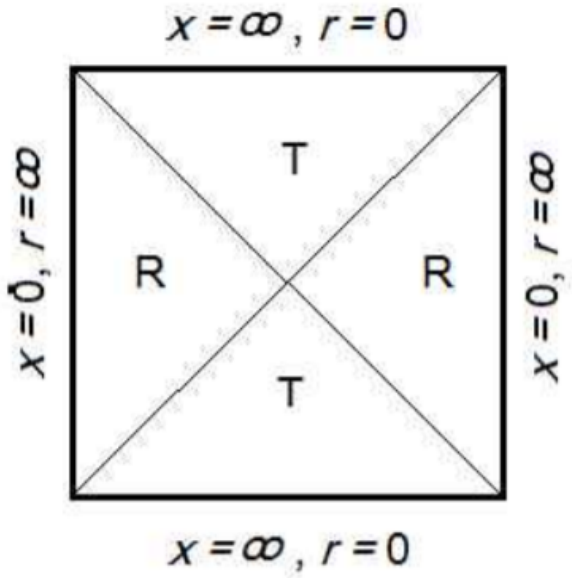

Figure 3.1.: Penrose diagram for solution 1 for $B_0 > 0$. The R and T correspond to static and non-static regions, respectively. Figure taken from reference [2].

The scalar field function is given by

$$\phi(u) \propto -\frac{B_0}{k^8 u^3} - \frac{u}{k^4}. \tag{3.7}$$

For any choice of the sign of B_0, ϕ is always decreasing for $u > 0$, while always increasing for $u < 0$. However, for $B_0 > 0$, the function $\phi(u)$ is always negative in the positive u axis, and always positive in the negative u axis. Despite the sign change in the first term for $B_0 < 0$, the same general behavior holds true.

- **Solution 2:** V = cst and n =1/2

In this case, the solution for the metric is

$$ds^2 = \frac{(9\beta^2 - x^2)^2}{9} dt^2 - \frac{9}{(9\beta^2 - x^2)^2} dx^2 - \frac{3}{9\beta^2 - x^2} d\Omega^2. \tag{3.8}$$

This spacetime has horizons at $x = \pm 3\beta$, where β is a constant with null Hawking temperature and infinite area, traits well observed in cold BHs in scalar-tensor solutions [100, 101]. This spacetime better represents a wormhole connecting these two horizons, separating static and non-static regions. We show the Penrose diagram for this solution in figure 3.2.1.

The function of the scalar field is given by

$$\phi(x) = \frac{4}{3\epsilon} \left(2x - \frac{9\beta}{2} \ln \left| \frac{3\beta + x}{3\beta - x} \right| \right) + \phi_0. \tag{3.9}$$

While this function is singular at the radial infinities and at the horizons, the kinetic term given by X is finite at both horizons. That is, while this solution does not show any singularity in the metric, its scalar field diverges in the same regions.

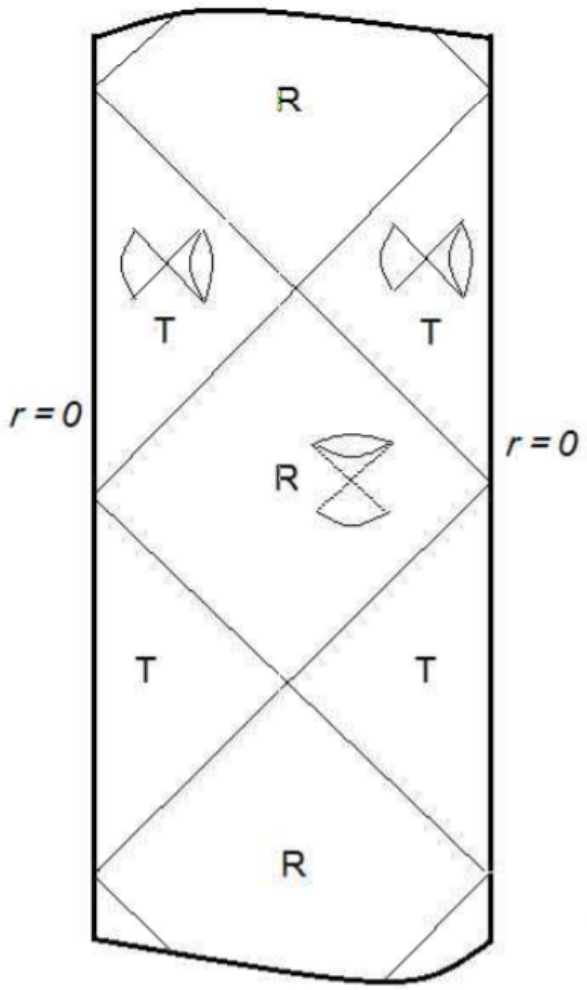

Figure 3.2.: Penrose diagram for solution 2. The R and T correspond to static and non-static regions, respectively, with the light-cones indicating the time direction. Figure taken from reference [2].

3.2.2. Rastall theory

One way to generalize GR theory, is to relax the conservation condition, that is, to allow $\nabla_\mu T^{\mu\nu} \neq 0$. The simplest way to achieve this, while still recovering the usual result for a flat spacetime[2], is to set the divergence of the SET proportional to the gradient of the Ricci curvature scalar R, that is

$$\nabla_\mu T^{\mu\nu} \propto \nabla^\nu R. \tag{3.10}$$

This proposal was first made by P. Rastall [102], and it may be interpreted as a phenomenological implementation of some unknown quantum effect in curved space time.

The field equation that satisfies this condition is given by

$$G_{\mu\nu} = \tilde{T}_{\mu\nu}, \tag{3.11}$$

[2] A reasonable condition, given that quantum-field theory gives well tested predictions in the flat spacetime.

with the new effective SET, $\tilde{T}$, defined via

$$\tilde{T}_{\mu\nu} = T_{\mu\nu} - \frac{b-1}{2} g_{\mu\nu} T, \tag{3.12}$$

where b is the free parameter of the theory (for $b = 1$, GR is recovered). Through the use of Bianchi identities, the SET conservation condition may be recast as

$$\nabla_\mu T^{\mu\nu} = \frac{b-1}{2} \nabla^\nu T. \tag{3.13}$$

This model of gravity has been studied in various different contexts, from BHs solutions [103], to the cosmological scale [104]. To our interest, we focus on spherically symmetric solutions with a canonical self-interacting scalar field, that is

$$T_{\mu\nu} = \epsilon \left(\partial_\mu \phi \partial_\nu \phi - \frac{1}{2} g_{\mu\nu} \partial_\lambda \phi \partial^\lambda \phi \right) + g_{\mu\nu} V(\phi). \tag{3.14}$$

And thus, the dynamical equation for the ϕ field is

$$\Box\phi + (b-1) \frac{\nabla_\alpha \phi \nabla_\beta \phi \nabla^\alpha \nabla^\beta \phi}{\partial_\lambda \phi \partial^\lambda \phi} = -\epsilon(3-2b) V_\phi. \tag{3.15}$$

The striking result obtained in reference [105], was the discovery that the metric of the two spherically-symmetric solutions obtained for this model were exactly the same as in the k-essence theory. We, once again, briefly discuss these two solutions, explicitly distinguishing its differences for the scalar field.

- **Solution 1:** $V = 0$ and $b = -1$

The line element for this case is exactly the same as in equation (3.6). This may either describe a homogeneous but anisotropic cosmological solution, or a BH where the spatial infinity is singular.

Despite its similarities, the scalar field behavior is different from equation (3.7). It reads

$$\phi(u) = \sqrt{\frac{3}{2}} \ln(u) + \phi_0, \tag{3.16}$$

a steadily increasing function, with a single divergence when $u = 0$.

- **Solution 2:** $V = cst$ and $b = 0$

Alike to the k-essence case, the metric solution is given by (3.8), giving a cold-BH-like solution.

Once again, contrasting equation (3.9), this time the scalar field function reads

$$\phi'(x) = \pm\beta\sqrt{2}\sqrt{3 - \frac{2}{\cosh^2(\beta x)}}. \tag{3.17}$$

The integration of this equation is possible, but not simple. What we have to have in mind is that its general behavior is either always increasing, choosing the positive sign, or decreasing, choosing the negative sign.

3.3. The duality between the two theories

K-essence theory and Rastall gravity comes from two very different frameworks: the former is a generalization for scalar fields and the latter a non-conservative theory. Having obtained some identical solutions begs the question: is there any deeper connection between these two theories?

Following reference [106], we change the notation setting as follows

1. $F(X,\phi) = F_0 X^n - 2V(\phi)$,
2. $\phi = \phi(u)$, where u may be either a spatial or the time coordinate,
3. The metric is given by
$$ds^2 = \eta e^{2\alpha(u)} du^2 + h_{ij} dx^i dx^j, \tag{3.18}$$
4. T, ϕ and V are the total SET, scalar field and the interacting potential for k-essence; $\tilde{T}$, ψ and W, the corresponding functions for Rastall.

We set i and k as the number of coordinates other than u, the determinant of h_{ik} may be written as $det(h_{ik}) = e^{2\sigma(u)} h_1(x^i)$ and we have $X = e^{-2\alpha(u)}(\partial_u \phi)^2$.

With this, the k-essence equations in section 3.2.1, may be rewritten. Its SET components are given by

$$T^\nu_\mu(\phi) = \eta F_X \partial_\mu \phi \partial^\nu \phi - \frac{1}{2}\delta^\nu_\mu F, \tag{3.19}$$

with the following components

$$\begin{aligned} T^u_u(\phi) &= (n - 1/2) F_0 X^n + V, \\ T^i_i(\phi) &= -\frac{1}{2} F_0 X^n + V, \end{aligned} \tag{3.20}$$

while the respective scalar field equation becomes

$$e^{-2n\alpha} \partial_u \phi^{2(n-1)} [(2n-1)\partial_u \partial_u \phi + \sigma_u \partial_u \phi - (2n-1)\partial_u \alpha \partial_u \phi] = -\frac{1}{nF_0} V_\phi. \tag{3.21}$$

Similarly, the SET for Rastall gravity, section 3.2.2 may be written as

$$\tilde{T}^\nu_\mu(\psi) = \epsilon(\partial_\mu \psi \partial^\nu \psi - \frac{1}{2}\partial_\lambda \psi \partial^\lambda \psi), \tag{3.22}$$

with the following non-vanishing components

$$\begin{aligned} \tilde{T}^u_u(\psi) &= \frac{\epsilon}{2} b\eta e^{-2\alpha} (\partial_u \psi)^2 + (3 - 2a) W, \\ \tilde{T}^i_i(\psi) &= \frac{\epsilon}{2} (b-2)\eta e^{-2\alpha} (\partial_u \psi)^2 + (3 - 2a) W, \end{aligned} \tag{3.23}$$

while the scalar field equation takes the form

$$e^{-2\alpha} [b\partial_u \partial_u \psi + \partial_u \psi (\partial_u \sigma - b\partial_u \alpha)] = -\epsilon\eta(3 - 2b) W_\psi, \tag{3.24}$$

where $W_\psi = \frac{dW}{d\psi}$ and $\eta = sign(g_{uu})$.

3.3.1. Scalar-vacuum comparison

In sections 3.2.1 and 3.2.2, we established that the solutions for both theories coincide for the scalar-vacuum case, that is, no other matter field besides the scalar field is present. The condition to guarantee that both theories will have the same metric solution requires that both right-hand sides of the effective EFE, to be the same. Thus we check that both interacting potentials in equations (3.20) and (3.23) must obey the following condition

$$V(\phi) = (3 - 2b)W(\psi). \tag{3.25}$$

Now we do the same for the kinetic part

$$(\partial_u \psi)^2 = \epsilon \eta n F_0 (\partial_u \phi)^{2n} e^{2(1-n)\alpha}. \tag{3.26}$$

Lastly, we equate the ratios of both kinetic parts, equations (3.19) and (3.22), to find a relationship between the free parameter of both theories

$$(2 - b)n = 1. \tag{3.27}$$

Given that equations (3.25), (3.26) and (3.27) are simultaneously satisfied, then Rastall and k-essence models are identical. Some particular solutions will be discussed in section 3.3.4.

3.3.2. Cosmology with matter

This duality may also be observed in some cosmological solutions with matter fields. We restrict ourselves to metrics of the type

$$ds^2 = dt^2 - a(t)^2(dx^2 + dy^2 + dz^2), \tag{3.28}$$

which is just a particular case of equation (3.18). We assume the matter content to be of a perfect fluid, so that

$$T_\mu^{\nu(m)} = diag(\rho, -p, -p, -p), \tag{3.29}$$

with the usual definitions of ρ as the density and p the pressure. For this case, the total SET will be composed of both the scalar and matter field, thus

$$T_\mu^\nu = T_\mu^{\nu(m)} + T_\mu^{\nu(\phi)}. \tag{3.30}$$

The k-essence main equations are

$$\begin{aligned} 3H^2 &= \frac{1}{2}(2n-1)F_0\dot{\phi}^{2n} + V + \rho_k, \\ 3H^2 + 2\dot{H} &= -\frac{1}{2}F_0\dot{\phi}^{2n} + V - p_k, \\ \dot{\phi}^{2(n-1)}[(2n-1)\ddot{\phi} + 3H\dot{\phi}] &= -\frac{1}{nF_0}V_\phi, \end{aligned} \tag{3.31}$$

where the subscript k denotes the density and pressure related to k-essence, and $H = \frac{\dot{a}}{a}$ as the Hubble parameter. The matter SET conservation, $\nabla_\nu T_\mu^{\nu(m)} = 0$, yields

$$\dot{\rho_k} + 3H(\rho_k + p_k) = 0. \tag{3.32}$$

While the SET for $T_\mu^{\nu(\psi)}$ is given by equation (3.14), and $T_\mu^{\nu(m)}$ by equation (3.29), the $\tilde{T}_\mu^\nu$ is then the sum of $\tilde{T}_\mu^{\nu(\psi)}$ given by equation (3.23), with its respective part of the matter content as

$$\begin{aligned}\tilde{T}_t^{t(m)} &= \frac{1}{2}[(3-b)\rho + 3(b-1)p] \equiv \tilde{\rho},\\ \tilde{T}_i^{i(m)} &= \frac{1}{2}[(1-b)\rho + (3b-5)p] \equiv -\tilde{p}.\end{aligned} \tag{3.33}$$

These two tilde components may be interpreted as the "effective" density and pressure in Rastall theory. From these two equations, we notice that

$$\begin{aligned}\tilde{\rho} + \tilde{p} &= \rho + p,\\ \tilde{\rho} - \tilde{p} &= \rho - p = \frac{1-b}{2}(\rho - 3p).\end{aligned} \tag{3.34}$$

With these relations, we can write the full set of Rastall equations as

$$\begin{aligned}3H^2 &= \frac{1}{2}\epsilon b\dot{\psi}^2 + (3-2b)W + \tilde{\rho},\\ 3H^2 + 2\dot{H} &= \frac{1}{2}\epsilon(b-2)\dot{\psi}^2 + (3-2b)W - \tilde{p}.\end{aligned} \tag{3.35}$$

The continuity equation depends on how we assume the non-conservation of the full SET to behave in respect to equation (3.13). We analyze two particular cases.

3.3.2.1. Case 1: No mixing of scalar field and matter

In this instance the SET of the scalar field, ψ, and the matter field obey the non-conservation equation given in (3.13) separately. Hence

$$\begin{aligned}\nabla_\nu T_\mu^{\nu(\psi)} &= \frac{b-1}{2}\nabla_\mu T^{(\psi)},\\ \nabla_\nu T_\mu^{\nu(m)} &= \frac{b-1}{2}\nabla_\mu T^{(m)}.\end{aligned} \tag{3.36}$$

The first of these two conditions yields the following dynamic equation for the scalar field

$$b\ddot{\psi} + 3H\dot{\psi} = -\epsilon(3-2b)W_\psi, \tag{3.37}$$

while the second condition, for the matter field, the continuity equation reads

$$\dot{\tilde{\rho}} + 3H(\rho + p) = 0. \tag{3.38}$$

This model is fully described by equations (3.35, 3.37, 3.38).

The Null Energy Condition (NEC) is satisfied for $\rho + p > 0$ [107]. From relation (3.34), we see that if this condition is satisfied for both ρ and p, so does for the "effective" $\tilde{\rho}$ and $\tilde{p}$. However, from the i component of equation (3.33), we see that the "effective" pressure of Rastall theory may be either negative or positive, depending on the density and pressure of the k-essence model.

Equations (3.35) are identical to (3.31) if we set $\rho_k = \tilde{\rho}$ and $p_k = \tilde{p}$ (transforming the variables ϕ to ψ, the parameter n to b and the potential W to V trough the use of equations (3.25, 3.26, 3.27)). This identity may also been seen from both continuity equations in (3.32) and (3.38).

The equation relating both scalar fields is

$$(\partial_u\psi)^2 = \epsilon\eta n F_0(\partial_u\phi)^{2n}e^{2(1-n)\alpha}, \tag{3.39}$$

through the use of equation (3.26).

3.3.2.2. Case 2: Conservative matter

While the non-conservation condition still holds for the scalar field, this is not the case for the matter field

$$\begin{aligned} \nabla_\nu T_\mu^{\nu(\psi)} &= \frac{b-1}{2}\nabla_\mu T^{(\psi)}, \\ \nabla_\nu T_\mu^{\nu(m)} &= 0, \end{aligned} \tag{3.40}$$

which may be rewritten as

$$\nabla_\nu T_\mu^{\nu(\psi)} = \frac{b-1}{2}(\nabla_\mu T^{(\psi)} + \nabla_\mu T^{(m)}), \tag{3.41}$$

and the resulting equation for the scalar field is

$$(b\ddot{\psi} + 3H\dot{\psi})\dot{\psi} = -\epsilon(3-2b)W_\psi\dot{\psi} + \frac{b-1}{2}\epsilon(\dot{\rho} - 3\dot{p}). \tag{3.42}$$

It is important to notice that this equation mixes both SET contents, the scalar field ψ and the matter components ρ and p, even though the fluid is conserved just like in GR. This model is completely described by equations (3.32, 3.35, 3.42).

Once again, using $V = (3-2b)W$ and comparing the Friedmann-like equations (3.35) with their k-essence counterparts (3.31), we obtain

$$\epsilon\dot{\psi}^2 = nF_0\dot{\phi}^{2n}. \tag{3.43}$$

Instead of a relationship between the constants as in equation (3.27) for the scalar-vacuum case, now this connection is performed via

$$\epsilon\dot{\psi}^2\left(b + \frac{1-2n}{n}\right) = (b-1)(\rho - 3p), \tag{3.44}$$

due to (3.34). The same algebraic relation between n and b is recovered only in the radiation case, $\rho = 3p$.

If we change the ψ scalar field to ϕ, through relation (3.43), we get back to the scalar field equation in k-essence case as in (3.31).

Equation (3.44) is connecting the temporal behavior of the scalar field ψ with the matter content, ρ and p. Assuming a constant potential, we may use this equation back into (3.42) to obtain

$$2\ddot{\psi}\dot{\psi} + \frac{6n}{2n-1}H\dot{\psi}^2 = 0. \tag{3.45}$$

This equation may be integrated once, leading to

$$\dot{\psi}^2 = \psi_0 a^{-\frac{6n}{2n-1}}, \tag{3.46}$$

with ψ_0 as an integration constant.

Assuming that both the pressure and density have an equation of state (EoS) related via $p = \omega\rho$, we get

$$\rho = \rho_0 a^{-3(1+\omega)}, \tag{3.47}$$

that is, the parameters ω and n are related by

$$\omega = \frac{1}{2n-1}, \tag{3.48}$$

while Rastall's parameter b remains arbitrary.

For the same EoS, equation (3.44) reads as

$$\epsilon\dot{\psi}^2 = \left[\frac{n(b-1)(1-3\omega}{bn-2n+1}\right]\rho. \tag{3.49}$$

Plugging this back into the frist Friedmann-like equation from the Rastall framework, equation (3.35), we obtain

$$\begin{aligned} 3H^2 &= V + \frac{\rho}{2n-1}\left[\frac{2nb(b-1)(n-2)}{bn-2n+1} + 2(2b-3) + 2n(3-b)\right], \\ 3H^2 &= V + \frac{\rho}{2}\left[\frac{b(b-1)(1+\omega)(1-3\omega)}{(b-2)(1+\omega)+2\omega} + (3-b) + 3\omega(b-1)\right], \end{aligned} \tag{3.50}$$

where the first equation is relating the parameters b and n, and the second one relating b and ω.

Since the right-hand side must be positive, setting a particular choice for either n and V, or ω and V, it is possible to restrict the possible values on b. For example: i) If we choose $V = 0$ and $\omega = 0$ as well (cold matter), the parameter b is constrained by $b < 3/2$ or $b > 2$; ii)Now setting $V = cst$ and $\omega = 1$ (stiff matter) we have $H^2 = V = cst > 0$, that is, an expanding de Sitter universe.

Although more complex potentials and/or EoS are possible, turning the analysis much more challenging, the constant ω value covers most of the interesting cases in cosmology.

3.3.3. Perturbations and the speed of sound considerations

The k-essence theory ruled by a power-law model with a vanishing interacting potential ($V = 0$) is equivalent, in the cosmological framework, to a perfect fluid with an EoS of the type $p = \omega\rho$, related via (3.48). The speed of sound for adiabatic perturbations of a fluid propagate via

$$v_s^2 = \frac{dp}{d\rho} = \omega. \tag{3.51}$$

A well known result for scalar field perturbations of the type $F(X, \phi)$ [108], is that its sound speed is given by

$$v_s^2 = \frac{F_X}{F_X + 2XF_{XX}}, \tag{3.52}$$

which is valid for a general potential $V(\phi)$. Given the power law, as in equation (3.4), the previous equation becomes

$$v_s^2 = \frac{1}{2n-1}, \tag{3.53}$$

in full agreement with both equations (3.48) and (3.51). Thus, there is a complete equivalence between a perfect fluid and k-essence without a potential, not only for a cosmological background but even on the perturbative level, as far as adiabatic perturbations are concerned. For the particular case of $\omega < 0$, that is $n < 1/2$, the speed of sound becomes imaginary and, therefore, the model is perturbatively unstable. This stands true for both a perfect fluid and k-essence. Although a general interaction potential alters the scalar field dynamics, its perturbative propagation speed is still the same as with $V = 0$, coinciding with reference [109].

However, in the theory of Rastall this result may differ. As it is stated in references [110, 111], the speed of sound for the scalar field is

$$v_s^2 = \frac{2-b}{b}. \tag{3.54}$$

We can see that the scalar-vacuum and Case 1, equations (3.53) and (3.54), are identical through the use of (3.27). We must also emphasize that the fluid in these models obey different EoS, conform $\rho_k = \tilde{\rho}$ and $p_k = \tilde{p}$. However, since in Rastall the fluid is represented by its "effective" components $\tilde{\rho}$ and $\tilde{\rho}$, the SET written in terms of these components are conservative, therefore

$$v_s^2 = \frac{d\tilde{p}}{d\tilde{\rho}} = \frac{dp_k}{d\rho_k}. \tag{3.55}$$

With this, we conclude that both theories in the scalar-vacuum and Case 1 framework, coincide even at the adiabatic peturbative level.

On the other hand, for Case 2 where the matter content is conserved individually, the relation between the parameters is more intricate, as it is possible to see through equation (3.44). Thus, it is possible that a stable model in one theory may be unstable in the other, or vice versa; since equation (3.27) does not hold true anymore, b is essentially independent of n up to some possible restrictions on their range. In this case, non-adiabatic perturbations may appear due to the coupling of matter with the scalar field.

3.3.4. Some special cases

In this section we explicitly discuss some particular cases for some choice of either the k-essence parameter n or Rastall's b.

3.3.4.1. Special case 1: $n = 1/2$

Through direct substitution, the k-essence scalar field equation becomes

$$3H = -2F_0^{-1}V_\phi. \tag{3.56}$$

Therefore, for a constant potential, the scalar factor vanishes, $H = 0$, hence the solution is a flat spacetime. Although this condition may be obtained in Rastall theory as well, in the context of the duality this is a trivial case. Even so, the remaining Friedmann equations, the first two equations in (3.31), should still be taken into account. The Rastall dual solution for this case is given by $b = 0$, $V = 3W$ and

$$2\epsilon\dot{\psi}^2 = F_0\dot{\phi}. \tag{3.57}$$

Assuming that the matter conserves, Case 2, the duality still holds true, even so with the parameter b remaining arbitrary. We can confirm this result by substituting equation (3.57) back into equation (3.42) (while using the Friedmann equations in (3.35)) to obtain back equation (3.56).

This case main trait is that non-trivial solutions are obtained only for a variable potential V.

3.3.4.2. Special case 2: $b = 3/2$

For this exact value, Rastall's potential leads to $W = 0$, then the potential also vanishes for k-essence, that is, $V = 0$.

In the scalar-vacuum and Case 1, we have $\tilde{\rho} = 3\tilde{p}$ from equation (3.33), consequently its dual k-essence counterpart contains matter with $\rho_k = 3p_k$. We may switch to the n parameter using relation (3.27), which yields $n = 2$, so that the ϕ field also behaves as radiation.

As for Case 2, since equation (3.27) does not hold true anymore, the general description is applicable.

3.3.4.3. Special case 3: $b = 2$

Equations (3.48) and (3.54) give zero values of pressure and the speed of sound of a scalar field in Rastall's theory. For the k-essence theory this would correspond to $n = \infty$, as we can see from (3.53).

For Case 2, relation (3.27) is valid only, and only if, the conserved matter is pure radiation obeying $\rho = 3p$, thence the speed of sound in the two theories are different for the scalar fields. That is, despite the duality existing for the isotropic background, it is not valid in the perturbative level.

3.3.4.4. Special case 4: $b = 0$

For the scalar-vacuum and Case 1, this instance is identical to the Special case 1, $n = 1/2$.

In Case 2 the scalar field equation for ψ is

$$3H\epsilon\dot{\psi}^2 = -3\dot{W} - \frac{1}{2}(\dot{\rho} - 3\dot{p}), \tag{3.58}$$

which is not a dynamical equation, acting more as a constraint relation since it only contains first-order derivative. Even so, the duality still works for this case: using equations, (3.39) and (3.35) back into the previous equation, we obtain the scalar field equation as in (3.31), which is a second-order equation unless $n = 1/2$.

3.3.5. Explicit examples

Let us now consider some specific examples of the equivalence, assuming a zero or constant potential, and dust as a possible matter contribution.

3.3.5.1. Scalar-vacuum

We consider the scalar-vacuum model with zero potential. The k-essence equations yields

$$\begin{aligned} \dot{\phi} &= \phi_0 a^{-\frac{3}{2n-1}}, \\ H^2 &= \frac{2n-1}{6} F_0 \phi_0^{2n} a^{-\frac{6n}{2n-1}}, \end{aligned} \tag{3.59}$$

where we assumed ϕ_0 as a constant. In terms of the cosmic time we obtain

$$\begin{aligned} a &= a_0 t^{\frac{2}{3(1+\omega)}}, \\ \dot{\phi} &= \phi_1 t^{-\frac{2\omega}{1+\omega}}, \end{aligned} \tag{3.60}$$

where a_0 is a constant and we merged some constants into ϕ_1. To get to this result we assumed that the k-essence perfect fluid has the EoS stated by $p = \omega\rho$, trough the use of equation (3.48).

While the geometric solution, $a(t)$, is the same for the dual theories, the scalar field is given by

$$\dot{\psi} \propto a^{-\frac{3(1+\omega)}{2}} = a^{-\frac{3}{b}} \propto t^{-1}, \tag{3.61}$$

where we should identify, using equation (3.54),

$$\omega = \frac{2-b}{b}. \tag{3.62}$$

We see that the k-essence scalar field ϕ depends on the EoS parameter ω, in contrast to this, the Rastall counterpart does not, reading

$$\psi = \ln(t) + cst. \tag{3.63}$$

Adding a constant potential, which may be interpreted as a cosmological constant, keeps the scalar field equations (3.59) and (3.61) unaltered in terms of $a(t)$. But, in consequence of this, the time dependence becomes more complex, and this situation will not be investigated here.

In the presence of matter the form of the duality depends on how matter couples to the scalar field.

3.3.5.2. Dust and Rastall-Case 1 models

We assume that the k-essence theory contains a pressureless fluid, besides the scalar field ϕ, so that

$$p_k = 0, \quad \rho_k = \rho_1 a^{-3}, \tag{3.64}$$

with ρ_1 as a constant. For the Case 1, where there is no mixing of the SETs, we have

$$\begin{aligned} \frac{1}{2}[(3-b)\rho + 3(b-1)p] &= \tilde{\rho} = \rho_k, \\ \frac{1}{2}[(b-1)\rho + (5-3b)p] &= \tilde{p} = 0, \end{aligned} \tag{3.65}$$

leading to

$$\begin{aligned} \rho &= \frac{5-3b}{2(3-2b)}\rho_k, \\ p &= \frac{1-b}{5-3b}\rho = \frac{1-b}{2(3-2b)}\rho_k, \end{aligned} \tag{3.66}$$

with both parameters of the fluid evolving with a^{-3}. That is, even with a pressureless fluid in the k-essence model, the Rastall dual solution acquires pressure [3]. The scalar fields ϕ and ψ both satisfies the relation (3.27).

If we add a constant potential, with V and W related via relation (3.25), equations (3.64, 3.66) remain unchanged. That is, this is a model with a dust matter field, a cosmological constant due to the constant potential and a scalar field. For the dual part of this solution, Rastall model have an "effective" pressure while still keeping $\rho_k = 0$.

In opposition to this case, we may introduce a pressureless fluid in Rastall-Case 1 model. With this, the k-essence dual equations are

$$\begin{aligned} \rho_k = \tilde{\rho} &= \frac{1}{2}(3-b)\rho, \\ p_k = \tilde{p} &= \frac{1}{2}(b-1)\rho, \end{aligned} \tag{3.67}$$

and we may solve equation (3.38) to obtain

$$\rho_k \propto p_k \propto a^{-\frac{6}{3-b}} = a^{-3(1+\omega_k)}, \tag{3.68}$$

where we defined the EoS parameter of the fluid in the k-essence theory as

$$\omega_k = \frac{b-1}{3-b} = \frac{n-1}{n+1}. \tag{3.69}$$

Thus, we see that this model is quite different from the dust one introduced in k-essence theory.

[3] Except for the value that returns to GR, $b = 1$.

3.3.5.3. Dust and Rastall-Case 2 models

Assuming, once again, a pressureless perfect fluid as in equation (3.64), but now under the Case 2 of Rastall theory, we get

$$\epsilon\dot{\psi}^2\left(b-\frac{2n-1}{n}\right)=(b-1)\rho\propto a^{-3}. \tag{3.70}$$

In accordance to equation (3.43), for $b\neq 1$, we find

$$\begin{aligned}\dot{\psi}&\propto a^{-3/2},\\ \dot{\phi}&\propto a^{-\frac{3}{2n}}.\end{aligned} \tag{3.71}$$

Combining (3.31) with (3.43), setting $V_\phi=0$, we check that this corresponds to the case $n\to\infty$. So, just like as in GR for pure dust model, we get $a\propto t^{2/3}$. Consequently, for scalar fields

$$\begin{aligned}\phi&\propto t,\\ \dot{\psi}\propto a^{-3/2}&\propto t^{-1}.\end{aligned} \tag{3.72}$$

We can arrive in a restriction for the parameter b using $\dot{\psi}=\psi_0/t$, $\rho=\rho_0/t^2$ into (3.70)

$$\epsilon\psi_0^2(b-2)=(b-1)\rho_0. \tag{3.73}$$

We conclude that Rastall parameter depends on the contribution of both the matter and scalar field contents. Moreover, the speed of sound of the scalar field does not follow the adiabatic relation as in Case 1.

A cosmological constant can be easily introduced in the form of $V=(3-b)W=cst$. The scalar field again follows the law (3.70), and the whole configuration reduces to the ΛCDM model where Λ is given by the constant potential and the matter component consists of the scalar field and ordinary matter. All background relations of the ΛCDM model are preserved in this case, but the degeneracy between the scalar field and usual matter is broken at the perturbative level. Due to the fact that the ΛCDM model is subject to problem at the perturbative level in the non-linear regime (see references [112, 113]), such a more complex configuration in k-essence and Rastall models may lead to interesting results to be studied in the future.

3.4. The stability of these two theories

With the structure of the solutions investigated in sections 3.2.1 and 3.2.2, then their duality in section 3.3, we now investigate if the solutions obtained are stable, or not, under first-order perturbation analysis. First we will work on the k-essence theory, closely following reference [114] and [115]. After developing the method we turn ourselves to Rastall theory, where we then use reference [116] as our main lead.

3.4.1. K-essence stability

3.4.1.1. Main equations

We first write the main equations for the stability problem. Some equations shall be simply rewritten for the instances where some notation is changed, but I also hope to make the reader's life a bit easier, saving you the work of turning pages back and forth just to recall the equations.

The k-essence Lagrangian is

$$\mathcal{L} = \sqrt{-g}[R - F(X,\phi)], \quad X = \eta\partial_\lambda\phi\partial^\lambda\phi, \quad \eta = \pm 1, \tag{3.74}$$

and we focus ourselves in a power-law of the type

$$F(X,\phi) = F_0 X^n - 2V(\phi), \quad F_0 = cst. \tag{3.75}$$

The field-equations for this theory are

$$G^\nu_\mu = -T^{\nu(\phi)}_\mu, \tag{3.76}$$

$$T^{\nu(\phi)}_\mu = \eta F_X \partial_\mu\phi\partial^\nu\phi - \frac{1}{2}\delta^\nu_\mu F, \tag{3.77}$$

$$\eta\nabla_\lambda(F_X\phi^\lambda) = \frac{1}{2}F_\phi. \tag{3.78}$$

We write a general static spherically-symmetric metric as

$$ds^2 = e^{2\gamma}dt^2 - e^{2\alpha}du^2 - e^{2\beta}d\Omega^2, \tag{3.79}$$

where the background components depend solely on the radial coordinate, and the perturbations, followed by a δ, of both u and t as

$$\begin{aligned}
\gamma(u,t) &= \gamma(u) + \delta\gamma(u,t),\\
\alpha(u,t) &= \alpha(u) + \delta\alpha(u,t),\\
\beta(u,t) &= \beta(u) + \delta\beta(u,t),\\
\phi(u,t) &= \phi(u) + \delta\phi(u,t).
\end{aligned} \tag{3.80}$$

From now on the dots represents derivatives in respect to the time coordinate t, and primes the corresponding derivatives in respect to the radial coordinate u. To maintain X positive, we set $\eta = 1$, therefore the kinetic term becomes

$$\begin{aligned}
X &= e^{-2\alpha}\phi'^2,\\
\delta X &= 2e^{-2\alpha}(\phi'\delta\phi' - \phi'\delta\alpha),
\end{aligned} \tag{3.81}$$

with the following corresponding non-zero SET components

$$\begin{aligned}
T^t_t = T^\theta_\theta = T^\phi_\phi &= -\frac{F}{2},\\
T_{tu} &= -F_X\dot{\phi}\phi',\\
T^u_u &= -\frac{F}{2} + XF_X.
\end{aligned} \tag{3.82}$$

To further simplify the set of EFE and the Klein-Gordon-like equation, we impose a further restriction into the function $F(X,\phi)$, fixing it as $F(X)$ only.

With all of this, we can finally write down equations (3.76) and (3.78) as

$$-e^{2\alpha-\beta} + \beta'(\beta' + 2\gamma') = \left(\frac{F}{2} - XF_X\right)e^{2\alpha}, \tag{3.83}$$

$$-e^{2(\alpha-\beta)} + 2\beta'' + 3\beta'^2 - 2\alpha'\beta' = \frac{F}{2}e^{2\alpha}, \tag{3.84}$$

$$e^{2(\alpha-\beta)} + e^{2(\alpha-\gamma)}\ddot{\beta} - \beta'' - \beta'(\gamma' - \alpha' + 2\beta') = -\frac{e^{2\alpha}}{2}(F - XF_X), \tag{3.85}$$

$$\dot{\beta}' + \dot{\beta}\beta' - \dot{\alpha}\beta' - \dot{\beta}\gamma' = \frac{F_x}{2}\dot{\phi}\phi', \tag{3.86}$$

$$F_X e^{\alpha+2\beta-\gamma}\ddot{\phi} - \left(F_X e^{-\alpha+2\beta+\gamma}\phi'\right)' = 0, \tag{3.87}$$

preserving only linear terms with respect to time derivatives.

So far, this set of equations was written in its most general form, without fixing any radial coordinate (where u may depend on $u = u(z)$, for example), and without fixing any perturbation gauge for the "delta" functions as well. With this, we now choose the simplest gauge to deal with perturbation in the context of spherically-symmetric solutions, $\delta\beta = 0$, which greatly simplify our equations.

If the radial function e^{β} has a minimum at some u, as it is the case for wormholes spacetimes, this gauge imposes a physical restriction on the wormhole, forcing its throat to be at rest. This leaves the throat radius invariable, while perturbations must in general admit a temporal dependence [101]. However, we can safely choose this gauge for our case, since for other solutions (i.e. BHs), these regions are usually critical points of the radial function u and they don't present any physical critical restriction [115].

Setting this gauge, equation (3.86) reads

$$\delta\alpha = -\frac{n}{2\beta'}X^{n-1}\phi'\delta\phi, \tag{3.88}$$

and we can show that all the remaining Einstein equations hold as consequence of equations (3.83, 3.85) and (3.89), leading to no further restriction with this gauge choice [115]. The perturbed equation for the scalar field, (3.83), yields

$$-e^{2(\alpha-\gamma)}\delta\ddot{\phi} + \delta\phi'' + \phi'\delta\sigma' + \sigma'\delta\phi' + \frac{F'_X}{F_X}\delta\phi' + \phi'\delta\left(\frac{F'_X}{F_X}\right) = 0, \tag{3.89}$$

where we defined

$$\sigma = 2\beta + \gamma - \alpha. \tag{3.90}$$

As the solutions studied in section 3.2.1 were obtained with a constant potential only, we may impose this condition directly into the function $F(X)$, while interpreting it as a cosmological constant. That is

$$F(X) = F_0X^n - 2\Lambda. \tag{3.91}$$

We may switch the variable $\delta\alpha$ to $\delta\phi$ using (3.89), and the same can be done for the other variables with the remaining equations (3.83, 3.84, 3.85). As a result, we obtain the wave equation for $\delta\phi$ as

$$-e^{2(\alpha-\gamma)}\delta\ddot{\phi} + (2n-1)\delta\phi'' + \delta\phi'[\sigma' - 2(n-1)\alpha'] - \frac{n^2}{\beta'^2}(e^{-2\beta} - \Lambda)e^{4\alpha}F_0X^n\delta\phi = 0. \tag{3.92}$$

Just like the previous case, the radial coordinate u is not yet fixed, then we pass on to the "tortoise" coordinate z via

$$\frac{du}{dz} = e^{\gamma-\alpha}. \tag{3.93}$$

Since we are looking after wave equations, we define the time dependence as

$$\delta\phi = \Psi(z)e^{i\omega t}, \tag{3.94}$$

followed by

$$\Psi(z) = f(z)\psi(z), \quad f(z) = exp\left[-\frac{\beta + (1-n)\gamma}{2n-1}\right]. \tag{3.95}$$

Thus, we obtained the master equation ruling the perturbation for this theory

$$(2n-1)\frac{d^2\psi(z)}{dz^2} + [\omega^2 - V(z)]\psi(z) = 0, \tag{3.96}$$

where $V(z)$ is the effective potential[4], which its full form is being omitted for now (due to its rather complicated form), but we are going to explicitly write it down it for the solutions that we are about to check.

3.4.1.2. Verifying the solution's stability

Now we will use equation (3.96), with the two k-essence solutions (with some slightly notation changes) obtained in section 3.2.1, to test their stability.

- **Solution 1:** $V = 0$ and $n = 1/3$

The first solution, equations (3.6) and (3.7), are

$$ds^2 = \frac{B(x)}{k^2 x}dt^2 - \frac{k^2 x}{B(x)}dx^2 - \frac{1}{k^2 x}d\Omega^2, \quad B(x) = B_0 - \frac{1}{2}k^2 x^4, \tag{3.97}$$

$$\frac{d\phi}{dx} = \phi_0 \left(\frac{B_0}{x^4} - \frac{k^2}{2}\right). \tag{3.98}$$

Since we want to test the stability of the BH solution, we impose $B_0 > 0$, with the radial coordinate range going from $x = 0$ to its horizon at $x = \frac{(2B_0)^{1/4}}{k}$.

We change the radial coordinate to the tortoise coordinate, through equation (3.93), set its time dependence, (3.94), and write everything in terms of ψ, (3.95), to finally use the master equation (3.96). After all these transformations, we obtain

$$\partial_z^2 \psi(z) - [3\omega^2 + V(x)]\psi(z) = 0, \tag{3.99}$$

with its effective potential given by

$$V(x) = -F_1 B(x) + \frac{5B_0^2}{4k^2x^4} + \frac{31B_0}{4k^2} - \frac{3x^4}{16}. \tag{3.100}$$

At first sight, we see that the role of energy is given by $-3\omega^2$, therefore if the eigenvalues are not restricted from above, they definitely are not from below. That is, this suggests that this solution is unstable, and we have to verify this result formulating the boundary conditions for the function $\psi(z)$.

First we have to check how the coordinates act within the radial coordinate range. The general behavior near $x \to 0$ is

$$z \propto x^2, \quad V \approx \frac{5B_0}{4k^2x^4} \approx z^{-2}, \tag{3.101}$$

while near the horizon, $x \to \frac{(2B_0)^{1/4}}{k}$,

$$z \to \infty, \quad V \to cst. \tag{3.102}$$

By definition of perturbation theory, we cannot allow the perturbative term, $\delta\phi$, to grow faster than the background function, ϕ, itself. According to equation (3.98) $\delta\phi$ may grow as x^{-3} when $x \to 0$, and it must be finite as it approaches the horizon, that is, as $x \to \frac{(2B_0)^{1/4}}{k}$. Switching back to the tortoise coordinate z, relation (3.93), the $\delta\phi$ term reads

$$\psi \approx z^{-1/4}, \tag{3.103}$$

[4]Not to be confused with the interaction potential in the scalar field lagrangian.

as $z \to 0$, and

$$\psi \approx e^{z}, \tag{3.104}$$

as $z \to \infty$. Thus, the eigenfrequencies are neither restricted from below nor above, $|\omega^2|$ can be arbitrarily large. We conclude that this BH solution is unstable in the region between $x = 0$ and its horizon.

- **Solution 2:** $V = cst$ and $n = 1/2$

Now we focus our attention to the second solution, equations (3.8) and (3.9), are

$$ds^2 = \frac{(9\beta^2 - x^2)^2}{9\beta^4}dt^2 - \frac{9\beta^4}{(9\beta^2 - x^2)^2}dx^2 - \frac{3\beta^4}{9\beta^2 - x^2}d\Omega^2, \tag{3.105}$$

$$\phi(x) = \pm\frac{4}{3F_0\beta^4}\left(-2x + \frac{9\beta}{2}\ln\left|\frac{3\beta + x}{x - 3\beta}\right|\right) + \phi_0, \tag{3.106}$$

since the potential is constant, we interpret it as the cosmological constant and define it as $\Lambda = 3/\beta^2$. The BH solution is between two horizons, set by $-3\beta < x < 3\beta$.

This time the procedure is much simpler than the previous case, the wave equation, as in (3.92), yields

$$\delta\ddot{\phi} = h(u)\delta\phi, \tag{3.107}$$

with the definition for the function $h(u)$ as

$$h(u) = \frac{27}{b^4\cosh^2(bu)}[1 + 2\tanh^2(bu)], \tag{3.108}$$

which we must stress that is positive definite.

We integrate equation (3.107) once

$$\delta\dot{\phi}^2 = h(u)\delta\phi^2 + C_0(u), \tag{3.109}$$

and setting $C_0(u) = 0$ we integrate it once again

$$\delta\phi(t, u) = e^{\pm\sqrt{h(u)} + C_1(u)}. \tag{3.110}$$

It is clear that due to the arbitrariness of $C_1(u)$ this function will always grow with time. Thus, we conclude that this solution is unstable as well.

3.4.2. Rastall stability

3.4.2.1. Main equations

As we did in the section prior to this one, we quickly review the main equations of the model, while extending them to the perturbation analysis.

The general field equations, for both the geometric part and the scalar field, are

$$R_{\mu\nu} = \epsilon\left(\partial_\mu\phi\partial_\nu\phi + \frac{1 - b}{2}g_{\mu\nu}\partial_\lambda\phi\partial^\lambda\phi\right) - g_{\mu\nu}W(\phi), \tag{3.111}$$

$$\Box\phi + (b - 1)\frac{\partial^\alpha\phi\partial^\beta\phi\partial_\alpha\partial_\beta\phi}{\partial_\lambda\phi\partial^\lambda\phi} = -W_\phi. \tag{3.112}$$

where, for simplicity, we defined $W(\phi) = (3-2b)V(\phi)$. Keeping the same notation for the metric as in (3.79), we have the following perturbed equations

$$-e^{2(\alpha-\gamma)}(\delta\ddot{\alpha} + 2\delta\ddot{\beta}) + \delta\gamma'' + \delta\gamma'(\gamma' - \alpha' + 2\beta') + \gamma'(\delta\gamma' - \delta\alpha' + 2\delta\beta') = -\epsilon(1-b)\phi'\delta\phi' - e^{2\alpha}(2W\delta\alpha + W_\phi\delta\phi), \quad (3.113)$$

$$-e^{2(\alpha-\gamma)}\delta\ddot{\alpha} + \delta\gamma'' + 2\delta\beta'' - \delta\alpha'(\gamma' + 2\beta') - \alpha'(\delta\gamma' + 2\delta\beta') + 2\gamma'\delta\gamma' + 4\beta'\delta\beta' = -\epsilon(3-b)\phi'\delta\phi' - e^{2\alpha}(2W\delta\alpha + W_\phi\delta\phi), \quad (3.114)$$

$$-e^{2(\alpha-\gamma)}\delta\ddot{\beta} + \delta\beta'' + \delta\beta'(\gamma' - \alpha' + 2\beta') + \beta'(\delta\gamma' - \delta\alpha' + 2\delta\beta') - 2e^{2(\alpha-\beta)}(\delta\alpha - \delta\beta) = -\epsilon(1-b)\phi'\delta\phi' - e^{2\alpha}(2W\delta\alpha + W_\phi\delta\phi), \quad (3.115)$$

$$\delta\dot{\beta}' + (\beta' - \gamma')\delta\dot{\beta} - \beta'\delta\dot{\alpha} = -\frac{\epsilon}{2}\phi'\delta\dot{\phi}, \quad (3.116)$$

$$-e^{2(\alpha-\gamma)}\delta\ddot{\phi} + b\delta\phi'' + (\gamma' - b\alpha' + 2\beta')\delta\phi' + \phi'(\delta\gamma' - b\delta\alpha' + 2\delta\beta') = \epsilon e^{2\alpha}(2W_\phi\delta\alpha + W_{\phi\phi}\delta\phi), \quad (3.117)$$

since we are dealing with first-order perturbation theory, we kept only the linear terms for each perturbed variable.

3.4.2.2. Master equation and a discrepancy

Following the same reasoning as before, we keep our arbitrary radial coordinate u and set the perturbation gauge $\delta\beta = 0$. Therefore, the field equations become

$$-e^{\alpha-\gamma}\delta\ddot{\alpha} + \delta\gamma'' + \delta\gamma'(2\gamma' - \alpha' + 2\beta') - \gamma'\delta\alpha' = -\epsilon(1-b)\phi'\delta\phi' - e^{2\alpha}(2W\delta\alpha + W_\phi\delta\phi), \quad (3.118)$$

$$-e^{\alpha-\gamma}\delta\ddot{\alpha} + \delta\gamma'' - \delta\alpha'(\gamma' + 2\beta') - (\alpha' - 2\gamma')\delta\gamma' = -\epsilon(3-b)\phi'\delta\phi' - e^{2\alpha}(2W\delta\alpha + W_\phi\delta\phi), \quad (3.119)$$

$$\beta'(\delta\gamma' - \delta\alpha') - 2e^{2(\alpha-\beta)}\delta\alpha = -\epsilon(1-b)\phi'\delta\phi' - e^{2\alpha}(2W\delta\alpha + W_\phi\delta\phi), \quad (3.120)$$

$$-\beta'\delta\dot{\alpha} = -\frac{\epsilon}{2}\phi'\delta\dot{\phi}, \quad (3.121)$$

$$b\delta\phi'' + (\gamma' - b\alpha' + 2\beta')\delta\phi' + (\delta\gamma' - b\delta\alpha')\phi' - e^{2(\alpha-\gamma)}\delta\ddot{\phi} = \epsilon e^{2\alpha}(2W_\phi\delta\alpha + W_{\phi\phi}\delta\phi). \quad (3.122)$$

The easiness on using this particular gauge can be seen through equation (4.21). We can integrate it to acquire

$$\begin{aligned} \delta\alpha &= \eta(u)\delta\phi + \xi(u), \\ \eta &= \frac{\epsilon\phi'}{2\beta'}. \end{aligned} \quad (3.123)$$

We solve for $\delta\gamma'$ by subtracting equation (3.118) from (3.119). We get

$$\delta\gamma' = \eta\delta\phi' - \eta'\delta\phi. \quad (3.124)$$

However, we acquire a relation for $\delta\gamma'$ using equation (3.120) as well, which gives

$$2\beta'\delta\gamma' = \epsilon b\phi'\delta\phi' + e^{2\alpha}\left[2(e^{-2\beta} - W)\delta\alpha - W_\phi\delta\phi\right]. \quad (3.125)$$

In order to attain the master equation, we use relations (3.123) and (3.124) back into the equation that contains the dynamical equation for the perturbed scalar field, equation (3.122). Thence

$$-e^{2(\alpha-\gamma)}\delta\ddot{\phi}+b\delta\phi''+[2\beta'+\gamma'-b\alpha'+\eta(1-b)\phi']\delta\phi'-[(1+b)\eta'\phi'+\epsilon e^{2\alpha}(2\eta W_{\phi}+W_{\phi\phi})]\delta\phi=0. \quad (3.126)$$

This equation plays the same role as in the k-essence model, equation (3.92): it should lead to the result concerning the stability of the solutions of the model.

3.4.2.3. Verifying the solution's stability

Using the same framework as before, we develop the stability condition for both solutions in Rastall theory.

- **Solution 1:** $V=0$ and $b=-1$

The geometric and scalar field equations, with some notation changes, are given by

$$ds^2=A(x)dt^2-\frac{dx^2}{A(x)}-\sqrt{\frac{3}{2C^2}}\frac{d\Omega^2}{x}, \quad A(x)=\frac{K}{x}-\frac{C}{\sqrt{6}}x^3, \quad (3.127)$$

$$\phi(x)=\sqrt{\frac{3}{2}}ln(x)+\phi_0, \quad (3.128)$$

given that ϕ_0, C and K are all constants.

Then, we plug these background quantities into the wave equation for the perturbation, equation (3.126), yielding

$$e^{-4\gamma}\delta\ddot{\phi}+\delta\phi''+\frac{2}{x}\delta\phi'=0. \quad (3.129)$$

We may use both relations that we obtained for $\delta\gamma'$ to obtain

$$\begin{aligned}\delta\gamma' &= \sqrt{\frac{3}{2}}\delta\phi', \\ &= -\left(\frac{3}{2}\delta\phi'+\sqrt{6}e^{2(\alpha-\beta)}\delta\phi\right),\end{aligned} \quad (3.130)$$

using a variable separation of the type $\delta\phi(t,x)=F(t)\psi(x)$, the last equality in equation (3.130) may be integrated to obtain

$$-\frac{\ddot{F}}{F}=\frac{\psi''}{\psi}+\frac{2}{x}\frac{\psi'}{\psi}=cst, \quad (3.131)$$

where we have defined

$$\psi(x)=\left(K-\frac{C}{\sqrt{6}x^4}\right)^{-1/2}. \quad (3.132)$$

However, solving the differential equation for $\psi(x)$ using (4.35), we get

$$\psi(x)\propto\frac{e^{-x}+e^{x}}{x}, \quad (3.133)$$

which is vastly different from the definition of (3.132). Thus we arrived into an inconsistency.

- **Solution 2:** $V=cst$ and $b=0$

Moving onward to the second solution, already setting $V = cst = \Lambda = \beta^2$, we have

$$ds^2 = \frac{9\beta^4}{\cosh^4(bu)}dt^2 - du^2 - \frac{\cosh^2(bu)}{3\beta^2}d\Omega^2, \tag{3.134}$$

$$\phi'(u) = \pm\beta\sqrt{6 - \frac{4}{\cosh^2(bu)}}. \tag{3.135}$$

The master equation, equation (3.122), reads

$$e^{-2\gamma}\delta\ddot{\phi} - \phi'\delta\gamma = 0. \tag{3.136}$$

And from this point we can already see an odd behavior: while we have a second time derivative term, there is no evolution term for the radial coordinate u. Even so, from one of the expressions for $\delta\gamma'$, equation (3.125), we have

$$\delta\gamma' = \frac{3}{2}\phi'\delta\phi, \tag{3.137}$$

then we use the other expression for the same variable, equation (3.124), which gives

$$\eta\delta\phi' - \eta'\delta\phi = \frac{3}{2}\phi'\delta\phi. \tag{3.138}$$

This equation is integrable, obtaining

$$\delta\phi(t,u) = F(t)\frac{\phi'}{\beta'}e^{-3\beta}, \tag{3.139}$$

for an arbitrary function $F(t)$. With $\delta\phi$ written in terms of the background functions, we use it back into the master equation (3.136), which reads

$$\frac{2}{3}\frac{\ddot{F}}{F} = \phi'^2 e^{-4\beta} = cst. \tag{3.140}$$

Finally, using the background solutions, (3.134) and (3.135), we check that this does not hold true. Thus, once again we arrive into an inconsistency.

In this section we were able to prove that while the background solutions are stable in the k-essence context, we arrive in an inconsistency when analyzing them for Rastall theory. We cannot conclude, through this analysis, if the solutions are stable or not. We further investigate Rastall theory in the next chapter, tackling one of its main issues.

Seeking out a Lagrangian for Rastall theory

4.1. Introduction

In the previous chapter we made a quick review of two, at first vastly different, theories of gravity in section 3.2, where each of them possess different assumptions and motivations to be considered and, even so, we arrived in the same (geometrical) solution for some particular cases. Taking "coincidences" as a hint on where to further investigate, we compared both theories directly to unveil some new connection between them, we checked under which conditions they behave alike in section 3.3.

With some more clarity of how these theories are intertwined, we verified that both BHs solutions found are unstable in k-essence. Following the same general framework, we showed in section 3.4 that linear time-dependent spherically-symmetric perturbations simply do not exist for Rastall theory. We arrived in inconsistencies in the method applied.

Of course, the first question that we may ask ourselves about such issue is: why? However, up to this point, we have been hiding an important peculiarity of Rastall theory, we *induced* the field equations, it was not derived from a Lagrangian formalism. Simply because it does not exist[1]. We take this as a possibility on the inconsistencies found in the previous chapter, therefore, we are motivated to try to find a Lagrangian that reproduces Rastall field equations.

With that in mind, we investigate the proposals for a Lagrangian formalism in Rastall theory and their consequences.

4.2. Seeking out a Lagrangian for Rastall theory

Rastall field equations are

$$G_{\mu\nu} = T_{\mu\nu} - \frac{b-1}{2} g_{\mu\nu} T, \tag{4.1}$$

$$\nabla_\mu T^{\mu\nu} = \frac{b-1}{2} \nabla^\nu T. \tag{4.2}$$

We already stated that Rastall is an exotic theory due to its non-conservative nature, and now it seems a good time to address its main issues. Visser [118] argues that Rastall's theory could be always recast as standard GR, a point argued against in reference [119]. In some sense, this controversy does not touch the fundamental original approach by Rastall, stated as a modification of the conservation laws due to space-time curvature which is, in our opinion, the more appealing

[1] One could take a step further and even argue if a Lagrangian is really necessary to a fundamental theory of gravity [117].

and physically sound aspect of Rastall gravity. It is also not evident how Visser's argument applies to multi-fields models, since the redefinition in the SET are less evident in this case. We remember, concerning this point, that our universe contains many different components which can only approximately be represented by a single fluid approach.

However, the main argument against Rastall theory is that (4.1) was not deduced following a Lagrangian formalism. We just inferred the field equations that satisfy the conditions desired. The first proposal for finding a Lagrangian for this model was given in reference [120], where the author himself realized that Lagrangian function found was not a scalar density.

More recently, motivated by several different modifications of the Einstein-Hilbert Lagrangian, theories of the type $f(R,\mathcal{L}_m)$ [121] and $f(R,T)$ [122], where $\mathcal{L}_m$ is the usual matter Lagrangian and T is the trace of the SET, were shown to inherently possess $\nabla_\mu T^{\mu\nu}$ different from zero. This led some authors [123, 124, 125] to attempt to find a connection between Rastall theory and the aforementioned models. In these references, the authors propose a similar Rastall Lagrangian of the type $f(R,T)=R+\alpha T$, however, it was not throughly investigated how the addition of matter affetcs the relationship with Rastall's proposal. Specifically in reference [123], it is also claimed that Rastall gravity may be recast using the following prescription $f(R,\mathcal{L}_m)=\alpha R+\mathcal{G}(\mathcal{L}_m)$, where $\mathcal{G}(\mathcal{L}_m)$ is a general function of $\mathcal{L}_m$.

In light of all of this, in the next pages we will analyze the $f(R,\mathcal{L}_m)$ model and show how it cannot recover Rastall gravity. Then, we explicitly calculate how $f(R,T)$ gravity behaves for several different choices of SETs, and demonstrate that it is possible to obtain a similar structure as that given by Rastall gravity but only for perfect fluids. This chapter follows reference [126].

4.2.1. Rastall theory as a $f(R,\mathcal{L}_m)$ theory

As an extension of $f(R)$ models [127], a specific non-minimal coupling of the matter Lagrangian was proposed as a way to investigate non-geodesic motion of massive test particles [128]. The complete generalization of this model, now perceived as an $f(R,\mathcal{L}_m)$ theory, possesses the following Lagrangian formulation

$$\mathcal{L}=\sqrt{-g}f(R,\mathcal{L}_m)+\sqrt{-g}\mathcal{L}_m. \tag{4.3}$$

The correspondent field equations for the metric field is given by

$$f_R R_{\mu\nu}+(g_{\mu\nu}\Box-\nabla_\mu\nabla_\nu)f_R-\frac{1}{2}[f(R,\mathcal{L}_m)-f_{(\mathcal{L}_m)}\mathcal{L}_m]g_{\mu\nu}=f_{(\mathcal{L}_m)}T_{\mu\nu}, \tag{4.4}$$

where we define $f_R=\frac{\partial f}{\partial R}$, $f_{(\mathcal{L}_m)}=\frac{\partial f}{\partial \mathcal{L}_m}$ and adopt the usual definition of the SET as

$$\begin{aligned} T_{\mu\nu}&=-\frac{2}{\sqrt{-g}}\frac{\delta(\sqrt{-g}\mathcal{L}_m)}{\delta g^{\mu\nu}},\\ &=g_{\mu\nu}\mathcal{L}_m-2\frac{\delta\mathcal{L}_m}{\delta g^{\mu\nu}}. \end{aligned} \tag{4.5}$$

In reference [123] it is claimed that choosing $f(R,\mathcal{L}_m)=\alpha R+\mathcal{G}(\mathcal{L}_m)$, where $\mathcal{G}(\mathcal{L}_m)$ is a general function of the matter Lagrangian, Rastall gravity is recovered for any choice of $\mathcal{G}$. The field equations for this case are

$$G_{\mu\nu}=\frac{1}{\alpha}[\mathcal{G}'T_{\mu\nu}+(\mathcal{G}-\mathcal{G}'\mathcal{L}_m)g_{\mu\nu}], \tag{4.6}$$

and using the Bianchi identities, the conservation equations read

$$\nabla^\mu T_{\mu\nu}=\frac{\nabla_\nu(\mathcal{G}'\mathcal{L}_m-\mathcal{G})-T_{\mu\nu}\nabla^\mu\mathcal{G}'}{\mathcal{G}'}, \tag{4.7}$$

where the prime in $\mathcal{G}$ denotes the derivative with respect to $\mathcal{L}_m$.

Through inspection of equation (4.6), one sees that the only way to recover a structure similar to equation (4.1), is to set the function multiplying $T_{\mu\nu}$ to a constant, that is, $\mathcal{G}' = cst$. With thiI see ps choice we are left with

$$\mathcal{G} = c_1\mathcal{L}_m + c_2 \tag{4.8}$$

where $c_{1,2}$ are integration constants, which recovers GR. Non-linear dependences of $\mathcal{G}$ on $\mathcal{L}_m$ lead to strong departures from GR but also from Rastall's gravity.

We check that a general choice of $\mathcal{G}(\mathcal{L}_m)$ cannot recover Rastall gravity. For instance, considering scalar fields such that $\mathcal{L}_m = \partial_\lambda\phi\partial^\lambda\phi$ reduces the above formulation to the k-essence class of theories [129] instead of Rastall's theory.

4.2.2. Rastall theory as a $f(R,T)$ theory

Another way to generalize GR is to assume that the cosmological constant Λ, at first a constant in the EFEs, might be a dynamical term (see reference [130] for a review in several different proposals). One possible formulation to that idea is to assume that the cosmological parameter may depend on the trace of the SET, T. This is known as $\Lambda(T)$ gravity [131], which is now recognized as a particular case of $f(R,T)$ theory.

Despite this dependence on T, that might be motivated due to some exotic fluid, there is a misleading cyclical definition: in the Lagrangian they use T, which is defined by a variational principle of the very same lagrangian. A possible solution to this issue, as it was done in reference [124], is to assume that the trace of T comes from a general and arbitrary tensor contraction, not related to the SET. To recover a Rastall-like field equations, it is necessary to identify T as the usual trace of the SET, which is the standard approach in $f(R,T)$ theories. In what follows we ignore this (very important) conceptual aspect and we focus only on its consequences.

The general Lagrangian for these theories is given by

$$\mathcal{L} = \sqrt{-g}f(R,\mathcal{L}_m) + \sqrt{-g}\mathcal{L}_m. \tag{4.9}$$

Using the same definition for the SET as in equation (4.5), the field equations are

$$f_R R_{\mu\nu} + (g_{\mu\nu}\Box - \nabla_\mu\nabla_\nu)f_R - \frac{1}{2}[f(R,\mathcal{L}_m) - f_{(\mathcal{L}_m)}\mathcal{L}_m]g_{\mu\nu} = f_{(\mathcal{L}_m)}T_{\mu\nu}, \tag{4.10}$$

where

$$\Theta_{\mu\nu} = g^{\alpha\beta}\frac{\delta T_{\alpha\beta}}{\delta g^{\mu\nu}}. \tag{4.11}$$

If we restrict ourselves to the particular case

$$f(R,T) = \alpha R + \beta T, \tag{4.12}$$

where both α and β are constants of the model, the field equations are

$$G_{\mu\nu} = \frac{1-\beta}{\alpha}T_{\mu\nu} + \frac{\beta}{2\alpha}(Tg_{\mu\nu} - 2\Theta_{\mu\nu}), \tag{4.13}$$

with its respective conservation equation

$$\nabla_\mu T^{\mu\nu} = \frac{\beta}{2(\beta-1)}(\nabla^\nu T - 2\nabla_\mu\Theta^{\mu\nu}). \tag{4.14}$$

In reference [123], it was assumed $\Theta_{\mu\nu} = 0$ and the free parameters were set as

$$\begin{aligned} \alpha &= 1 - \beta, \\ \beta &= \frac{b-1}{b-2}, \end{aligned} \tag{4.15}$$

where they claimed that this was Rastall theory. However, as we are going to show, assuming that $\Theta_{\mu\nu}$ vanishes has several theoretical consequences.

Now we evaluate $\Theta_{\mu\nu}$ for some SETs, where we use the following relations

$$\begin{aligned} \frac{\delta g^{\alpha\beta}}{g^{\mu\nu}} &= \delta^{\alpha}_{\mu}\delta^{\beta}_{\nu}, \\ \frac{\delta g_{\alpha\beta}}{g^{\mu\nu}} &= -g_{\alpha\lambda}g_{\beta\gamma}\delta^{\lambda}_{\mu}\delta^{\gamma}_{\nu} = -g_{\alpha\mu}g_{\beta\nu}. \end{aligned} \tag{4.16}$$

4.2.2.1. Electromagnetic case

As in reference [121], the standard Lagrangian for the electromagnetism in vacuum is

$$\mathcal{L}_m = -F_{\mu\nu}F^{\mu\nu}, \tag{4.17}$$

then equation (4.11) yields

$$\Theta_{\mu\nu} = -T_{\mu\nu}. \tag{4.18}$$

The correspondent EFE, equation (4.13) becomes

$$G_{\mu\nu} = \frac{1}{\alpha}T_{\mu\nu}, \tag{4.19}$$

thus

$$\nabla_{\mu}T^{\mu\nu} = 0, \tag{4.20}$$

which is GR with a trivial redefinition of the electromagnetic field. We should have expected this result since the electromagnetic SET is traceless.

So far, we did not obtain any unexpected result, since Rastall recovers GR for this case as well.

4.2.2.2. Perfect-fluid case

We use the SET of the perfect fluid as

$$T_{\mu\nu} = (\rho + p)u_{\mu}u_{\nu} - pg_{\mu\nu}, \tag{4.21}$$

which gives

$$\Theta_{\mu\nu} = -2T_{\mu\nu} - pg_{\mu\nu}. \tag{4.22}$$

Therefore, the respective field equation (4.13) is

$$G_{\mu\nu} = \frac{1+\beta}{\alpha}T_{\mu\nu} + \frac{\beta}{2\alpha}g_{\mu\nu}(T + 2p). \tag{4.23}$$

For the special case $\beta = -1$, the metric field and conservation equations are

$$\begin{aligned} G_{\mu\nu} &= -\frac{1}{2\alpha}[g_{\mu\nu}(T + 2p)], \\ \nabla^{\nu}T &= -2\nabla^{\nu}p. \end{aligned} \tag{4.24}$$

From the last equation, it gives us the EoS

$$p = \rho + \Lambda, \tag{4.25}$$

with Λ being an integration constant. This EoS represents stiff matter with a cosmological constant for $\Lambda \neq 0$, or without it for $\Lambda = 0$. In general, for an arbitrary β, the modified EFEs are not equivalently to either GR nor Rastall theory. This set of equations will be necessary for the hydrodinamical correspondence in the sections to come.

4.2.2.3. Scalar field case

The general Lagrangian of a self-interacting scalar field ϕ is

$$\mathcal{L}_m = -\frac{1}{2}\nabla_\lambda\phi\nabla^\lambda\phi + V(\phi). \tag{4.26}$$

The respective function for $\Theta_{\mu\nu}$[2] yields

$$\Theta_{\mu\nu} = -2T_{\mu\nu} + \frac{1}{2}g_{\mu\nu}T - g_{\mu\nu}V. \tag{4.27}$$

The modified EFEs are then given by

$$G_{\mu\nu} = \frac{1}{\alpha}[(1+\beta)T_{\mu\nu} - \beta g_{\mu\nu}T + \beta g_{\mu\nu}V]. \tag{4.28}$$

Setting $\beta = -1$, both the EFE and the conservation equation reads

$$\begin{aligned} G_{\mu\nu} &= \frac{(T-V)}{\alpha}g_{\mu\nu}, \\ \nabla^\mu V &= 0. \end{aligned} \tag{4.29}$$

That is, for this particular case the field ϕ is not dynamical and, from the SET conservation equation, we check that the potential is constant

$$V = \Lambda. \tag{4.30}$$

We rewrite these two equations in terms of the scalar field ϕ in order to better visualize the differences with respect to GR

$$\begin{aligned} G_{\mu\nu} &= \frac{1+\beta}{\alpha}\left(\nabla_\mu\phi\nabla_\nu\phi - \frac{1}{2}g_{\mu\nu}\nabla_\lambda\phi\nabla^\lambda\phi + g_{\mu\nu}V\right), \\ \Box\phi &= -\frac{1+2\beta}{1+\beta}V_\phi, \end{aligned} \tag{4.31}$$

keeping the usual notation of $V_\phi = \frac{dV}{d\phi}$. We once again recover GR through a trivial redefinition of V and ϕ via

$$\begin{aligned} \sqrt{\frac{1+\beta}{\alpha}}\phi &\to \phi', \\ \frac{1+2\beta}{\alpha}V &\to V'. \end{aligned} \tag{4.32}$$

We remark that depending on the sign of $\frac{1+\beta}{\alpha}$, the scalar field can be either normal or phantom, and the potential may be attractive or repulsive. Nonetheless, the general structure of these equations does not correspond to Rastall gravity.

[2] In reference [121], there is a factor 2 missing, probably a typo.

4.2.2.4. Self-interacting scalar field and fluid correspondence

In reference [132], a direct correspondence between the scalar field and perfect fluid was studied. We first outline the procedure, and then use it to our case.

For a lagrangian of the type

$$\begin{aligned} \mathcal{L} &= \sqrt{-g}\mathcal{L}(X,\phi), \\ X &= \frac{1}{2}\nabla_\lambda\phi\nabla^\lambda\phi, \end{aligned} \tag{4.33}$$

we can make a correspondence with thermodynamic quantities. Assuming $\mathcal{L}(X,\phi) = X - V(\phi)$ its pressure, density and four-velocity of a fluid, are respectively related to the scalar field as

$$\begin{aligned} p &= \mathcal{L}, \\ \rho &= 2X\mathcal{L}_X - \mathcal{L}, \\ u_\mu &= \nabla_\mu\left(\frac{\phi}{\sqrt{2X}}\right). \end{aligned} \tag{4.34}$$

With this, we can directly induce the following relations

$$\begin{aligned} \rho &= X + V, \\ p &= X - V. \end{aligned} \tag{4.35}$$

To distinguish both terms, we use "f" for the fluid components and "ϕ" for the scalar fluid ones. With equation (4.35), both SETs are related via

$$\begin{aligned} T^f_{\mu\nu} &= (\rho + p)u_\mu u_\nu - p g_{\mu\nu}, \\ &= \nabla_\mu\phi\nabla_\nu\phi - \frac{1}{2}g_{\mu\nu}\nabla_\lambda\phi\nabla^\lambda\phi + g_{\mu\nu}V(\phi) = T^\phi_{\mu\nu}. \end{aligned} \tag{4.36}$$

Similarly, the function $\Theta_{\mu\nu}$ of the fluid may be recast in terms of the scalar field SET as

$$\begin{aligned} \Theta^f_{\mu\nu} &= -T^f_{\mu\nu} - p g_{\mu\nu} = -2T^\phi_{\mu\nu} - (X - V)g_{\mu\nu}, \\ &= -T^f_{\mu\nu} + \frac{1}{2}g_{\mu\nu}T^\phi - g_{\mu\nu}V. \end{aligned} \tag{4.37}$$

Using the hydrodynamical representation, the modified EFEs become

$$G_{\mu\nu} = \frac{1+\alpha}{1-\alpha}T_{\mu\nu} + \frac{\alpha(\rho - p)}{2(1-\alpha)}g_{\mu\nu}. \tag{4.38}$$

Using the fluid/scalar field correspondence, we see that equation (4.38) is the standard scalar field equation. In particular, a rather simple case is obtained when setting $\rho = p$, which can be seen from relations (4.35) that it represents a free scalar field.

We recognize that there seems to be non-trivial situations in the fluid representation (besides the scalar field one) when $\rho \neq p$. Likewise, we think that this correspondence may be further investigated when the potential is exponential, which coincide to a fluid with $p = \omega\rho$, with ω constant. However, we will not investigate such cases here.

4.2.3. ΛCDM

Through the previous sections, we were able to see that we could not recover Rastall using any of the proposed frameworks. We side-track a bit in the next section to recover an important result using the scalar field/fluid correspondence. We show how the $f(R,T)$ model recovers ΛCDM model, as in reference [104].

4.2.3.1. Background evolution

First we rewrite equations (4.24) while setting $\alpha = 1 + \beta$. That is, the modified EFEs, and the respective conservation equations, are

$$\begin{aligned} G_{\mu\nu} &= T_{\mu\nu} + \frac{\beta}{2(1+\beta)} g_{\mu\nu}(T + 2p), \\ \nabla_\mu T^{\mu\nu} &= -\frac{\beta}{2(1+\beta)} \nabla^\nu (T + 2p). \end{aligned} \tag{4.39}$$

To obtain a cosmological solution, we assume a metric of the type

$$ds^2 = dt^2 - a(t)^2 \delta_{ij} dx^i dx^j, \tag{4.40}$$

where the matter content assumed to be of a perfect fluid, with its SET given by (4.24), and both the pressure and density depending on the time coordinate t as

$$\begin{aligned} \rho &= \rho(t), \\ p &= p(t). \end{aligned} \tag{4.41}$$

The resulting equations are

$$\begin{aligned} 3H^2 &= \frac{2+3\beta}{2(1+\beta)}\rho - \frac{\beta}{2(1+\beta)}p, \\ \left[\frac{2+3\beta}{2(1+\beta)}\right]\dot{\rho} - \frac{\rho}{2(1+\beta)}\dot{p} + 3H(\rho + p) &= 0. \end{aligned} \tag{4.42}$$

For the next step, we can decompose the fluid into two different components

$$\begin{aligned} \rho &= \rho_m + \rho_\Lambda, \\ p &= p_m + p_\Lambda = -\rho_\Lambda, \end{aligned} \tag{4.43}$$

that is, pressureless matter (denoted by the subscript m, $p_m = 0$) and a cosmological term (denoted by the standard notation Λ, $p_\Lambda = -\rho_\Lambda$). We are able to write equations (4.42) as

$$\begin{aligned} 3H^2 &= \frac{2+3\beta}{2(1+\beta)}\rho_m + \frac{1+2\beta}{1+\beta}\rho_\Lambda, \\ \frac{2+3\beta}{2(1+\beta)}\dot{\rho}_m + \frac{1+2\beta}{1+\beta}\dot{\rho}_\Lambda + 3H\rho_m &= 0. \end{aligned} \tag{4.44}$$

To allow structures to be formed in the late-universe, we impose that the matter component conserves separately[3]. That is, the continuity equation for this fluid reads

$$\dot{\rho}_m + 3H\rho_m = 0, \tag{4.45}$$

which may be integrated to obtain its evolution in time

$$\rho_m = \frac{\rho_{m0}}{a^3}, \tag{4.46}$$

where ρ_{m0} is the integration constant defined as the matter density at present time.

[3]Something really similar to what we have done in section 3.3.2.2 for Case 2 in the Rastall/k-essence duality.

Thus, equations (4.44) become

$$\begin{aligned} 3H^2 &= \frac{2+3\beta}{2(1+\beta)}\rho_m + \frac{1+2\beta}{1+\beta}\rho_\Lambda, \\ \left[\frac{\beta}{2(1+\beta)}\right]\dot{\rho}_m &+ \frac{1+2\beta}{1+\beta}\dot{\rho}_\Lambda = 0. \end{aligned} \tag{4.47}$$

The second equation of this pair can be integrated, yielding

$$\rho_\Lambda = -\frac{\beta}{2(1+2\beta)}\rho_m + \rho_{\Lambda 0}, \tag{4.48}$$

where $\rho_{\Lambda 0}$ is the integration constant defined as the cosmological constant density at present time. Ultimately, we get to

$$\begin{aligned} 3H^2 &= \rho_m + \bar{\rho}_{\Lambda 0}, \\ \bar{\rho}_{\Lambda 0} &= \frac{1+2\beta}{1+\beta}\rho_{\Lambda 0}. \end{aligned} \tag{4.49}$$

Hence, the ΛCDM model re-appears. All the background tests are thus equally satisfied, as explained in reference [104].

In this section we were able to show that from a intrinsically non-conservative modified theory of gravity, $f(R,T)$, the ΛCDM model was re-obtained. On the other hand, the cosmological constant does not behave as in GR, since the non-conservation of this component changes its evolution.

4.2.3.2. Evolution of matter perturbation

We have shown that ΛCDM model is recovered in the background equations. Now we take a step further showing that this is also the case in the perturbative level. We recast the two main equations in a more suitable way

$$\begin{aligned} R_{\mu\nu} &= T_{\mu\nu} - \frac{1+2\beta}{2(1+\beta)}g_{\mu\nu}T - \frac{\beta}{1+\beta}g_{\mu\nu}p, \\ \nabla_\mu T^{\mu\nu} &= -\frac{\beta}{2(1+\beta)}\nabla^\nu(T+2p). \end{aligned} \tag{4.50}$$

These equations are written in its covariant form, thus we are free to choose the syncronous gauge, defined by $h_{\mu t} = 0$ [133]. We choose the standard linearly perturbed FLRW metric as well, keeping the same notation from chapter 2, where the perturbed metric quantities are denoted as $h_{\mu\nu}$. We may simplify the equations introducing the following definition

$$h = \frac{h_{kk}}{a^2}. \tag{4.51}$$

Just like as we did in equations (4.43), we divide the SET into two different fluids

$$T^{\mu\nu} = T^{\mu\nu}_m + T^{\mu\nu}_\Lambda, \tag{4.52}$$

with

$$\begin{aligned} T^{\mu\nu}_m &= \rho_m u^\mu u^\nu, \\ T^{\mu\nu}_\Lambda &= \rho_\Lambda g^{\mu\nu}. \end{aligned} \tag{4.53}$$

Following the same reasoning as before, we assume that the matter SET conserves

$$\nabla_\mu T_m^{\mu\nu} = 0, \tag{4.54}$$

and the conservation equation (4.50) yields

$$\nabla_\mu T_\Lambda^{\mu\nu} = -\frac{\beta}{2(1+\beta)}\nabla^\nu(T_t + 2p_t), \tag{4.55}$$

where the subscript t stands for the total contribution.

As we have showed, the background solutions works out just as in reference [104], therefore we can follow the same steps for the perturbative part as well. With this, the perturbed equations are

$$\begin{aligned} \frac{\ddot{h}}{2} + H\dot{h} &= \frac{1}{2(1+\beta)}\delta\rho_m - \frac{1+2\beta}{1+\beta}\delta\rho_\Lambda, \\ \frac{\delta\rho_m}{\rho_m} &= \frac{\dot{h}}{2}, \\ \delta\dot{\rho}_\Lambda &= -\frac{\beta}{2(1+2\beta)}\delta\dot{\rho}_m. \end{aligned} \tag{4.56}$$

Using the standard definition of the density contrast as

$$\delta_m = \frac{\delta\rho_m}{\rho_m}, \tag{4.57}$$

we can merge equations (4.56) together to obtain

$$\ddot{\delta}_m + 2H\dot{\delta}_m - \frac{1}{2}\rho_m\delta_m = 0. \tag{4.58}$$

Therefore, the evolution of small matter fluctuations in the model under consideration is also identical to the one in the ΛCDM model of GR. Despite the similarities, an important difference is that the cosmological constant introduced in the $f(R,T)$ theory is not really a constant, but has an evolution dictated by the non-conservative character of the theory. This feature is the same as it was found in reference [104] for the standard Rastall gravity.

Charged BH and radiating solutions in entangled relativity

5.1. Introduction

Entangled relativity [134, 135, 136, 137] is a theory of relativity that fulfills Einstein's original idea that "there can be no G-field [space-time] without matter" [138], while at the same time it recovers many predictions of general relativity—without any novel field, see [135] and references therein. Einstein originally thought that general relativity augmented with a cosmological constant Λ would possess the wanted property that "physical qualities of space are *completely* determined by matter alone" [139]; whereas it was obviously not the case with general relativity without a cosmological constant since a flat space-time is obviously solution of vacuum in that case [138]. Indeed, the existence of space-time without matter means that inertia *can* be defined relative to *space* only, whereas Einstein had in mind that inertia—and, of course, angular momentum—could only be defined relatively to surrounding matter [140, 141, 142]. One has to keep in mind that in 1918, according to Einstein, the impossibility of the existence of space-time (hence gravity and inertia) without matter—that follows from *his interpretation* of some of the ideas of Mach [140, 143, 141, 142], which *he* named *Mach's principle* [138]—was one of the three requirements of a satisfying general theory of relativity, together with the need of covariant equations—which follow from the *principle of relativity*—and the fact that the metric tensor determines the metric properties of space, the inertial behavior of bodies in this space, as well as the gravitational effects—which follow from the *principle of equivalence* [138]. Hence, de Sitter's solution [144] of GR with a cosmological constant—but in vacuum otherwise—was quite unsatisfactory to Einstein, as it meant that "the Λ-term does not fulfill the purpose [*he*] *intended* [...] that no $g_{\mu\nu}$-field must exist without matter that generates it" [139]. In other words, Einstein believed in the *relativity of inertia* [141, 142] that, despite his initial hopes, turned out not to be valid (at least in general) in the framework of GR [141, 142]. This is arguably a very serious ontological issue of GR [142, 145].

Nevertheless, BH solutions in vacuum of GR—such as the Schwarzschild and the Kerr metrics—play an important role in explaining many different phenomena, from the observations of the Event Horizon Telescope [146, 147] to the detection of gravitational waves [15, 73]. Therefore, it is important to check whether or not the usual vacuum solutions of GR—which are good mathematical idealization of astrophysical BHs—are also good approximations of BHs in entangled relativity.

While vacuum solutions should not exist in entangled relativity, nothing prevents the density of matter field outside the event horizon to be arbitrarily small—notably recovering some usual astrophysical conditions. In what follows, we shall name such a condition a *near vacuum situation*.

In the present chapter, we shall present an exact spherical solution of entangled relativity that can be approximated by the Schwarzschild metric in a near vacuum situation. We shall then argue that this result could actually come from a general property that makes that vacuum solutions of GR good approximations of near vacuum solutions of entangled relativity. It is therefore argued that astrophysical BHs of entangled relativity are likely indistinguishable from the ones of GR in many cases. This chapter closely follows reference [148].

5.2. Action and field equation

The action of entangled relativity is given by [135]

$$S = -\frac{\xi}{2c}\int \mathrm{d}^4x\sqrt{-g}\frac{\mathcal{L}_m^2}{R}, \tag{5.1}$$

where the constant ξ has the dimension of the usual coupling constant of GR $\kappa \equiv 8\pi G/c^4$—where G is the Newtonian constant and c the speed of light. R is the usual Ricci scalar constructed upon the space-time metric $g_{\alpha\beta}$, with determinant g; while $\mathcal{L}_m$ is a scalar Lagrangian representing the matter fields. ξ defines a novel fundamental scale that is relevant at the quantum level only, and therefore is notably not related to the size of BHs; whereas the Planck scale—defined from κ and which is related to the size of BHs—no longer is fundamental, nor constant, in entangled relativity [135]. [1] The impossible existence of gravity without matter, and vice versa, is obvious from the action. It comes from the fact that one has replaced the usual additive coupling between matter and geometry by a pure multiplicative coupling. For $\mathcal{L}_m \neq 0$, the metric field equation reads

$$R_{\mu\nu} - \frac{1}{2}g_{\mu\nu}R = -\frac{R}{\mathcal{L}_m}T_{\mu\nu} + \frac{R^2}{\mathcal{L}_m^2}\left(\nabla_\mu\nabla_\nu - g_{\mu\nu}\Box\right)\frac{\mathcal{L}_m^2}{R^2}, \tag{5.2}$$

with

$$T_{\mu\nu} \equiv -\frac{2}{\sqrt{-g}}\frac{\delta\left(\sqrt{-g}\mathcal{L}_m\right)}{\delta g^{\mu\nu}}. \tag{5.3}$$

Note that the trace of Eq. (5.2) reads

$$3\frac{R^2}{\mathcal{L}_m^2}\Box\frac{\mathcal{L}_m^2}{R^2} = -\frac{R}{\mathcal{L}_m}\left(T - \mathcal{L}_m\right). \tag{5.4}$$

Also note that the stress-energy tensor is no longer conserved in general, as one has

$$\nabla_\sigma\left(\frac{\mathcal{L}_m}{R}T^{\alpha\sigma}\right) = \mathcal{L}_m\nabla^\alpha\left(\frac{\mathcal{L}_m}{R}\right). \tag{5.5}$$

But entangled relativity is more easily understood in its dilaton equivalent[2] form that reads [134, 135]

$$S = \frac{1}{c}\frac{\xi}{\tilde{\kappa}}\int d^4x\sqrt{-g}\left[\frac{\phi R}{2\tilde{\kappa}} + \sqrt{\phi}\mathcal{L}_m\right], \tag{5.6}$$

[1] As also discussed in [137, 149], this might be a way out of the ontological paradox of conventional quantum gravity that, in Freeman Dyson's words [150], "nature conspires to forbid any measurement [through the creation of BHs] of distance with error smaller than the Planck length", because the effective Planck scale [135]—which fixes the size of a BH's event horizon for a given mass—depends on the field equations in entangled relativity.

[2] This dilaton theory is equivalent, at least at the classical level, as long as $\mathcal{L}_m/R < 0$. Notably, it seems that one must always consider cases such that $(R, \mathcal{L}_m) \neq 0$ when one uses the dilaton form of entangled relativity, although R and $\mathcal{L}_m$ can be arbitrarily small in principle. We shall come back on this point in the later on.

where $\tilde{\kappa}$ is a positive effective coupling constant between matter and geometry, with the dimension of κ. $\tilde{\kappa}$ takes its value from the asymptotic behavior of the effective scalar degree of freedom in Eq. (5.1) [134, 135], as well as the considered normalisation of ϕ. $\tilde{\kappa}/\sqrt{\phi}$, which defines an effective Planck scale, notably fixes the size of BHs with a given mass. The equivalence between the two actions is similar to the equivalence between $f(R)$ theories and the corresponding specific scalar-tensor theories [151]. From this alternative action, one can easily see why entangled relativity reduces to GR when the variation of the scalar-field degree of freedom vanishes. The dilaton field equations read

$$G_{\alpha\beta} = \tilde{\kappa}\frac{T_{\alpha\beta}}{\sqrt{\phi}} + \frac{1}{\phi}\left[\nabla_\alpha\nabla_\beta - g_{\alpha\beta}\Box\right]\phi, \tag{5.7}$$

$$\sqrt{\phi} = -\tilde{\kappa}\mathcal{L}_m/R, \tag{5.8}$$

where $G_{\alpha\beta}$ is the Einstein tensor and the conservation equation reads

$$\nabla_\sigma\left(\sqrt{\phi}T^{\alpha\sigma}\right) = \mathcal{L}_m\nabla^\alpha\sqrt{\phi}, \tag{5.9}$$

The trace of the metric field equation can therefore be rewritten as follows

$$\frac{3}{\phi}\Box\phi = \frac{\tilde{\kappa}}{\sqrt{\phi}}\left(T - \mathcal{L}_m\right). \tag{5.10}$$

The equivalence between Eqs. (5.7-5.10) and (5.2-5.5) is pretty straightforward to check. This simply means that, indeed, the action (5.1) possesses an additional gravitational scalar degree of freedom with respect to GR.

The good thing with this extra degree of freedom is that it is not excited in all situations where $\mathcal{L}_m \sim T$. This leads to a phenomenology that closely resembles the one of GR [152, 135, 153, 154, 137]; whereas it is expected to differ from the one of GR in all other situations—see e.g. [136] or [149]. As a consequence, the theory seems to be viable from an observational perspective, while at the same time it offers potential interesting new avenues—as we will see, notably in Sec. 5.3.1. The electromagnetic field being the easiest (and perhaps the only) matter field with infinite range to consider, we will only study the case of the electromagnetic Lagrangian $\mathcal{L}_m = -F^2/(2\mu_0)$ in what follows, where μ_0 is the magnetic permeability.[3] With this Lagrangian, the electromagnetic field equation reads

$$\nabla_\sigma\left(\sqrt{\phi}F^{\mu\sigma}\right) = \nabla_\sigma\left(\frac{\mathcal{L}_m}{R}\ F^{\mu\sigma}\right) = 0. \tag{5.11}$$

Let us note that the equivalence of the original action of entangled relativity in Eq. (5.1) with an Einstein-Maxwell-dilaton theory—see Eqs. (5.6) and (5.12)—seems to indicate that the theory is well-behaved with respect to various aspects, such as the Ostrogradsky instabily [156, 157] or the well-posedness of the initial value problem [158, 159, 160, 161]. Indeed, Einstein-Maxwell-dilaton theories are second-order theories that are notably known to have a well-posed initial-value problem [162, 163]. This is similar to what happens with fourth-order $f(R)$ theories [159, 160, 156].

[3] In natural units, we consider $\mathcal{L}_m = -F^2/2$ instead of $\mathcal{L}_m = -F^2/4$, in order to follow the definition used in the literature [155]. In particular, it means that the electromagnetic stress-energy tensor reads $T^{\mu\nu} = 2\left(F^{\mu\alpha}F^{\nu}{}_{\alpha} - \frac{1}{4}g^{\mu\nu}F_{\alpha\beta}F^{\alpha\beta}\right)$ in natural units.

5.3. Charged BH

In its scalar-tensor form (5.6), entangled relativity is just a specific case of a dilaton theory, for which the solution for charged BH has been investigated by many authors during the first superstring revolution [164, 165]. Indeed, defining the Einstein frame metric by $\tilde{g}_{\alpha\beta} = e^{-2\varphi/\sqrt{3}} g_{\alpha\beta}$, with $\phi = e^{-2\varphi/\sqrt{3}}$, the action in the Einstein frame reads

$$S = \frac{1}{c}\frac{\xi}{\kappa}\int d^4x\sqrt{-\tilde{g}}\left[\frac{1}{2\kappa}\left(\tilde{R} - 2\tilde{g}^{\alpha\beta}\partial_\alpha\varphi\partial_\beta\varphi\right) - e^{-\varphi/\sqrt{3}}\frac{\tilde{F}^2}{2\mu_0}\right], \tag{5.12}$$

where $\tilde{F}^2 = \tilde{g}^{\alpha\sigma}\tilde{g}^{\beta\epsilon}\tilde{F}_{\sigma\epsilon}\tilde{F}_{\alpha\beta}$, where $\tilde{F}_{\alpha\beta} := F_{\alpha\beta}$. One has used the conformal invariance of the electromagnetic action. From now on, in order to follow the literature, we use natural units. This action corresponds exactly to the one considered in [155, 166, 167, 168] with $a = (2\sqrt{3})^{-1}$. The spherical solution therefore reads

$$\mathrm{d}\tilde{s}^2 = -\tilde{\lambda}^2\mathrm{d}t^2 + \tilde{\lambda}^{-2}\mathrm{d}r^2 + \tilde{\rho}^2\left(\mathrm{d}\theta^2 + \sin^2\theta\mathrm{d}\psi^2\right), \tag{5.13}$$

with

$$\tilde{\lambda}^2 = \left(1 - \frac{r_+}{r}\right)\left(1 - \frac{r_-}{r}\right)^{\left(1-a^2\right)/\left(1+a^2\right)}, \tag{5.14}$$

and

$$\tilde{\rho}^2 = r^2\left(1 - \frac{r_-}{r}\right)^{2a^2/\left(1+a^2\right)}, \tag{5.15}$$

whereas the field solutions read

$$\tilde{F} = -\frac{Qe^{2a\varphi}}{\tilde{\rho}^2}dt\wedge dr = -\frac{Q}{r^2}dt\wedge dr, \tag{5.16}$$

for an electric charge, and

$$e^{2a\varphi} = \left(1 - \frac{r_-}{r}\right)^{2a^2/\left(1+a^2\right)}, \tag{5.17}$$

where we normalized the scalar-field such that its background value φ_0 corresponds $\varphi_0 = 0$. r_+ is an event horizon, whereas r_- is a curvature singularity for $a \neq 0$. They are related to the mass and charge, M and Q, by

$$2M = r_+ + \left(\frac{1-a^2}{1+a^2}\right)r_-, \tag{5.18}$$

and

$$Q^2 = \frac{r_-r_+}{1+a^2}. \tag{5.19}$$

Performing the inverse conformal transformation $g_{\alpha\beta} = e^{2\varphi/\sqrt{3}}\tilde{g}_{\alpha\beta}$ in order to have the solution of the action Eq. (5.6), one gets

$$\mathrm{d}s^2 = -\lambda_0^2\mathrm{d}t^2 + \lambda_r^{-2}\mathrm{d}r^2 + \rho^2\left(\mathrm{d}\theta^2 + \sin^2\theta\mathrm{d}\varphi^2\right), \tag{5.20}$$

with

$$\lambda_0^2 = \left(1 - \frac{r_+}{r}\right)\left(1 - \frac{r_-}{r}\right)^{15/13}, \tag{5.21}$$

$$\lambda_r^2 = \left(1 - \frac{r_+}{r}\right)\left(1 - \frac{r_-}{r}\right)^{7/13}, \tag{5.22}$$

$$\rho^2 = r^2\left(1 - \frac{r_-}{r}\right)^{6/13}. \tag{5.23}$$

The scalar-field solution on the other hands reads

$$\phi = \left(1 - \frac{r_-}{r}\right)^{-4/13}. \tag{5.24}$$

The solution (5.20-5.24) has been verified via Mathematica, the code is accessible on GitHub [169]. It is therefore the first known BH solution of entangled relativity.

$r_- \to 0$ corresponds to a near vacuum situation described in the introduction. In this limit, the scalar-field tends to a constant field and the metric in Eq. (5.20) tends to the Schwarzschild solution in a near vacuum situation.

This represents the first example for which an exact solution of entangled relativity is shown to be well approximated in a near vacuum situation by the usual Schwarzschild solution in vacuum. This is an indication that the outside metric of the Schwarzschild solution can be an accurate mathematical idealisation of a non-rotating astrophysical BH in entangled relativity.

5.3.1. Discussion on the validity of the solution beyond the event horizon

While the solution (5.20-5.24) seems perfectly well behaved within the event horizon at a mathematical level, we would like to argue that this region might not correspond to the solution after the collapse of an astrophysical object, therefore only the region outside the event horizon might be relevant at the physical level. The reason being that nothing guarantees that singularities occur after the collapse of compact objects in entangled relativity.

Indeed, the effective coupling $8\pi G_{eff}/c^4 := -R/\mathcal{L}_m$ between matter and curvature in the metric field equation (5.2) is not necessarily positive everywhere since it notably depends on the on-shell value of matter fields $\mathcal{L}_m$. As a consequence, gravity is potentially not attractive everywhere in entangled relativity, but also repulsive in some places. In particular, if one assumes that $\mathcal{L}_m = K - V$, where K and V are the kinetic and potential energy densities, it seems plausible that $\mathcal{L}_m$ flips its sign at high enough energy, when kinetic energy should dominate matter dynamics. It may not mean that the effective coupling between matter and curvature in the metric field equation becomes negative. But if it does—such that gravity can indeed become repulsive at a given high energy threshold—one can genuinely assume that the solution will not look like (5.20-5.24) within the event horizon. Unfortunately, investigating this issue seems to require an accurate description of matter fields at (arbitrarily) high energy; while it is believed that the standard model of particles is not accurate at (arbitrarily) high energy.

The transition between the attractive and repulsive cases seems to be singular, or at least ambiguous, in the metric field equation (5.2), since one has to go through $\mathcal{L}_m = 0$. However, this is likely not the case for the following reason. One can see that the metric field equation that derives from the action (5.1) actually originally reads for all $\mathcal{L}_m$,

$$\frac{\mathcal{L}_m^2}{R^2}\left(R_{\mu\nu} - \frac{1}{2}g_{\mu\nu}R\right) = -\frac{\mathcal{L}_m}{R}T_{\mu\nu} + \left(\nabla_\mu\nabla_\nu - g_{\mu\nu}\Box\right)\frac{\mathcal{L}_m^2}{R^2}, \tag{5.25}$$

instead of Eq. (5.2), as it usually appears in the literature for its resemblance with the usual form of the equation of Einstein. Therefore, one can see that any metric that leads to a non-null Ricci scalar is likely consistent with $\mathcal{L}_m = 0$ on-shell. As a consequence, the transition between $\mathcal{L}_m < 0$ and $\mathcal{L}_m > 0$ is likely not singular if one has $R \neq 0$ at the transition. If that happens, not only the transition would be regular, but it would also correspond to a transition from attractive to repulsive gravity—that is, from $\mathcal{L}_m/R < 0$ to $\mathcal{L}_m/R > 0$ in Eq. (5.2)—given that the effective coupling between matter and curvature can be written as $8\pi G_{eff}/c^4 := -R/\mathcal{L}_m$. This very interesting topic is left for further studies.

5.4. Pure electromagnetic radiation

The case of pure electromagnetic radiation is of interest because radiating solutions of GR seems to satisfy entangled relativity as well, despite an apparent ambiguity in the field equations.

Indeed, from the trace of Einstein's equation of GR, and from the conformal invariance of electromagnetism, one deduces that any purely radiative solution of GR must be such that $R = T = 0$. Also, even though one has $T_{\mu\nu} \neq 0$, the electromagnetic Lagrangian $\mathcal{L}_m = B^2 - E^2$ vanishes on-shell in entangled relativity as well, since $E^2 = B^2$ for pure radiation. Therefore, assuming any purely radiative solution of GR, one has $\mathcal{L}_m = R = T = 0$.

Nevertheless, $\phi = \tilde{\kappa}^2\mathcal{L}_m^2/R^2 = \phi_0$, where ϕ_0 is a constant, is consistent with all the field equations of entangled relativity, because in that case, they reduce exactly to the one of the Einstein-Maxwell theory. Hence, any purely radiative solution of GR seems likely to be solution in entangled relativity as well. The division $\mathcal{L}_m^2/R^2$, however, is ambiguous, despite it being a constant.

At this stage, we do not conclude that purely radiative solutions of GR are also solutions of entangled relativity, but that it seems that it might very well be. In any case, these solutions, such as Vaidya's radiating Schwarzschild solution [170, 171], may be used in order to study the behavior of entangled relativity in the limit $(\mathcal{L}_m, T, R) \to 0$. Another possibility to study such cases might be achieved by analysing a solution that is both charged and radiating, and then taking the limit when its charge goes to zero. This issue is left for further studies.

Nevertheless, note that even if it turns out that a pure radiative field cannot be solution in entangled relativity (5.1), this might not be a fundamental issue for the theory, as the quantum trace anomaly of self-interacting fields in a curved background should induce small, but non-null, values of the Ricci scalar, the trace of the stress-energy tensor and the Lagrangian that appears in the field equations [172, 137]. Quantum trace anomalies may therefore imply that the theory is well behaved everywhere. Investigation of this aspect is left for further studies.

5.5. Discussion

Now we argue that, in general, vacuum solutions of GR can be good approximations of some near vacuum BH solutions of entangled relativity. Indeed, in a near vacuum situation—that is $T_{\mu\nu} \sim 0$—the scalar-field in Eq. (5.10) can be approximated as being sourceless. As a consequence, a constant scalar-field is a good approximation as well, and the metric field equation becomes itself well approximated by the one of GR without a cosmological constant.[4]

This means that while BHs in entangled relativity are not entirely the same as in GR, their differences might be insignificant in situations that correspond to a scalar-field which equation is mostly sourceless. In particular, this argument seems to indicate that an astrophysical rotating BH in entangled relativity could be well approximated by the external Kerr metric of GR.

Otherwise, it is known that BHs might grow some *hair* due to a variation (either temporal or spatial) of the background value of the scalar-field in scalar-tensor theories [**?**]. Let us note that, whether or not this may be true in entangled relativity as well, the scalar-field is not expected to vary significantly neither temporally nor spatially. Indeed, with respect to the former, the scalar-field is attracted toward a constant in entangled relativity during the expansion of the universe [153, 154, 137]; whereas, because the scalar-field is also not sourced by pressure-less

[4] Given the small value of the inferred cosmological constant in GR from the apparent acceleration of the expansion of the universe, BH solutions of GR with and without a cosmological constant are alike on scales well below the Hubble scale. Hence, we will not enter into such details.

matter fields in the weak field regime [152], one does not expect a significant spatial variation of the scalar-field either. Both cases follow from the *intrinsic decoupling* of the scalar-field at the level of the scalar-field equation for $\mathcal{L}_m \sim T$ [152, 153, 154, 173, 137].

Before concluding, we would like to stress again that one should not take seriously the exact solutions beyond the event horizon. Indeed, in order to describe any compact object inside the BH in this model, one must have a high energy description of matter fields in order to tell what happens there in entangled relativity. The reason being that gravity becomes repulsive in entangled relativity for matter fields that are such that $\mathcal{L}_m/R > 0$ [149],[5] and one cannot exclude the possibility that this situation could happen after a phase transition of matter fields at high energy. In particular, this may be a way to avoid BH singularities [174] without the absolute need of a quantum field description of gravity [149].

[5] See the first term of the right hand side of Eq. (5.2).

Conclusions

We conclude this thesis summarizing the main result achieved in each part.

In chapter 2 we first investigated the theory behind the last stage of the coalescence of two BHs, quasi-normal modes oscillation. In section 2.2, we detailed how perturbation theory is applied in this context. We developed the first-order perturbation of the Einstein tensor; then, we showed how the invariance under rotation of the two-dimensional sub-space splits the perturbations in either one of the two categories: *axial* or *polar* parity; we classified these components using the SVT decomposition, and related each component to a spin-weighted spherical harmonic.

We attained our attention to some specific solutions in the context of GR, in section 2.3. First, singular BHs: Schwarzschild, Reissner-Nordström and Schwarzschild de-Sitter; then regular BHs: Bardeen and Hayward. For each case we discussed the BH's main properties like, horizons, singularities and how the parameters change the solutions. We showed the effective potential for the *gravitational*, *electromagnetic* and *scalar* test-fields for each one and discussed its main properties.

Then we focused our attention into obtaining the quasi-normal frequencies given by these potentials. In section 2.4 we quickly reviewed the analytical method of the Pöschl-Teller potential. This method is well suited for frequencies in the eikonal limit, while also being an exact case for some particular BHs solutions.

Thereafter, in section 2.5, we developed the WKB method, a well refined scheme where the quasi-normal frequencies are a good approximation to the numerical result. In section 2.6 we used the third-order WKB method to fully investigate how each of the solutions behave under the variation of the parameters. The general results that we obtained were: all the BHs investigated are expected to be stable; the mass always decrease the real frequency of oscillation, while it becomes less damped; the solutions which possess a charge are barely sensible to the variation of ℓ and in all cases, the real frequency decreases as the overtone number increases, the opposite occurs to the imaginary frequency.

We finish this chapter with 2.7 where we delve ourselves into the observational part of the ringdown phase of the coalescence. First we analyse a model-independent strain, constructed from a damped sinusoidal wave, and we show how we can use this to obtain the final intrinsic parameter of the remnant BH. Next, we choose a different wave strain $h(t)$ using a first-principles model. BOB recovers the information from the system in its binary stage, from the ISCO position, up to the final BH. The whole model relies on tracing back the null bundle of light rays from the remnant BH to the unstable orbit.

We close this chapter by showing some results using BOB. We show that for both GW150914 and GW170104 the spin parameter a agrees with the previous published results. However, the value that we obtained for the mass is reasonably higher.

In chapter 3 onward, we move on to a more theoretical part of this thesis. First we investigate

how two seemingly different theories, k-essence, a model with an arbitrary function of the kinetic term for the scalar field, and Rastall, a non-conservative theory of gravity, have similarities for some particular BH-like cases. We take our time in section 3.2 to review these two models, detailing their main structure and motivations first, and then stating the spherically-symmetric solutions obtained. We make note that the geometric solutions are the same in both cases, while the scalar field solution differ from each other.

Given this "coincidence", we analyze how deep this relationship between these two models go in section 3.4. For the scalar-vacuum case, this duality occurs with simple relations between the potentials, scalar fields and the free parameter of the theories. For a FLRW metric, given a perfect fluid, the two types that we investigate are: Case 1 - No mixing of the scalar field and the matter field, where both SETs obey Rastall non-conservative condition; Case 2 - Conservative matter, where only the matter SET obeys the conservation equation.

The duality has been established for Case 1 of Rastall's theory with an arbitrary EoS of matter. It has been found that the EoS of matter is different in the mutually dual k-essence and Rastall models; however, it is argued that the respective speeds of sound are the same. Since the speeds of sound characterizing the scalar fields (ϕ in k-essence theory and ψ in Rastall's) also coincide, we conclude that the duality is maintained not only for the cosmological backgrounds but also for adiabatic perturbations.

For Case 2 of Rastall's theory, it has been found that the duality exists only with fluids having the EoS $p = \omega\rho$, which is the same for k-essence and Rastall models. Moreover, in the k-essence model, the scalar field obeys the same effective EoS. However, on the perturbative level the mutually dual models behave, in general, differently.

Some special cases have been discussed, showing how there emerge some restrictions on the free parameters of each theory.

An example has been considered in which a cosmological model completely equivalent to the ΛCDM model of GR is obtained at the background level, but different features must appear at the perturbative level.

Established some conditions for both theories to behave alike each other, we move on onto checking if the BHs solutions are stable in both formalisms in section 3.4. After showing the whole first-order formalism for k-essence, we show that the two BHs are unstable. However, such stability analysis in the Rastall case is inconsistent: linear time-dependent spherically symmetric perturbations simply do not exist.

In chapter, 4, we focus in Rastall's theory and tackle some theoretical issues that it possess. In section 4.2, we look after the proposals for a lagrangian for Rastall theory. First, we showed that theories of type $f(R, \mathcal{L}_m)$ cannot reproduce Rastall gravity. Even assuming $f(R, \mathcal{L}_m) = \alpha R + \mathcal{G}(\mathcal{L}_m)$, this structure either recovers GR, or strongly deviates from Rastall gravity.

We demonstrated that despite the structural similarities with Rastall, the only way to cast this theory in the framework of $f(R, T)$, was through the hydrodynamical representation of a scalar field.

In a cosmological setting, the latter model, is able to reproduce one of the most intriguing results of Rastall theory: the recent cosmic history of the ΛCDM model is reproduced, but with the extra feature of having a clustering of dark energy.

We end this thesis with chapter 5 where we discuss some BH solutions in a novel theory of gravity, entangled relativity. BHs in this model are somewhat more complex to study than in GR, as we explored in section 5.2, given that vacuum does not seem to be allowed by the theory. Therefore one has to study solutions that involve matter fields, before contingently taking the limit toward vacuum in order to have a more realistic representation of astrophysical BHs—which are usually thought to evolve in a near vacuum environment. Using previous results developed in

the framework of string theory, we presented an exact spherically charged solution of entangled relativity in section 5.3. The solution tends to the Schwarzschild's solution in a near vacuum limit—that is, when the charge of the BH goes to zero.

Additionally, in section 5.4, we argued that any solution of pure radiation in GR, such as Vaidya's solution, might also be solution of entangled relativity, although more careful analyses are required to pin the argument on a more firm mathematical ground.

In any case, both Vaidya's and the charged BG solutions are well approximated by the external solution of the Schwarzschild metric in a near vacuum situation, providing evidence that an astrophysical spherical black hole in entangled relativity can be approximated by a Schwarzschild BH.

Otherwise, we have argued that this result is likely generic in near vacuum situations, such that an astrophysical rotating BH in entangled relativity can also likely be approximated by a Kerr BH, as we concluded in section 5.5.

Spherical Harmonics

The goal of this appendix is to settle the foundation for the equations in section 2.2. The main reference in this section is from [25], however we are using the notation from Regge and Wheeler [16].

First we define the metric of a sphere in two-dimensions as

$$\Omega_{ij}(\theta,\phi) = \begin{pmatrix} 1 & 0 \\ 0 & \sin\theta \end{pmatrix}. \tag{A.1}$$

With this we can write the Laplace equation of two a dimensional space in a sphere via

$$\begin{aligned} \Box Y_l^m(\theta,\phi) &= 0, \\ \Omega^{ij}\nabla_i\partial_j Y_l^m(\theta,\phi) &= 0, \end{aligned} \tag{A.2}$$

with $Y_l^m(\theta,\phi)$ denoting the spherical harmonics.

With the metric of the 2-sphere in equation (A.1), we can develop the D'Alembertian operator as follows

$$\Box = \frac{1}{\sin\theta}\partial_\theta(\sin\theta\partial_\theta) + \frac{1}{\sin^2\theta}\partial_\phi^2. \tag{A.3}$$

Then we can set up the eigenvalue problem as

$$\Box Y_\ell^m = \lambda Y_\ell^m, \tag{A.4}$$

which, by the usual separation of variables given as

$$Y_\ell^m(\theta,\phi) = \Theta(\theta)\Phi(\phi), \tag{A.5}$$

leads to

$$\sin\theta\partial_\theta(\sin\theta\partial_\theta\Theta) + \ell(\ell+1)\sin^2\theta\Theta = m^2\Theta, \tag{A.6}$$

$$\partial_\phi^2\Phi + m^2\Phi = 0. \tag{A.7}$$

The solution for Θ and Φ, respectively, are

$$\Theta(\theta) = P_\ell^m(\cos\theta), \qquad \Phi(\phi) = e^{\pm im\phi}, \tag{A.8}$$

where P_ℓ^m is the usual definition of the associated Legendre polynomial.

Hence, the full solution is given by the spherical harmonics defined as

$$Y_\ell^m(\theta,\phi) = A_\ell^m P_\ell^m(\cos\theta)e^{im\phi}, \tag{A.9}$$

where we have defined the normalization constant A_l^m as

$$A_\ell^m = \sqrt{\frac{(2\ell+1)(\ell-m)!}{4\pi(\ell+m)!}}, \tag{A.10}$$

to satisfy the following orthonormality condition

$$\int_{\theta=0}^{\pi}\int_{\phi=0}^{2\pi} Y_\ell^m Y_{\ell'}^{m'*} d\Omega = \delta_{\ell\ell'}\delta_{mm'}. \tag{A.11}$$

Bibliography

[1] B. P. Abbott et al. *Tests of general relativity with GW150914*. Phys. Rev. Lett. **116** 221101 (2016). [Erratum: Phys.Rev.Lett. 121, 129902 (2018)]. arXiv:1602.03841. [Cited on pages xii and 32.]

[2] K. Bronnikov, J. Fabris, and D. Rodrigues. *On horizons and wormholes in k-essence theories*. Grav. Cosmol. **22** 26 (2016). arXiv:1511.08036. [Cited on pages xii, 36, 37, and 38.]

[3] B. P. Abbott et al. *Observation of Gravitational Waves from a Binary Black Hole Merger*. Phys. Rev. Lett. **116** 061102 (2016). arXiv:1602.03837. [Cited on pages 1 and 29.]

[4] B. P. Abbott et al. *Gravitational Waves and Gamma-rays from a Binary Neutron Star Merger: GW170817 and GRB 170817A*. Astrophys. J. Lett. **848** L13 (2017). arXiv:1710.05834. [Cited on page 1.]

[5] A. G. Riess et al. *Observational evidence from supernovae for an accelerating universe and a cosmological constant*. Astron. J. **116** 1009 (1998). arXiv:astro-ph/9805201. [Cited on page 1.]

[6] K. Akiyama et al. *First M87 Event Horizon Telescope Results. I. The Shadow of the Supermassive Black Hole*. Astrophys. J. Lett. **875** L1 (2019). arXiv:1906.11238. [Cited on page 1.]

[7] U. Gunther, A. Starobinsky, and A. Zhuk. *Multidimensional cosmological models: Cosmological and astrophysical implications*. Phys. Rev. D **69** 044003 (2004). arXiv:hep-ph/0306191. [Cited on page 1.]

[8] P. Villanueva-Domingo, O. Mena, and S. Palomares-Ruiz. *A brief review on primordial black holes as dark matter*. 2021. arXiv:2103.12087. [Cited on page 1.]

[9] S. Perkins and N. Yunes. *Probing Screening and the Graviton Mass with Gravitational Waves*. Class. Quant. Grav. **36** 055013 (2019). arXiv:1811.02533. [Cited on page 1.]

[10] E. P. Verlinde. *On the Origin of Gravity and the Laws of Newton*. JHEP **04** 029 (2011). arXiv:1001.0785. [Cited on page 1.]

[11] W. Israel. *Event Horizons in Static Vacuum Space-Times*. Phys. Rev. **164** 1776 (1967). URL: https://link.aps.org/doi/10.1103/PhysRev.164.1776. [Cited on page 3.]

[12] K. Schwarzschild. *On the gravitational field of a mass point according to Einstein's theory*. Sitzungsber. Preuss. Akad. Wiss. Berlin (Math. Phys.) **1916** 189 (1916). arXiv:physics/9905030. [Cited on page 3.]

[13] S. Carroll, S. Carroll, and Addison-Wesley. *Spacetime and Geometry: An Introduction to General Relativity*. Addison Wesley 2004. URL: https://books.google.com.br/books?id=1SKFQgAACAAJ. [Cited on page 3.]

[14] A. Einstein. *Näherungsweise Integration der Feldgleichungen der Gravitation. Approximative Integration of the Field Equations of Gravitation*. Sitzungsber.Preuss.Akad.Wiss.Berlin (Math.Phys.) (1916). URL: http://cds.cern.ch/record/632328. [Cited on page 3.]

[15] B. P. Abbott et al. *Observation of gravitational waves from a binary black hole merger*. Physical Review Letters **116** 1 (2016). [Cited on pages 3 and 65.]

[16] T. Regge and J. A. Wheeler. *Stability of a schwarzschild singularity*. Physical Review **108** 1063 (1957). [Cited on pages 3, 4, 12, and 75.]

[17] F. J. Zerilli. *Gravitational field of a particle falling in a schwarzschild geometry analyzed in tensor harmonics*. Physical Review D **2** 2141 (1970). [Cited on pages 3 and 12.]

[18] C. V. Vishveshwara. *Stability of the Schwarzschild metric*. Physical Review D **1** 2870 (1970). [Cited on page 4.]

[19] R. A. Konoplya and A. Zhidenko. *Quasinormal modes of black holes: From astrophysics to string theory*. Reviews of Modern Physics **83** 793 (2011). [Cited on pages 4 and 6.]

[20] E. Berti, V. Cardoso, and A. O. Starinets. *Quasinormal modes of black holes and black branes*. Classical and Quantum Gravity **26** (2009). URL: https://arxiv.org/pdf/0905.2975.pdfhttp://arxiv.org/abs/0905.2975%0Ahttp://dx.doi.org/10.1088/0264-9381/26/16/163001. [Cited on pages 4 and 12.]

[21] K. D. Kokkotas and B. G. Schmidt. *Quasi-normal modes of stars and black holes*. Living Reviews in Relativity **2** (1999). [Cited on page 4.]

[22] S. W. Hawking. *Black hole explosions?* Nature **248** 30 (1974). [Cited on page 4.]

[23] W. G. Unruh and R. M. Wald. *Information Loss*. Rept. Prog. Phys. **80** 092002 (2017). arXiv:1703.02140. [Cited on page 4.]

[24] O. F. Piattella. *Lecture Notes in Cosmology*. UNITEXT for Physics. Springer Cham 2018. arXiv:1803.00070. [Cited on page 6.]

[25] K. Martel and E. Poisson. *Gravitational perturbations of the Schwarzschild spacetime: A practical covariant and gauge-invariant formalism*. Physical Review D **71** 104003 (2005). URL: https://link.aps.org/doi/10.1103/PhysRevD.71.104003. [Cited on pages 7 and 75.]

[26] E. T. Newman and R. Penrose. *Note on the Bondi-Metzner-Sachs Group*. Journal of Mathematical Physics **7** 863 (1966). [Cited on page 7.]

[27] K. S. Thorne. *Multipole expansions of gravitational radiation*. Reviews of Modern Physics **52** 299 (1980). [Cited on page 7.]

[28] S. A. Teukolsky. *Perturbations of a rotating black hole. 1. Fundamental equations for gravitational electromagnetic and neutrino field perturbations*. Astrophys. J. **185** 635 (1973). [Cited on page 11.]

[29] S. Hawking and R. Penrose. *The Singularities of gravitational collapse and cosmology.* Proc. Roy. Soc. Lond. A **A314** 529 (1970). [Cited on page 11.]

[30] R. Penrose. *Gravitational collapse: The role of general relativity.* Riv. Nuovo Cim. **1** 252 (1969). [Cited on page 12.]

[31] S. Chandrasekhar. *On Algebraically Special Perturbations of Black Holes.* Proceedings of the Royal Society A: Mathematical, Physical and Engineering Sciences **392** 1 (1984). URL: http://rspa.royalsocietypublishing.org/cgi/doi/10.1098/rspa.1984.0021. [Cited on page 12.]

[32] V. Cardoso and J. P. S. Lemos. *Quasinormal modes of Schwarzschild anti-de Sitter black holes: Electromagnetic and gravitational perturbations.* Phys. Rev. **D64** 84017 (2001). [Cited on page 12.]

[33] S. Chandrasekhar. *The mathematical theory of black holes.* The Oxford University Press 1983. [Cited on page 12.]

[34] K. D. Kokkotas and B. F. Schutz. *Black-hole normal modes: A WKB approach. III. the reissner-nordström black hole.* Physical Review D **37** 3378 (1988). [Cited on pages 13 and 21.]

[35] E. Berti and K. D. Kokkotas. *Quasinormal modes of Kerr-Newman black holes: Coupling of electromagnetic and gravitational perturbations.* Physical Review D - Particles, Fields, Gravitation and Cosmology **71** 1 (2005). URL: https://arxiv.org/pdf/gr-qc/0502065.pdf. [Cited on page 13.]

[36] F. Kottler. *Über die physikalischen Grundlagen der Einsteinschen Gravitationstheorie.* Annalen der Physik **361** 401 (1918). URL: https://onlinelibrary.wiley.com/doi/abs/10.1002/andp.19183611402. [Cited on page 14.]

[37] J. M. Maldacena. *The Large N limit of superconformal field theories and supergravity.* Int. J. Theor. Phys. **38** 1113 (1999). [Cited on page 14.]

[38] V. Faraoni. *Embedding black holes and other inhomogeneities in the universe in various theories of gravity: a short review.* Universe **4** 109 (2018). [Cited on page 14.]

[39] N. Hidekazu. *On a new cosmological solution of Einstein's field equations of gravitation.* Sci.˜Rep.˜Tohoku Univ.˜Eighth Ser. **35** (1951). [Cited on page 14.]

[40] J. Guven and D. Núñez. *Schwarzschild-de Sitter space and its perturbations.* Phys. Rev. D **42** 2577 (1990). URL: https://link.aps.org/doi/10.1103/PhysRevD.42.2577. [Cited on page 14.]

[41] A. Zhidenko. *Quasi-normal modes of Schwarzschild-de Sitter black holes.* Classical and Quantum Gravity **21** 273 (2004). URL: http://arxiv.org/abs/gr-qc/0307012%0Ahttp://dx.doi.org/10.1088/0264-9381/21/1/019. [Cited on pages 14 and 15.]

[42] J. M. Bardeen. *Non-singular general-relativistic gravitational collapse.* In *Proc. Int. Conf. GR5, Tbilisi* volume 174 1968. [Cited on page 15.]

[43] E. Ayón-Beato and A. García. *The Bardeen model as a nonlinear magnetic monopole.* Physics Letters, Section B: Nuclear, Elementary Particle and High-Energy Physics **493** 149 (2000). [Cited on page 16.]

[44] K. A. Bronnikov. *Regular magnetic black holes and monopoles from nonlinear electrodynamics*. Phys. Rev. **D63** 044005 (2001). arXiv:gr-qc/0006014. [Cited on page 16.]

[45] M. E. Rodrigues and M. V. S. Silva. *Bardeen regular black hole with an electric source*. Journal of Cosmology and Astroparticle Physics **2018** (2018). [Cited on page 16.]

[46] J. A. d. F. Pacheco. *Primordial Regular Black Holes: Thermodynamics and Dark Matter*. Universe **4** 62 (2018). arXiv:1805.03053. [Cited on pages 16 and 17.]

[47] S. Fernando and J. Correa. *Quasinormal modes of the Bardeen black hole: Scalar perturbations*. Physical Review D - Particles, Fields, Gravitation and Cosmology **86** 1 (2012). [Cited on page 16.]

[48] S. C. Ulhoa. *On the Quasinormal Modes for Gravitational Perturbations of the Bardeen Black Hole*. Brazilian Journal of Physics **44** 380 (2014). [Cited on page 16.]

[49] S. Dey and S. Chakrabarti. *A note on electromagnetic and gravitational perturbations of the Bardeen de Sitter black hole: quasinormal modes and greybody factors*. Eur. Phys. J. C **79** 504 (2019). arXiv:1807.09065. [Cited on page 17.]

[50] S. A. Hayward. *Formation and evaporation of nonsingular black holes*. Physical Review Letters **96** 1 (2006). [Cited on page 17.]

[51] P. Chunilal Vaidya. *The gravitational field of a radiating star*. Indian Academy of Sciences Proceedings Section **33** 264 (1951). [Cited on page 17.]

[52] R. Kumar, S. G. Ghosh, and A. Wang. *Shadow cast and deflection of light by charged rotating regular black holes*. Phys. Rev. D **100** 124024 (2019). arXiv:1912.05154. [Cited on page 17.]

[53] P. M. Davidson. *Bemerkungen zur Quantenmechanik des anharmonischen Oscillators*. Zeitschrift für Physik **87** 364 (1934). [Cited on page 18.]

[54] J. Lekner. *Reflectionless eigenstates of the sech^2 potential*. American Journal of Physics **75** 1151 (2007). [Cited on page 18.]

[55] E. Brown and L. Hernández De La Pena. *A Simplified Pöschl-Teller Potential: An Instructive Exercise for Introductory Quantum Mechanics*. Journal of Chemical Education **95** 1989 (2018). [Cited on page 18.]

[56] V. Ferrari and B. Mashhoon. *New approach to the quasinormal modes of a black hole*. Phys. Rev. D **30** 295 (1984). [Cited on page 18.]

[57] A. F. Cardona and C. Molina. *Quasinormal modes of generalized Pöschl-Teller potentials*. Classical and Quantum Gravity **34** 1 (2017). [Cited on page 19.]

[58] V. Cardoso and J. P. Lemos. *Quasinormal modes of the near extremal Schwarzschild-de Sitter black hole*. Phys. Rev. D **67** 084020 (2003). arXiv:gr-qc/0301078. [Cited on page 19.]

[59] C. Molina. *Quasinormal modes of d-dimensional spherical black holes with near extreme cosmological constant*. Phys. Rev. D **68** 064007 (2003). arXiv:gr-qc/0304053. [Cited on page 19.]

[60] L. D. Landau and E. M. Lifshitz. *Quantum Mechanics* volume 3. Butterworth-Heinemann 3 edition 1981. [Cited on page 19.]

[61] C. M. Bender and S. A. Orszag. *Advanced Mathematical Methods for Scientists and Engineers I* volume 1. Springer-Verlag New York 1 edition 1978. [Cited on page 19.]

[62] P. Tipler and G. Mosca. *Physics for Scientists and Engineers*. Physics for Scientists and Engineers. W. H. Freeman and Company New York 2004. URL: https://books.google.com.br/books?id=2HRFckqcBNoC. [Cited on page 20.]

[63] B. Mashhoon. *Quasi-normal modes of a black hole.* In *Third Marcel Grossmann Meeting on General Relativity* pages 599–608 1983. [Cited on page 20.]

[64] S. Iyer and C. M. Will. *Black-hole normal modes: A WKB approach. I. Foundations and application of a higher-order WKB analysis of potential-barrier scattering*. Physical Review D **35** 3621 (1987). [Cited on page 21.]

[65] S. Iyer. *Black Hole Normal Modes: a WKB Approach. II. Schwarzschild Black Holes*. Phys. Rev. **D35** 3632 (1987). [Cited on page 21.]

[66] E. Seidel and S. Iyer. *Black-hole normal modes: A WKB approach. IV. Kerr black holes*. Physical Review D **41** 374 (1990). URL: https://journals.aps.org/prd/pdf/10.1103/PhysRevD.41.374. [Cited on page 21.]

[67] R. Konoplya. *Quasinormal behavior of the d-dimensional Schwarzschild black hole and higher order WKB approach*. Phys. Rev. D **68** 024018 (2003). arXiv:gr-qc/0303052. [Cited on page 21.]

[68] V. Cardoso, J. L. Costa, K. Destounis, P. Hintz, and A. Jansen. *Quasinormal modes and Strong Cosmic Censorship*. Phys. Rev. Lett. **120** 31103 (2018). [Cited on page 23.]

[69] J. L. Cervantes-Cota, S. Galindo-Uribarri, and G.-F. Smoot. *A Brief History of Gravitational Waves*. Universe **2** 22 (2016). arXiv:1609.09400. [Cited on page 27.]

[70] C. W. Misner, K. S. Thorne, and J. A. Wheeler. *Gravitation*. 1973. [Cited on page 27.]

[71] R. Feynman. *An Expanded Version of the Remarks by R.P. Feynman on the Reality of Gravitational Waves* 1957. URL: https://edition-open-sources.org/sources/5/34/index.html. [Cited on page 27.]

[72] J. Weber. *Anisotropy and Polarization in the Gravitational-Radiation Experiments*. Phys. Rev. Lett. **25** 180 (1970). URL: https://link.aps.org/doi/10.1103/PhysRevLett.25.180. [Cited on page 28.]

[73] B. P. Abbott et al. *GWTC-1: A Gravitational-Wave Transient Catalog of Compact Binary Mergers Observed by LIGO and Virgo during the First and Second Observing Runs*. Phys. Rev. X **9** 031040 (2019). arXiv:1811.12907. [Cited on pages 29 and 65.]

[74] R. Abbott et al. *GWTC-2: Compact Binary Coalescences Observed by LIGO and Virgo During the First Half of the Third Observing Run*. 2020). arXiv:2010.14527. [Cited on page 29.]

[75] A. H. Mroue et al. *Catalog of 174 Binary Black Hole Simulations for Gravitational Wave Astronomy*. Phys. Rev. Lett. **111** 241104 (2013). arXiv:1304.6077. [Cited on page 29.]

[76] M. Boyle et al. *The SXS Collaboration catalog of binary black hole simulations*. Class. Quant. Grav. **36** 195006 (2019). arXiv:1904.04831. [Cited on page 29.]

[77] R. H. Price. *Nonspherical Perturbations of Relativistic Gravitational Collapse. I. Scalar and Gravitational Perturbations*. Phys. Rev. D **5** 2419 (1972). URL: https://link.aps.org/doi/10.1103/PhysRevD.5.2419. [Cited on page 29.]

[78] R. H. Price. *Nonspherical Perturbations of Relativistic Gravitational Collapse. II. Integer-Spin, Zero-Rest-Mass Fields*. Phys. Rev. D **5** 2439 (1972). URL: https://link.aps.org/doi/10.1103/PhysRevD.5.2439. [Cited on page 29.]

[79] E. S. C. Ching, P. T. Leung, W. M. Suen, and K. Young. *Wave propagation in gravitational systems: Late time behavior*. Phys. Rev. D **52** 2118 (1995). arXiv:gr-qc/9507035. [Cited on page 29.]

[80] W. K. Hastings. *Monte Carlo sampling methods using Markov chains and their applications*. Biometrika **57** 97 (1970). URL: https://doi.org/10.1093/biomet/57.1.97 arXiv:https://academic.oup.com/biomet/article-pdf/57/1/97/23940249/57-1-97.pdf. [Cited on page 29.]

[81] N. Metropolis, A. W. Rosenbluth, M. N. Rosenbluth, A. H. Teller, and E. Teller. *Equation of State Calculations by Fast Computing Machines*. The Journal of Chemical Physics **21** 1087 (1953). URL: https://doi.org/10.1063/1.1699114 arXiv:https://doi.org/10.1063/1.1699114. [Cited on page 29.]

[82] E. Berti, V. Cardoso, and C. M. Will. *On gravitational-wave spectroscopy of massive black holes with the space interferometer LISA*. Phys. Rev. D **73** 064030 (2006). arXiv:gr-qc/0512160. [Cited on page 29.]

[83] M. Giesler, M. Isi, M. A. Scheel, and S. Teukolsky. *Black Hole Ringdown: The Importance of Overtones*. Phys. Rev. X **9** 041060 (2019). arXiv:1903.08284. [Cited on page 29.]

[84] K. D. Kokkotas. *Gravitational waves*. Acta Phys. Polon. B **38** 3891 (2007). [Cited on page 30.]

[85] E. Newman and R. Penrose. *An Approach to gravitational radiation by a method of spin coefficients*. J. Math. Phys. **3** 566 (1962). [Cited on page 30.]

[86] P. Szekeres. *The Gravitational compass*. J. Math. Phys. **6** 1387 (1965). [Cited on page 30.]

[87] A. Buonanno and T. Damour. *Effective one-body approach to general relativistic two-body dynamics*. Phys. Rev. D **59** 084006 (1999). arXiv:gr-qc/9811091. [Cited on page 30.]

[88] T. Damour and A. Nagar. *The Effective One Body description of the Two-Body problem*. Fundam. Theor. Phys. **162** 211 (2011). arXiv:0906.1769. [Cited on page 30.]

[89] S. T. McWilliams. *Analytical Black-Hole Binary Merger Waveforms*. Phys. Rev. Lett. **122** 191102 (2019). arXiv:1810.00040. [Cited on pages 30 and 31.]

[90] H. Yang, D. A. Nichols, F. Zhang, A. Zimmerman, Z. Zhang, and Y. Chen. *Quasinormal-mode spectrum of Kerr black holes and its geometric interpretation*. Phys. Rev. D **86** 104006 (2012). URL: https://link.aps.org/doi/10.1103/PhysRevD.86.104006. [Cited on page 31.]

[91] J. G. Baker, W. D. Boggs, J. Centrella, B. J. Kelly, S. T. McWilliams, and J. R. van Meter. *Mergers of nonspinning black-hole binaries: Gravitational radiation characteristics.* Phys. Rev. D **78** 044046 (2008). URL: https://link.aps.org/doi/10.1103/PhysRevD.78.044046. [Cited on page 31.]

[92] *Gravitational Wave Open Science Center.* https://www.gw-openscience.org/about/. Accessed: 2021-05-31. [Cited on page 32.]

[93] B. P. Abbott et al. *Properties of the Binary Black Hole Merger GW150914.* Phys. Rev. Lett. **116** 241102 (2016). arXiv:1602.03840. [Cited on page 32.]

[94] B. P. Abbott et al. *GW170104: Observation of a 50-Solar-Mass Binary Black Hole Coalescence at Redshift 0.2.* Phys. Rev. Lett. **118** 221101 (2017). [Erratum: Phys.Rev.Lett. 121, 129901 (2018)]. arXiv:1706.01812. [Cited on page 32.]

[95] T. Kaluza. *Zum Unitätsproblem der Physik.* Sitzungsber. Preuss. Akad. Wiss. Berlin (Math. Phys.) **1921** 966 (1921). arXiv:1803.08616. [Cited on page 35.]

[96] O. Klein. *The Atomicity of Electricity as a Quantum Theory Law.* Nature **118** 516 (1926). [Cited on page 35.]

[97] T. Clifton, P. G. Ferreira, A. Padilla, and C. Skordis. *Modified Gravity and Cosmology.* Phys. Rept. **513** 1 (2012). arXiv:1106.2476. [Cited on page 35.]

[98] C. Armendariz-Picon, T. Damour, and V. F. Mukhanov. *k - inflation.* Phys. Lett. B **458** 209 (1999). arXiv:hep-th/9904075. [Cited on page 36.]

[99] R. Kantowski and R. K. Sachs. *Some Spatially Homogeneous Anisotropic Relativistic Cosmological Models.* Journal of Mathematical Physics **7** 443 (1966). URL: https://doi.org/10.1063/1.1704952 arXiv:https://doi.org/10.1063/1.1704952. [Cited on page 36.]

[100] K. Bronnikov, G. Clement, C. Constantinidis, and J. Fabris. *Cold scalar tensor black holes: Causal structure, geodesics, stability.* Grav. Cosmol. **4** 128 (1998). arXiv:gr-qc/9804064. [Cited on page 37.]

[101] K. Bronnikov, G. Clement, C. Constantinidis, and J. Fabris. *Structure and stability of cold scalar - tensor black holes.* Phys. Lett. A **243** 121 (1998). arXiv:gr-qc/9801050. [Cited on pages 37 and 50.]

[102] P. Rastall. *Generalization of the Einstein Theory.* Phys. Rev. D **6** 3357 (1972). URL: https://link.aps.org/doi/10.1103/PhysRevD.6.3357. [Cited on page 38.]

[103] A. Oliveira, H. Velten, and J. Fabris. *Nontrivial static, spherically symmetric vacuum solution in a nonconservative theory of gravity.* Phys. Rev. D **93** 124020 (2016). arXiv:1602.08513. [Cited on page 39.]

[104] C. E. M. Batista, M. H. Daouda, J. C. Fabris, O. F. Piattella, and D. C. Rodrigues. *Rastall cosmology and the ΛCDM model.* Phys. Rev. D **85** 084008 (2012). URL: https://link.aps.org/doi/10.1103/PhysRevD.85.084008. [Cited on pages 39, 61, 63, and 64.]

[105] K. Bronnikov, J. Fabris, O. Piattella, and E. Santos. *Static, spherically symmetric solutions with a scalar field in Rastall gravity.* Gen. Rel. Grav. **48** 162 (2016). arXiv:1606.06242. [Cited on page 39.]

[106] K. A. Bronnikov, J. C. Fabris, O. F. Piattella, D. C. Rodrigues, and E. C. Santos. *Duality between k-essence and Rastall gravity*. Eur. Phys. J. C **77** 409 (2017). arXiv:1701.06662. [Cited on page 40.]

[107] V. Rubakov. *The Null Energy Condition and its violation*. Usp. Fiz. Nauk **184** 137 (2014). arXiv:1401.4024. [Cited on page 42.]

[108] C. Armendariz-Picon, V. F. Mukhanov, and P. J. Steinhardt. *A Dynamical solution to the problem of a small cosmological constant and late time cosmic acceleration*. Phys. Rev. Lett. **85** 4438 (2000). arXiv:astro-ph/0004134. [Cited on page 44.]

[109] O. Piattella, J. Fabris, and N. Bilic. *Note on the thermodynamics and the speed of sound of a scalar field*. Classical and Quantum Gravity **31** (2014). [Cited on page 44.]

[110] J. Fabris, M. Daouda, and O. Piattella. *Note on the Evolution of the Gravitational Potential in Rastall Scalar Field Theories*. Phys. Lett. B **711** 232 (2012). arXiv:1109.2096. [Cited on page 44.]

[111] C. Gao, M. Kunz, A. R. Liddle, and D. Parkinson. *Unified dark energy and dark matter from a scalar field different from quintessence*. Phys. Rev. D **81** 043520 (2010). URL: https://link.aps.org/doi/10.1103/PhysRevD.81.043520. [Cited on page 44.]

[112] W. De Blok. *The core-cusp problem*. Advances in Astronomy **2010** (2010). [Cited on page 48.]

[113] J. Bullock. *Notes on the missing satellites problem*. Local Group Cosmology **20** 95 (2013). [Cited on page 48.]

[114] K. Bronnikov, J. Fabris, and D. C. Rodrigues. *Instability of some k-essence spacetimes*. Int. J. Mod. Phys. D **29** 2050016 (2020). arXiv:1908.09126. [Cited on page 48.]

[115] K. A. Bronnikov and S. G. Rubin. *Black Holes, Cosmology and Extra Dimensions*. WSP 2012. [Cited on pages 48 and 50.]

[116] K. Bronnikov, J. C. Fabris, O. F. Piattella, D. C. Rodrigues, and E. C. Santos. *Rastall's theory of gravity: Spherically symmetric solutions and the stability problem*. 2020). arXiv:2007.01945. [Cited on page 48.]

[117] J. C. Fabris. *Conservation Laws in Gravitation and Cosmology*. 2012. arXiv:1208.4649. [Cited on page 56.]

[118] M. Visser. *Rastall gravity is equivalent to Einstein gravity*. Physics Letters B **782** 83 (2018). URL: http://www.sciencedirect.com/science/article/pii/S0370269318303927. [Cited on page 56.]

[119] F. Darabi, H. Moradpour, I. Licata, Y. Heydarzade, and C. Corda. *Einstein and Rastall Theories of Gravitation in Comparison*. Eur. Phys. J. C **78** 25 (2018). arXiv:1712.09307. [Cited on page 56.]

[120] L. L. Smalley. *Variational principle for a prototype Rastall theory of gravitation*. Nuovo Cimento B Serie **80** 42 (1984). [Cited on page 57.]

[121] T. Harko and F. S. Lobo. *$f(R,L_m)$ gravity*. Eur. Phys. J. C **70** 373 (2010). arXiv:1008.4193. [Cited on pages 57, 59, and 60.]

[122] T. Harko, F. S. Lobo, S. Nojiri, and S. D. Odintsov. *$f(R,T)$ gravity.* Phys. Rev. D **84** 024020 (2011). arXiv:1104.2669. [Cited on page 57.]

[123] W. De Moraes and A. Santos. *Lagrangian formalism for Rastall theory of gravity and Gödel-type universe.* Gen. Rel. Grav. **51** 167 (2019). arXiv:1912.06471. [Cited on pages 57 and 59.]

[124] R. V. d. Santos and J. A. C. Nogales. *Cosmology from a Lagrangian formulation for Rastall's theory.* 2017). arXiv:1701.08203. [Cited on pages 57 and 58.]

[125] H. Shabani and A. Hadi Ziaie. *A connection between Rastall-type and $f(R,T)$ gravities.* EPL **129** 20004 (2020). arXiv:2003.02064. [Cited on page 57.]

[126] J. C. Fabris, O. F. Piattella, D. C. Rodrigues, D. C. Rodrigues, and E. C. O. Santos. *A note on non-vanishing divergence of the stress-energy tensor in theories of gravity.* 2020). arXiv:2011.10503. [Cited on page 57.]

[127] H. A. Buchdahl. *Non-Linear Lagrangians and Cosmological Theory.* Monthly Notices of the Royal Astronomical Society **150** 1 (1970). URL: https://doi.org/10.1093/mnras/150.1.1 arXiv:https://academic.oup.com/mnras/article-pdf/150/1/1/8075909/mnras150-0001.pdf. [Cited on page 57.]

[128] O. Bertolami, C. G. Böhmer, T. Harko, and F. S. N. Lobo. *Extra force in $f(R)$ modified theories of gravity.* Phys. Rev. D **75** 104016 (2007). URL: https://link.aps.org/doi/10.1103/PhysRevD.75.104016. [Cited on page 57.]

[129] C. Armendariz-Picon, V. F. Mukhanov, and P. J. Steinhardt. *A Dynamical solution to the problem of a small cosmological constant and late time cosmic acceleration.* Phys. Rev. Lett. **85** 4438 (2000). arXiv:astro-ph/0004134. [Cited on page 58.]

[130] J. Overduin and F. Cooperstock. *Evolution of the scale factor with a variable cosmological term.* Phys. Rev. D **58** 043506 (1998). arXiv:astro-ph/9805260. [Cited on page 58.]

[131] N. J. Poplawski. *A Lagrangian description of interacting dark energy.* 2006). arXiv:gr-qc/0608031. [Cited on page 58.]

[132] O. F. Piattella, J. C. Fabris, and N. Bilić. *Note on the thermodynamics and the speed of sound of a scalar field.* Class. Quant. Grav. **31** 055006 (2014). arXiv:1309.4282. [Cited on page 61.]

[133] C.-P. Ma and E. Bertschinger. *Cosmological perturbation theory in the synchronous and conformal Newtonian gauges.* Astrophys. J. **455** 7 (1995). arXiv:astro-ph/9506072. [Cited on page 63.]

[134] H. Ludwig, O. Minazzoli, and S. Capozziello. *Merging matter and geometry in the same Lagrangian.* Phys. Lett. B **751** 576 (2015). arXiv:1506.03278. [Cited on pages 65, 66, and 67.]

[135] O. Minazzoli. *Rethinking the link between matter and geometry.* Phys. Rev. D **98** 124020 (2018). arXiv:1811.05845. [Cited on pages 65, 66, and 67.]

[136] D. Arruga, O. Rousselle, and O. Minazzoli. *Compact objects in entangled relativity.* Phys. Rev. D **103** 024034 (2021). URL: https://link.aps.org/doi/10.1103/PhysRevD.103.024034. [Cited on pages 65 and 67.]

[137] O. Minazzoli. *De Sitter space-times in entangled relativity.* Class. Quant. Grav. **38** 137003 (2021). arXiv:2011.14633. [Cited on pages 65, 66, 67, 70, and 71.]

[138] A. Einstein. *Prinzipielles zur allgemeinen Relativitätstheorie.* Annalen der Physik **360** 241 (1918). URL: https://onlinelibrary.wiley.com/doi/abs/10.1002/andp.19183600402 arXiv:https://onlinelibrary.wiley.com/doi/pdf/10.1002/andp.19183600402. [Cited on page 65.]

[139] A. Einstein. *Über Gravitationswellen.* Sitzungsberichte der Königlich Preußischen Akademie der Wissenschaften (Berlin pages 154–167 (1918). [Cited on page 65.]

[140] J. D. Norton. *Mach's Principle before Einstein.* In J. B. Barbour and H. Pfister, editors, *Mach's Principle: From Newton's Bucket to Quantum Gravity* page 9 1995. [Cited on page 65.]

[141] C. Hoefer. *Einstein's Formulations of Mach's Principle.* In J. B. Barbour and H. Pfister, editors, *Mach's Principle: From Newton's Bucket to Quantum Gravity* page 67 1995. [Cited on page 65.]

[142] A. Pais. *Subtle is the Lord. The science and the life of Albert Einstein.* 1982. [Cited on page 65.]

[143] H. H. von Borzeszkowski and R. Wahsner. *Mach's Criticism of Newton and Einstein's Reading of Mach: The Stimulating Role of Two Misunderstandings.* In J. B. Barbour and H. Pfister, editors, *Mach's Principle: From Newton's Bucket to Quantum Gravity* page 58 1995. [Cited on page 65.]

[144] W. de Sitter. *Einstein's theory of gravitation and its astronomical consequences. Third paper.* Monthly Notices of the Royal Astronomical Society **78** 3 (1917). [Cited on page 65.]

[145] *Mach's Principle: From Newton's Bucket to Quantum Gravity.* 1995. [Cited on page 65.]

[146] Event Horizon Telescope Collaboration. *First M87 Event Horizon Telescope Results. I. The Shadow of the Supermassive Black Hole.* Astrophysical Journal Letters **875** L1 (2019). arXiv:1906.11238. [Cited on page 65.]

[147] D. Psaltis et al. *Gravitational Test beyond the First Post-Newtonian Order with the Shadow of the M87 Black Hole.* Phys. Rev. Lett. **125** 141104 (2020). URL: https://link.aps.org/doi/10.1103/PhysRevLett.125.141104. [Cited on page 65.]

[148] O. Minazzoli and E. Santos. *Charged black hole and radiating solutions in entangled relativity.* 2021). arXiv:2102.10541. [Cited on page 66.]

[149] O. Minazzoli. *Spacetime might not be doomed after all.* arXiv e-prints page arXiv:2103.05313 (2021). arXiv:2103.05313. [Cited on pages 66, 67, and 71.]

[150] F. Dyson. *Is a Graviton Detectable?* International Journal of Modern Physics A **28** 1330041 (2013). [Cited on page 66.]

[151] S. Capozziello and M. De Laurentis. *F(R) theories of gravitation.* Scholarpedia **10** 31422 (2015). [Cited on page 67.]

[152] O. Minazzoli and A. Hees. *Intrinsic Solar System decoupling of a scalar-tensor theory with a universal coupling between the scalar field and the matter Lagrangian.* Physical Review D **88** 041504 (2013). arXiv:1308.2770. [Cited on pages 67 and 71.]

[153] O. Minazzoli. *On the cosmic convergence mechanism of the massless dilaton.* Physics Letters B **735** 119 (2014). arXiv:1312.4357. [Cited on pages 67, 70, and 71.]

[154] O. Minazzoli and A. Hees. *Late-time cosmology of a scalar-tensor theory with a universal multiplicative coupling between the scalar field and the matter Lagrangian.* Physical Review D **90** 023017 (2014). arXiv:1404.4266. [Cited on pages 67, 70, and 71.]

[155] C. F. E. Holzhey and F. Wilczek. *Black holes as elementary particles.* Nuclear Physics B **380** 447 (1992). arXiv:hep-th/9202014. [Cited on pages 67 and 68.]

[156] R. Woodard. *Avoiding Dark Energy with 1/R Modifications of Gravity* volume 720 page 403. 2007. [Cited on page 67.]

[157] R. P. Woodard. *Ostrogradsky's theorem on Hamiltonian instability.* Scholarpedia **10** 32243 (2015). revision #186559. [Cited on page 67.]

[158] R. M. Wald. *General relativity.* 1984. [Cited on page 67.]

[159] P. Teyssandier and P. Tourrenc. *The Cauchy problem for the $R+R^2$ theories of gravity without torsion.* Journal of Mathematical Physics **24** 2793 (1983). [Cited on page 67.]

[160] N. Lanahan-Tremblay and V. Faraoni. *The Cauchy problem of f(R) gravity.* Classical and Quantum Gravity **24** 5667 (2007). arXiv:0709.4414. [Cited on page 67.]

[161] N. Yunes and X. Siemens. *Gravitational-Wave Tests of General Relativity with Ground-Based Detectors and Pulsar-Timing Arrays.* Living Reviews in Relativity **16** (2013). [Cited on page 67.]

[162] P. Jai-akson, A. Chatrabhuti, O. Evnin, and L. Lehner. *Black hole merger estimates in Einstein-Maxwell and Einstein-Maxwell-dilaton gravity.* Phys. Rev. D **96** 044031 (2017). URL: https://link.aps.org/doi/10.1103/PhysRevD.96.044031. [Cited on page 67.]

[163] S. L. Liebling. *Maxwell-dilaton dynamics.* Phys. Rev. D **100** 104040 (2019). URL: https://link.aps.org/doi/10.1103/PhysRevD.100.104040. [Cited on page 67.]

[164] G. W. Gibbons and K.-I. Maeda. *Black holes and membranes in higher-dimensional theories with dilaton fields.* Nuclear Physics B **298** 741 (1988). [Cited on page 68.]

[165] D. Garfinkle, G. T. Horowitz, and A. Strominger. *Charged black holes in string theory.* Physical Review D **43** 3140 (1991). [Cited on page 68.]

[166] J. H. Horne and G. T. Horowitz. *Rotating dilaton black holes.* Physical Review D **46** 1340 (1992). arXiv:hep-th/9203083. [Cited on page 68.]

[167] P. H. Cox, B. Harms, and Y. Leblanc. *Dilaton black holes, naked singularities and strings.* EPL (Europhysics Letters) **26** 321 (1994). arXiv:hep-th/9207079. [Cited on page 68.]

[168] J. H. Kim and S.-H. Moon. *Electric charge in interaction with magnetically charged black holes.* Journal of High Energy Physics **2007** 088 (2007). arXiv:0707.4183. [Cited on page 68.]

[169] E. Santos. *Verifying entangled BH solution.nb*. `https://github.com/Edison-Santos/Mathematica_github.git` 2021. [Cited on page 69.]

[170] P. C. Vaidya. *A Radiation-absorbing Centre in a Non-statical Homogeneous Universe*. *Nature* **166** 565 (1950). [Cited on page 70.]

[171] J. B. Griffiths and J. Podolský. *Exact Space-Times in Einstein's General Relativity*. 2009. [Cited on page 70.]

[172] R. Schützhold. *Small Cosmological Constant from the QCD Trace Anomaly?* *Phys. Rev. Lett.* **89** 081302 (2002). `arXiv:gr-qc/0204018`. [Cited on page 70.]

[173] O. Minazzoli and A. Hees. *Dilatons with intrinsic decouplings*. *Physical Review D* **94** 064038 (2016). `arXiv:1512.05232`. [Cited on page 71.]

[174] R. Penrose. *Gravitational Collapse and Space-Time Singularities*. *Phys. Rev. Lett.* **14** 57 (1965). [Cited on page 71.]